Inês Vieira Peres Ventura

Characterization of glycoproteins involved in sea urchin adhesion

Dissertation to obtain the Master degree in Biomedical Research, performed under the scientific supervision of Doctor Cláudia Maria Fragão Pereira and co-supervision of Professor Romana Lopes Almeida dos Santos and presented to the Faculty of Medicine of the University of Coimbra

December, 2020

· U C ·

Universidade de Coimbra

Characterization of glycoproteins involved in sea urchin adhesion

Inês Vieira Peres Ventura

Dissertation presented to the Faculty of Medicine of the University of Coimbra. The work was performed in the Marine and Environmental Sciences Centre, in the Faculty of Sciences, University of Lisbon, under the scientific supervision of Doctor Cláudia Maria Fragão Pereira and co-supervision of Professor Romana Lopes Almeida dos Santos.

University of Coimbra

2020

The experimental work described in the present thesis was performed in the Bioadhesion and Biomimicry research group, at MARE, Faculty of Sciences, University of Lisbon, Portugal.

Financial support was granted by the by Fundação para a Ciência e Tecnologia through Project grants (IF/00006/2015/CP1276/CT0001; UIDP/04292/2020).

FCT Fundação para a Ciência e a Tecnologia

À minha família

ACKNOWLEDGEMENTS

Esta dissertação é tanto minha como de todos os que me apoiaram. Nunca poderei fazer jus a tudo o que fizeram por mim, mas espero que este pequeno reconhecimento seja um bom início.

Em primeiro lugar, gostaria de agradecer à minha orientadora Romana Santos. Não poderia ter escolhido alguém melhor. É um exemplo de força e determinação. Se existem palavras suficientes para lhe agradecer tudo o que fez por mim, não as tenho. Só lhe posso agradecer por me ter restituído o amor pela Ciência e por ter acreditado em mim. Obrigada por ter feito este percurso comigo. Por todas as palavras amigas, por todos os conselhos e por todas os momentos. Fico grata por termos partilhado um bocadinho desde percurso e espero que saiba que é um orgulho ser sua aluna. Posso dizer com todo o carinho que foi um privilégio conhecê-la.

Também gostaria de agradecer à minha orientadora, Cláudia Pereira, por estar sempre disponível para ajudar e sempre com uma palavra amiga. São poucas as pessoas que assim o são. Obrigada a ambas por terem feito todos os esforços possíveis para a conclusão desta dissertação. Tive muita sorte.

Ao coordenador do mestrado, Henrique Girão. Obrigada por me ter proporcionado esta experiência. Foi um prazer fazer parte do MIB e conhecê-lo.

À Professora Doutora Manuela Coelho. Por ser sempre um exemplo e um pequeno abrigo no mundo académico. Obrigada por me ter recebido sempre que me senti desorientada, sempre que precisei de um conselho amigo. Além de ter marcado o meu percurso académico como uma grande docente e pedagoga, também levo comigo todas as palavras amigas e ensinamentos repletos de carinho. Obrigada pela pessoa que é.

Ao serviço de espectrometria de Liverpool, pelo excelente trabalho realizado e pelo acompanhamento/sugestões dadas. Ao Professor Doutor Carlos Cordeiro (Laboratório de Bioquímica e Biologia Molecular FCT-ICR-MS-Lisboa), Prof. Dr. Rogério Tenreiro (Grupo de Microbiologia e Biotecnologia – Lab Bugworkers, M&B-BioISI, Tec Labs) e Dr.ª Filipa Silva (Grupo de Microbiologia e Biotecnologia – Lab Bugworkers, M&B-BioISI, Tec Labs) pela disponibilização de equipamentos.

À Mariana e à Lisa. Obrigada pela companhia, pela paciência e por todas as horas que passámos juntas no laboratório. Não podia ter pedido melhor companhia para este ano. Foram as mais divertidas e simpáticas companheiras que podia ter desejado. São únicas e se hoje me lembro deste ano com carinho, muito se deve a vocês.

Um muito obrigada a Coimbra. Aos amigos que essa cidade me deu, a minha vida é muito mais completa convosco. Francisca (Chica), Ana Rita, Luíza, Antónia, Daniela (Mila), David (Acéfalo), Inês (Benta), Diana (Obscura) e Filipa, obrigada. A quem viveu comigo, obrigada por terem tornado a saída de casa tão mais fácil e divertida. Era um prazer chegar a casa e conversar convosco. Ainda hoje me rio com tudo o que passámos. Aos restantes,

não podia ter pedido pessoas melhores. Em Coimbra, Lisboa ou noutra parte do mundo, cá estaremos. Adoro-vos a todos do fundo do coração. Não podia faltar um agradecimento à minha 2ª família. João, Helena, Ni e Joana. Obrigada por me terem acolhido, por todas as horas que passámos juntos e por tudo. Ainda hoje sinto falta de sair do trabalho e fazermos noites de jogos. De sair do trabalho e estar convosco. Se deixei algum pedacinho de mim em Coimbra, foram vocês. Foram das melhores coisas que me aconteceram.

A Lisboa, aos meus eternos amigos. Poderia ter pedido pessoas melhores? Ao Carlos e ao Rodrigo. À Santos e à Martins. À Araújo e à Sardinha. À Raposo e ao Jaime Jaime. À Mariya. A tantos outros que também me apoiaram. Obrigada. Do fundo do coração. Sou uma sortuda por vos ter conhecido e por vos ter na minha vida. Manela, Miguel, Kiko e Joana. Obrigada por terem entrado na minha vida e a terem completado. Por serem família e por me apoiarem sempre.

À minha família, a quem devo tudo e nunca me pede nada em troca. Primeiro, ao meu João. Nunca teria conseguido sem ti. Obrigada por todo esforço, pelo compromisso e por nunca me teres deixado desistir. Se consegui dar uma volta à minha vida, a ti o devo. Tenho muito orgulho em ti e em nós. À minha Leonor. A melhor parte do meu dia é chegar a casa e estar contigo. Espero que um dia vejas isto e saibas que o trabalho compensa. A mãe vai estar sempre aqui para ti. À minha mãe. Ao meu mundo. Obrigada. Não tenho palavras que cheguem para agradecer tudo o que fazes por mim. Foste/és e serás sempre o meu exemplo e a minha melhor amiga.

Por último, e mais importante, ao meu pai. Espero que te orgulhes por termos conseguido atingir este objectivo. Se o fiz, foi por ti. Obrigada por teres sido o melhor pai que poderia pedir. A ti, a nós, com todo o carinho e saudade deste mundo.

Obrigada a todos pelo apoio e carinho. Por me terem dado a oportunidade para vos conhecer e aprender convosco. A minha vida não teria sido a mesma.

TABLE OF CONTENTS

TABLE OF CONTENTS

FIGURE AND TABLE LIST

FIGURE LIST

TABLE LIST

ABBREVIATIONS LIST

A
AFM atomic force microscopy
Ala alanine
Arub *Asterias rubens* protein

C
CTL C-type lectin domain
Cys cysteine
C8 conserved cysteine residues

D
DBA ***Dolichos biflorus agglutinin***
Dopa 3,4-dihydroxyphenylalanine
DS Discoidin-like

E
ECL *Erythrina cristagalli* lectin
EGF epidermal growth factor-like

F
FDA food and drug administration

G
GlcNac N-acetylglucosamine
Gly glycine
Glx glutamate
GSL II *Griffonia simplicifolia* lectin II

I
ISH *in situ* hybridization

L
LEL *Lycopersicon esculetum* lectin
LM light microscopy
Lys lysine

M
Man7-OHTrp C2-mannosyl-7-hydroxytryptophan
MCT mutable connective tissue
Mfp mussel foot protein
Mlig-ap *Macrostomum lignano* adhesion protein
Mlile-ap *Macrostomum ileanae* adhesion protein
mRNA messenger ribonucleic acid

P
PHA phaseolus vulgaris lectin
PNA peanut agglutinin-lectin
PSA *Pisum sativum* agglutinin
Pro proline
PTM post-translational modifications
Pvfp *Perna viridis* foot protein

S
SBA Soybean agglutinin
SEM scanning electron microscopy
Ser serine
Spf1 sea star protein footprint 1
SNP single nucleotide polymorphism
STL *Solanum tuberosum* lectin

T
TEM transmission electron microscopy
Thr threonine
TIL trypsin inhibitor-like
Tyr tyrosine

U
Uegf Urinary epidermal growth factor

V
VVL *Vicia villosa* lectin
vWD von Willebrand factor

W
WGA *wheat* germ agglutinin

ABSTRACT

Abstract

Bioadhesion is vital for many aquatic organisms, since it is through the production of adhesive secretions that these animals attach, move and feed in their habitats (Flammang et al., 2016). Currently, the best studied bioadhesives are from organisms that attach permanently (mussels, barnacles) or transitorily (limpets), while little is still known about reversible adhesion (sea urchins, sea stars).

In a recent publication, our lab focused on the characterization of the glycidic fraction of sea urchin adhesives. Simão et al. (2020) analysed the adhesive organs (so-called tube feet, composed by an adhesive disc and a non-adhesive motile stem) and the secreted adhesive (footprint) using a battery of 22 lectins that recognize different glycans. The authors demonstrated the presence of glycoproteins with N-acetylgalactosamine (GalNac, detected by SBA) and N-acetylglucosamine (GlcNac) residues in *Paracentrotus lividus* adhesive disc epidermis and footprint, the later either in its simpler form (detected by GSL II) or in a specific chitobiose arrangement (a dimer of β-1,4-linked glucosamine units; detected by WGA, STL and LEL). LEL staining was particularly interesting, since it labelled what seems to be secretory granules, packed within the ducts of adhesive cells up to the level of the disc cuticle.

The aim of this project was to further investigate these *P. lividus* candidate adhesive/cohesive glycoproteins through (i) lectin pulldowns, taking advantage of their specificities for different glycans; (ii) identification of the pulled-down glycoproteins by mass-spectrometry, making use of the recently published transcriptome specific for *P. lividus* adhesive organs and (iii) select within the identified glycoproteins those that were previously pinpointed as putative adhesive candidates and perform an *in silico* analysis using bioinformatic tools to obtain a more detailed biochemical characterization.

Using this multidisciplinary approach, we pulled down high molecular weight glycoproteins containing GlcNac (simple and chitobiose) and GalNac (SBA). Within these, we identified and characterized five candidate adhesive/cohesive glycoproteins, that according to their biochemical characteristics can be separated as follows: (i) two large negatively charge proteins (Nectin and alpha-tectorin) and a smaller positively charge protein (uncharacterized protein), with a probable adhesive and/or cohesive function, (ii) an alpha-2-macroglobulin enzyme, possibly promoting adhesion/cohesion or having a protective role and (iii) a peroxidase, most likely involved in protein crosslinking, contributing to the cohesiveness of the secreted adhesive.

By providing a deeper characterization of these adhesive/cohesive glycoproteins, this work gives a step forward towards the development of stronger and biocompatible sea urchin-inspired bioadhesives.

Key words: sea urchin; tube feet; bioadhesive; glycoproteins; biomimetic adhesive

Resumo

A bioadesão tem sido descrita como essencial para os organismos marinhos pois é através da produção de secreções adesivas que estes se fixam, movem e alimentam nos seus habitats (Flammang et al., 2016). Atualmente, os adesivos mais estudados são os classificados como permanentes (mexilhão, cracas) ou transitórios (caracóis marinhos). Ainda não se conhece muito sobre os adesivos reversíveis (ouriços e estrelas do mar).

Numa publicação recente, o nosso laboratório caracterizou a fração glicídica dos adesivos dos ouriços do mar. Simão et al. (2020) analisaram os órgãos adesivos (denominados pés ambulacrários - compostos por um disco adesivo e um caule não-adesivo) e o adesivo secretado, recorrendo a uma bateria de 22 lectinas que reconhecem diferentes glícidos. Os autores detetaram glicoproteínas com resíduos de N-acetilglucosamina (GlcNac) na epiderme adesiva e no adesivo de *Paracentrotus lividus*. Este glícido foi identificado na sua forma mais simples (detetado por GSL II) e num arranjo específico (um dímero de glucosamina; detetado por WGA, STL e LEL). A imunomarcação com a LEL mostrou ser a mais específica, marcando estruturas semelhantes a grânulos secretores, empacotados nos ductos das células adesivas até à cutícula do disco.

O principal objetivo deste projeto foi caracterizar as potenciais glicoproteínas adesivas/coesivas através da (i) utilização de lectinas para obter diferentes frações enriquecidas com base na especificidade das mesmas para diferentes glícidos; (ii) identificação por espectrometria de massa das glicoproteínas obtidas em cada fração, tirando partido da existência de uma transcriptoma específico para os órgãos adesivos de *P. lividus* e (iii) seleção dentro das proteínas identificadas, daquelas que apontadas anteriormente como potenciais proteínas adesivas, de forma a realizar uma caracterização bioquímica mais aprofundada das mesmas como base numa análise *in sílico* utilizando ferramentas bioinformáticas.

Esta abordagem multidisciplinar permitiu obter glicoproteínas com elevado peso molecular, com resíduos de GlcNac (simples e em quitobiose) e GalNac. Destas, foi possível identificar e caracterizar cinco proteínas potencialmente adesivas/coesivas, que com base nas suas características bioquímicas podem ser separadas da seguinte forma: (i) duas proteínas grandes carregadas negativamente (Nectina e alfa-tectorina) e uma proteína pequena carregada positivamente (proteína não caracterizada), possivelmente com funções adesivas/coesivas (ii) a enzima alfa-macroglobulina, com uma possível função adesiva/coesiva ou de proteção do adesivo; e (iii) uma peroxidase, muito provavelmente envolvida na polimerização das proteínas do adesivo, contribuindo assim para a sua elevada coesão e insolubilidade.

RESUMO

Este estudo permitiu caracterizar em maior profundidade glicoproteínas potencialmente adesivas/coesivas, dando mais um passo para o futuro desenvolvimento de adesivos mais fortes e biocompatíveis inspirados em ouriços do mar.

Palavras chave: ouriços do mar; pés ambulacrários; bioadesivo; glicoproteínas; adesivo biomimético;

CHAPTER 1

General introduction

1.1. Adhesives

Currently, adhesives are considered as promising candidates over invasive mechanical procedures such as sutures (Ferreira et al., 2008; Vernengo, 2016; Zhu et al., 2018; Jain and Wairkar, 2019; Rathi et al., 2019). They are commercially available and are being used in different medical areas, namely neurosurgery, orthopaedical, periodontal, ophthalmic, cardiovascular, pneumothoracic, gastrointestinal, plastic and reconstructive surgery (Jackson, 2001; Dinte and Sylvester, 2018; Jain and Wairkar, 2019, Ge and Chen, 2020).

Beside sutures, various other materials like microporous surgical tapes, clips and staples are also used in surgeries (Sanders and Nagatomi, 2014). These procedures are easy to handle, have high tensile strength and no allergic or carcinogenic potential. However, they are time-consuming and require penetration of the surrounding tissues, causing additional damage and increasing potential for infection (Reece et al., 2001; Vernengo, 2016; O'Rorke et al., 2017; Xu et al., 2017; Zhu et al., 2018; Jain and Wairkar, 2019; Rathi et al., 2019). Additionally, these techniques are not a suitable solution in some surgical situations such as in friable tissues, minimally invasive surgeries or in large-scale traumas (Vernengo, 2016; Dinte and Sylvester, 2018; Rathi et al., 2019). Therefore, novel developments of suture-less techniques have been conducted to decrease surgeries time and accelerate patients' recovery, while alleviating their pain.

Adhesives use materials of either biological or synthetic origin in the adherence of-or-to biological surfaces (Palacio and Bhushan, 2012; Zhu et al., 2018; Rathi et al., 2019). They also help in attaching medical devices to tissues and post-operative sealing of air or gas leakages through an incision.

Ideally, they should possess strong bonding strength and elasticity, being easy to apply, biocompatible and biodegradable (Ferreira et al., 2008; Xu et al., 2017; Zhu et al., 2018; Jain and Wairkar, 2019; Rathi et al., 2019; Quan et al., 2019). Furthermore, it must act locally, not hindering the process of natural healing (Reece et al., 2001; Sanders and Nagatomi, 2014; Rathi et al., 2019). Depending on their function, they are classified as hemostats, adhesives and sealants (Ferreira et al., 2008; Vernengo, 2016; Dinte and Sylvester, 2018; Richter et al., 2018; Jain and Wairkar, 2019). Hemostats act as a hemostatic agent to form a clot in the presence of blood, while sealants mostly stop fluid leakage from the opening of tissues. Adhesives are responsible to re-approximate injured tissue, like in a wound or incision (Zhu et al., 2018; Richter et al., 2018; Jain and Wairkar, 2019). It has been noted that the same bioadhesive can have multiple actions.

The mechanism of adhesion is primarily based on two interactions viz. chemical and physiological (Jain and Wairkar, 2019; Rathi et al., 2019). The chemical interaction involves the formation of ionic or chemical bonds between the interfaces of adhesives and biological

substrate due to the interaction of different functional groups present in the adhesives (e.g. crosslinking and mechanical interlocking). On the other hand, physiological interaction involves adhesion through physiologically related mechanisms like the blood clotting process. On the basis of the adhesion interactions and the type of material used for the adhesives production, they are classified as synthetic, natural or biomimetic adhesives (Modjarrad and Ebnesajjad, 2013; Dinte and Sylvester, 2018; Ge and Chen, 2020). Their *in situ* application during surgeries or medical interventions depends on the biocompatibility of the used material.

Currently, the most appropriate approach depends on each individual medical situation.

1.1.1. Synthetic based-adhesives

Synthetic polymers, as polyurethanes, polyethylene glycol and cyanoacrylates and its derivatives, are used in the majority of adhesives applied in surgeries (Jain and Wairkar, 2019).

High tensile strength and good mechanical properties are their main advantages (Ferreira et al., 2008; Jain and Wairkar, 2019). However, all of them are considered to have drawbacks regarding toxicity or long-term mechanical performance. They suffer from poor biocompatibility, failing to meet the requirements of many surgical procedures (Zhu et al., 2018; Richter et al., 2018; Balkenende et al., 2019; Jain and Wairkar, 2019; Rathi et al., 2019; Pandey et al., 2020; Ge and Chen, 2020).

Table 1 – Synthetic based adhesives main characteristics | The adhesion mechanism and subsequent advantages and disadvantages are summarized for polyurethane (a polymer composed of organic units joined by urethane links), polyethylene glycol (a polymer formed by ethylene oxide and water) and the cyanoacrylate (different ester of cyanoacrylate acid).

	Adhesion mechanisms	Advantages		Disadvantages	References
Polyurethane	**Network polymerization** due to urea bond formation between adhesive isocyanate groups and amines present in tissue proteins	↑ wettability ↑ elasticity ↑ tissue adhesion	→ adhesion and tensile strength	↑ setting time ↑ toxicity	Ferreira P. et. al (2008); Jain, R. et. al (2019)
Polyethylene glycol	**Mechanical interlocking** due to adhesive fluids absortion and further gel formation	↑ biocompatibility (organic and aqueous solutions) ↑ flexibility		↑ swelling index ↑ degradation (long term use impairment)	Vernengo, A. et. al (2016); Jain, R. et. al (2019); Rathi, S. et. al (2019)
Cyanoacrylate	**Crosslinking or mechanical interlocking** after cyanoacrylates polymerization	↑ wettability ↑ setting time ↓ production cost		↑ toxicity ↑ inflammatory reactions ↑ carcinogenicity	Sanders, L. et. al (2014); Vernengo, A. et. al (2016); Zhu, W. et. al (2018); Jain, R. et. al (2019); Rathi, S. et. al (2019); Pandey, N. et. al (2020)

Recent developments of synthetic adhesives for internal applications have focused on polyethylene glycol and polyurethanes due to the potential risks for infection and cytotoxicity reported for cyanoacrylates (Jackson, 2001; Sanders and Nagatomi, 2014). Biocompatibility, degradability, and tunable mechanical properties are some of their attractive features (Modjarrad and Ebnesajjad, 2013; Sanders and Nagatomi, 2014). A common disadvantage is significant post-polymerization swelling, which can potentially cause compression on surrounding tissues or nerves (Quan et al., 2019). Consequently, their use is mainly restricted

to topical applications, creating the need to look for more biocompatible alternatives, such as natural bioadhesives.

1.1.2. Natural adhesives

Natural adhesives are obtained from biological constituents, being classified as protein-based bioadhesives like collagen and its derivatives, fibrin, gelatin and albumin and polysaccharide-based bioadhesives like chitosan and starch (Zhu et al., 2018; Jain and Wairkar, 2019; Rathi et al., 2019; Ge and Chen, 2020). The majority of these biopolymers mimic the mechanism of blood clotting, either being used directly or in combination with a cross-linking agent that forms covalent bonds with the tissue surface.

Being biodegradable, non-immunogenic and effective in physiological conditions, these types of adhesives can work over a wide range of temperatures, in different environments and under changing physicochemical conditions. Nevertheless, they have a high risk of diseases transmission due to possible contaminations of the blood derivatives present in the products and low tensile strength (Table 2) (Jackson, 2001; Ferreira et al., 2008; Sanders and Nagatomi, 2014; Jain and Wairkar, 2019; Rathi et al., 2019). Both fibrin and gelatin use thrombin pooled from human or bovine blood as cross-linking agent, risking the transmission of bloodborne pathogens and viruses, while albumin has been associated with tissue embolism and pseudoaneurysm (Spotnitz and Burks, 2008; Jain and Wairkar, 2019). Gelatin crosslinking can also be achieved with aldehydes and photochemical or enzymatic reactions (Vernengo, 2016; O'Rorke et al., 2017; Jain and Wairkar, 2019). Regarding collagen-based bioadhesives, their medical application is limited due to a swelling effecting resulting in tissue compression. Chitosan, due to its poor water solubility, hasn't been commercialized to a larger extent.

Table 2 - Natural based adhesives main characteristics | The adhesion mechanism and subsequent advantages and disadvantages are summarized for fibrin (a non-globular protein polymerized due to fibrinogen cleavage), collagen (an ECM structural protein) gelatin (derived from collagen hydrolysis), albumin (a globular protein) and chitosan (a polysaccharide composed by glucosamine - acetyl and deacetyl units.

	Adhesion mechanisms	Advantages	Disadvantages	References
Fibrin	**Fibrin crosslinking** by thrombin-catalysed cleavage of fibrinogen into fibrin, further polymerized forming insoluble clots	↑ biocompatibility	↑ risk of blood diseases transmission ↓ mechanical strength and adhesion (wet environment)	Weisel, J. W. (2005) Wesley, K. (2008) Jain, R. et al (2019) Rathi, S. et al (2019)
Collagen	**Crosslinking** by coagulation pathway activation due to blood and coagulation products adsorbed into the applied collagen fibers	↑ biocompatibility ↓ risk of diseases transmission	bioadhesive swelling due to tissue compression	Spotnitz, W. (2008) Jain, R. et al (2019) Rathi, S. et al (2019)
Gelatin	**Gelatin crosslinking** by thrombin-catalysed chemical gelation of the in situ gel formed upon hydratation	In situ gel formation ↑ biocompatibility	↑ risk of blood diseases transmission	Jain, R. et al (2019) Rathi, S. et al (2019)
Albumin	**Tissue crosslinking,** forming a mechanical seal independent of the blood coagulation process	↑ adhesion strength ↑ biocompatibility	associated to embolism and pseudoaneurysm	Xu, K. et al (2017) Rathi, S. et al (2019)
Chitosan	**Adhesive/tissue electrostatic atraction**, due to bond between a chitosan amino group and collagen tissue	↑ biodegradability ↑ biocompatibility	↓ water solubility	Jain, R. et al (2019)

Since fibrin and other extracellular matrix (ECM) components-based products are mostly derived from mammalian tissues, they have limited availability and higher production costs than synthetic ones (Modjarrad and Ebnesajjad, 2013; Sanders and Nagatomi, 2014).

1.1.3. Biomimetic adhesives

In nature, organisms have developed a diversified pool of survival strategies, based on mechanical (e.g. hooks, suckers or friction devices) or chemical principles (e.g adhesives). Biological adhesives present several advantages compared with other attachment systems as i) being able to bind surfaces with various chemistry and roughness ii) joining dissimilar materials and iii) improving stress distribution in the joint (Hennebert et al., 2015).

Due to these attractive features, basic science research has been elucidating animals' highly-evolved adhesion mechanisms to incorporate these chemical and physical strategies into medical adhesives, also known as biomimetic adhesives (Favi et al., 2012; Balkenende et al., 2019).

Currently, the majority of the engineered adhesives in the market exploit tissue/adhesive non-specific interactions (e.g van der Waals). Nonetheless, these adhesive interactions are dramatically weakened in the presence of the high dielectric and ionic strength of physiological fluids (Lee et al., 2011; Favi et al., 2012; Zhu et al., 2018; Guo et al., 2020). To overcome these limitations, marine adhesion is assuming increasing importance in providing model systems for mimicking wet adhesion (Favi et al., 2012; Waite, 2017; Lengerer et al., 2018; Balkenende et al., 2019; Almeida et al., 2020). Due to the different factors impacting marine adhesives composition and functioning (e.g evolutionary background, species biology and environmental constraints), the merge of these strategies into medical adhesives offers a tremendous opportunity to address unmet clinical challenges.

Mussels' permanent adhesion is arguably the most well-studied and emulated marine adhesive system (Waite, 2017; Balkenende et al., 2019). Its adhesive strategy is mediated by Dopa-mediated interfacial bonding, a catecholic amino acid, L-3,4-dihydroxyphenylalanine (Dopa), present in mussel adhesive proteins (MAP's) secreted during the adhesion process (Waite, 2017; Pandey et al., 2020; Guo et al., 2020). The combination of these catecholic moieties and diverse synthetic and natural polymers has inspired biomimetic adhesives with greater biocompatibility and adhesion strength, comparing with synthetic and natural adhesives (Favi et al., 2012; Pandey et al., 2020). However, catecholic groups generally suffer from oxidation in neutral and basic conditions, which significantly undermines adhesion strength, limiting their practical applications. Thus, the control of catechol redox chemistry is necessary for the modulation and optimization of Dopa-based adhesive properties. While mussels deliberately control the redox environment of the adhesive pad, regulating the inner adhesion and cohesion of the secreted proteins, we still lack a complete understanding of the mechanisms involved in this process. As such, achieving such redox balance in the catechol-

functionalized polymeric systems is still a tough problem and needs further investigation. Currently, mussel inspired adhesives do not have the ability to control the oxidation of Dopa or catecholic side groups grafted on polymers backbone, making these groups susceptible to uncontrollable oxidation and thus limiting their adhesiveness.

Up to now, the development of mussel-mimetic adhesives has generally focused on the catechol chemistry, but the biological system is far more complex. In natural MAP's, other amino acids residues (e.g cationic, anionic, hydrophobic and thiol groups) also contribute to the strong interfacial binding of mussels to a variety of surfaces, by maintaining a balance of different interactions. The synergetic effect between catecholic and cationic moieties in the mussel adhesion system awaits further investigation. Having this in consideration, despite the possible different applications, as tissue engineering, cellular engineering, drug delivery and surgical glues, this type of adhesives still has many drawbacks. No mussel-inspired bioadhesive has been approved by the FDA or is reported in clinical trials.

Other adhesives have gained increased interest in view of biomimetics as they have distinctive characteristics from those found in mussel adhesives or, being similar, can fill in the understanding of adhesive processes. The type of adhesion (e.g. permanent or reversible) is also relevant for the type of the developed adhesive and their biomedical applications.

Since the existent synthetic homologs insufficiently mimic the underwater properties of natural glues, a deeper understanding of the biological complexity of the bioadhesive composition and deposition is crucial in the preparation of the next generation of biomimetic adhesives.

1.2. Marine adhesion

Biological adhesion is a prerequisite for many organisms to accomplish critical tasks of life. Adhesion-related morphology, behavior and secretions are thus involved in a diverse array of ecological processes including, but not limited to, attachment to surfaces, locomotion, prey capture, building and defense (Clarke et al., 2020). Among the marine organisms that produce bioadhesive to attach permanently (e.g. mussels and barnacles) or reversibly (e.g. most echinoderms). Echinodermata have progressively gained relevance in adhesion studies, since most species of this phylum produce reversible adhesive secretions (Flammang, 2016; Lengerer et al., 2018; Wunderer et al., 2019; Federle and Labonte, 2019; Almeida et al., 2020;).

1.2.1. Echinoderms

There are five extant classes of echinoderms: Crinoidea (sea lilies and feather stars), Ophiuroidea (basket star), Asteroidea (sea stars), Echinoidea (sea urchins) and Holothuroidea (sea cucumbers) (Figure 1).

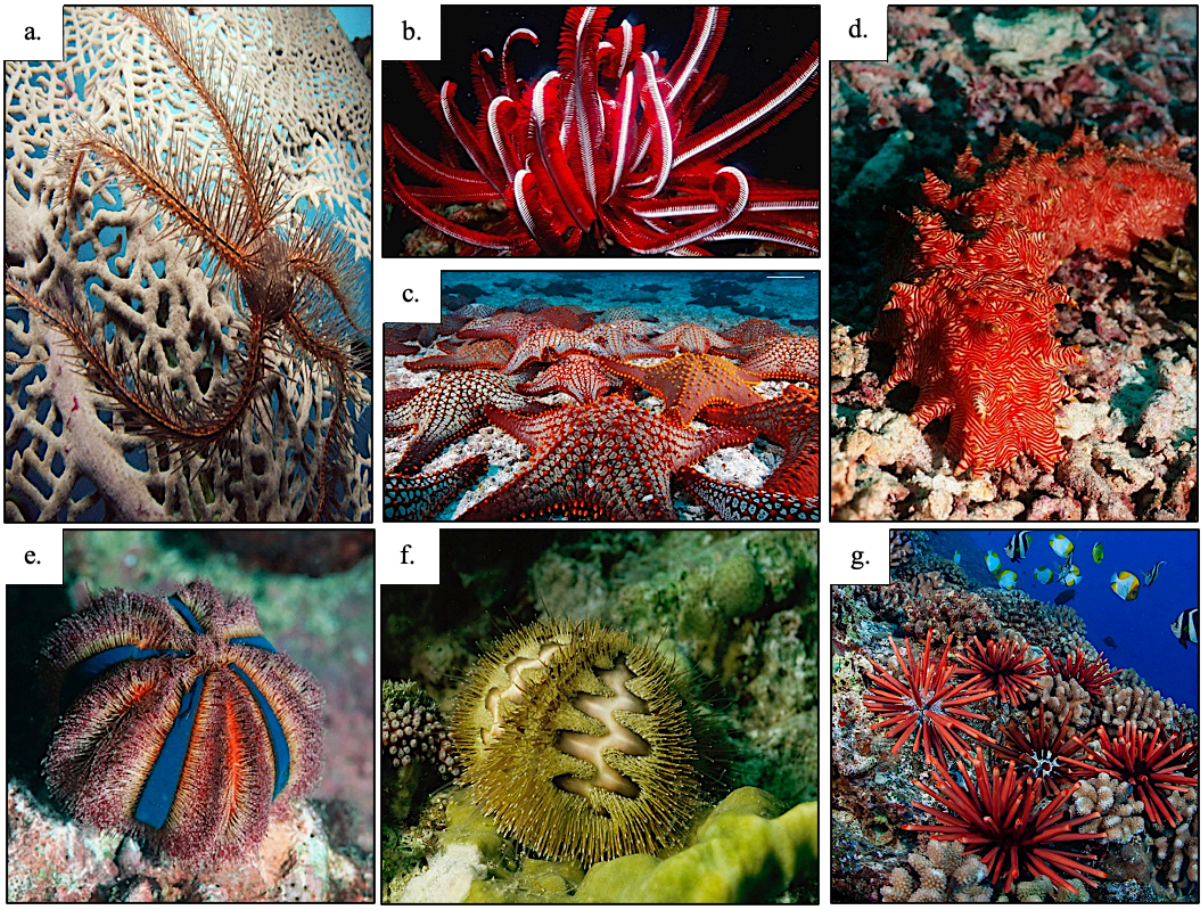

Figure 1 – Representative species of the five extant classes of echinoderms | a. Class Ophiuroidea, species *Gorgonocephalus caputmedusae* (common name: basket star). Only the larvae stage presents an external pentamerous radial symmetry, being the adult stage characterized by a bilateral symmetry. **b.** Class Crinoidea, species *Comanthus bennetti* (common name: feather star). Despite the pentameric pattern present in this class, the five characteristic arms are subdivided. **c.** Class Asteroidea, species *Pentaceraster cumingi* (common name: sea stars or starfish). **d.** Class Holothuroidea, specie *Thelenota rubralineata* (common name: sea cucumber). **e - g.** Class Echinoidea, species *Mespilia globulus*, (**e.**) *Microcyphus rousseaui* (**f.**) and *Heterocentrotus mammillatus* (**g.**) (common name: regular sea urchins) Adapted from National Geographic archive

The most striking characteristics of these groups are the pentamerous radial symmetry, the endodermal calcareous skeleton and the water-vascular system, a unique system of coelomic canals and surface appendages (Flammang, 2016; Zueva et al., 2018). Regarding the pentameric pattern, this is visible both externally (e.g. five ambulacral and interambulacral areas in sea urchins) and internally (e.g. five gonads).

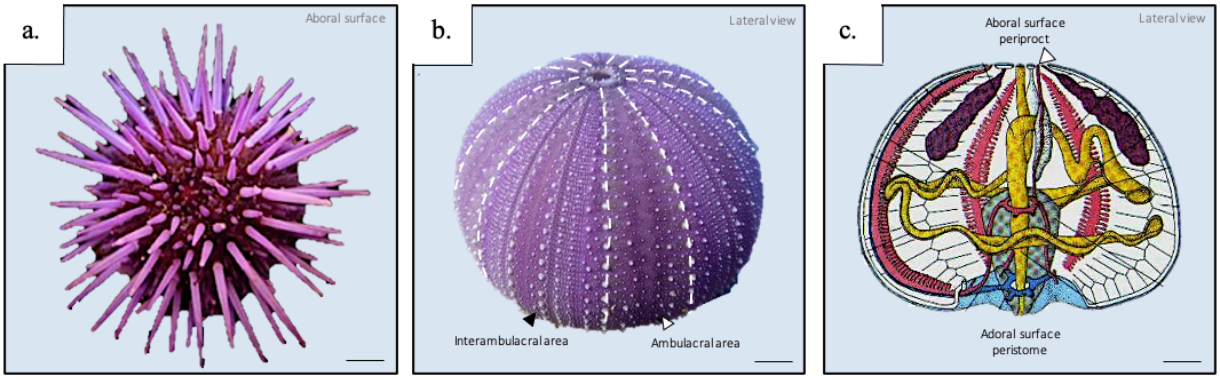

Figure 2 – Structural features of the Phylum Echinodermata | a – b. Sea urchin *Strongylocentrotus purpuratus* external morphology. **a.** *Strongylocentrotus purpuratus* aboral view. In this species, the spines don't show a specific spatial distribution, being spread all around the sea urchin test. **b.** Lateral view of *S. purpuratus* skeletal morphology. The skeleton, also known as test, consists of a number of plates, arranged in rows, also known as ambulacral zones (white arrow) which alternate with interambulacral zones (black arrow). The ambulacra (areas where the tube feet emerge through ambulacral pores) are outline in white. **c.** Representation of a sea urchin internal morphology (lateral view). All the systems are represented in the scheme. The nervous system is formed by five radial nerve cords, that innervate the tube feet, which converge to a ring (represented in blue). Reproductive system is formed by five gonads (in purple), located under the interambulacral zones. Digestive system (in dark yellow) consists in a coiled tube, joining the adoral mouth (facing the substrate) to the aboral anus. The ambulacral system, formed by radial and lateral canals and a ring canal, depends on the action of the ambulacral fluid hydrostatic pressure, regulated by ciliated pores in the madreporite plaque (white arrow). The madreporite functions as a pressure-equalizing valve, responsible for controlling the fluid volume in the water vascular system. (Original artwork)

The adult echinoid nervous system comprises five radial nerve cords, joined at their base, forming a ring surrounding the mouth (Figure 2 c.) (Burke et al., 2006; Franco et al., 2011). Each segment of the radial nerve cords contains a layer of neurons, innervating the external appendages (e.g. tube feet, spines and pedicellariae). This merge allows the tube foot to perform controlled and synchronized movements in a nervous stimuli response.

The reproductive system contains five gonads, displayed under the interambulacra. Each gonad has a single duct, opening in a genital plaque, as a gonopore. These five genital plaques and a modified plaque (madreporite), all surrounding the anus, form the periproct. These organisms are dioecious, with external fertilization.

The digestive system consists of a coiled tube, joining the adoral mouth to the aboral anus. A powerful teeth apparatus known as the Aristotle's lantern surrounds the mouth, being used to scrape algae and other food from rocks and even, in some sea urchins, to excavate hiding places in coral or rocks. The area comprising the mouth and Aristotle's lantern is known as peristome.

The ambulacral system, being a hydraulic system, depends on the action of the ambulacral fluid hydrostatic pressure. The ring canal, surrounding the esophagus, distributes the ambulacral fluid to the five radial canals (Figure 2 c.). These canals, underneath the ambulacral zones, deliver the fluid to all tube feet. Each tube foot has a small muscular sac, the ampulla, responsible for tube foot mobility. Tube foot can i) protract, resulting in the tube foot extension, ii) flex, leading to tube foot bending and iii) retract, by the contraction of the

tube foot longitudinal retractor muscle (see section 2.1.1. for further insights about tube foot histology). To protract, ampulla muscles contract, forcing the ambulacral fluid into the tube foot lumen, inducing gradual stretching of the adhesive organ. To retract, tube foot retractor muscles contract, expelling the ambulacral fluid back into the ampulla. When there is a differential contraction of these muscles, the tube foot bends to the more contracted side (Flammang, 1995). The tube feet, also named as the external appendages of the water-vascular system, are specialized organs responsible for the production of the adhesive secretions.

Although tube feet are present in every extant echinoderm species, only those of asteroids and regular sea urchins have been studied in detail in terms of adhesion.

1.2.1.1. Sea urchin tube foot morphology and structure

Tube feet have diversified into a variety of morphotypes (Flammang, 1995). Nevertheless, despite tube feet highly variable shapes, the disc-ending morphotype is the most interesting one in terms of adhesion (Flammang, 1995, 2016). For asteroids and regular sea urchins, Santos el al. (2006) reported tenacity values (adhesive force per unit area) similar to permanent adhesives (e.g. barnacles and mussels) (Waite, 2002; Holm et al., 2005; Matranga, 2005; Santos et al., 2005b; Santos and Flammang, 2006, 2008). Both echinoderm classes demonstrated superior tenacity values when compared with some bioadhesives currently on the market (Supplementary Table 1).

Disc-ending tube foot, consist on an enlarged and flattened distal extremity (disc) which makes contact with the substratum, and a proximal extensible cylinder (stem) that connects the disc to the test (Figure 3 a.) (Santos et al., 2005b; Almeida et al., 2020; Simão et al., 2020). Both the stem and the disc contain four tissue layers: an inner myomesothelium surrounding the water-vascular lumen, a connective tissue layer, a nerve plexus and an outer epidermis covered externally by a cuticle (Figure 3 b – c.) (Santos et al., 2005a, 2005b; Hennebert et al., 2011; Flammang, 2016; Lengerer et al., 2018; Simão et al., 2020). This histological structure is remarkably constant among Echinodermata tube feet, independently of the morphotypes (Santos and Flammang, 2005; Hennebert, 2010). In sea urchins, interspecific differences were described at the ultrastructural level (skeletal elements and secretory granules), but no relationship could be established with tube foot adhesive strength or the species habitat (Santos and Flammang, 2006, 2012).

At the level of the tube foot disc, the previously mentioned tissues are specialized for strong attachment. Both the connective tissue layer and the nerve plexus are thickened, and the epidermis is differentiated into a well-developed sensory-secretory epithelium. Externally, the epidermis is covered by a glycocalyx, the cuticle (also known as the “fuzzy coat”) (Ameye et al. 2000).

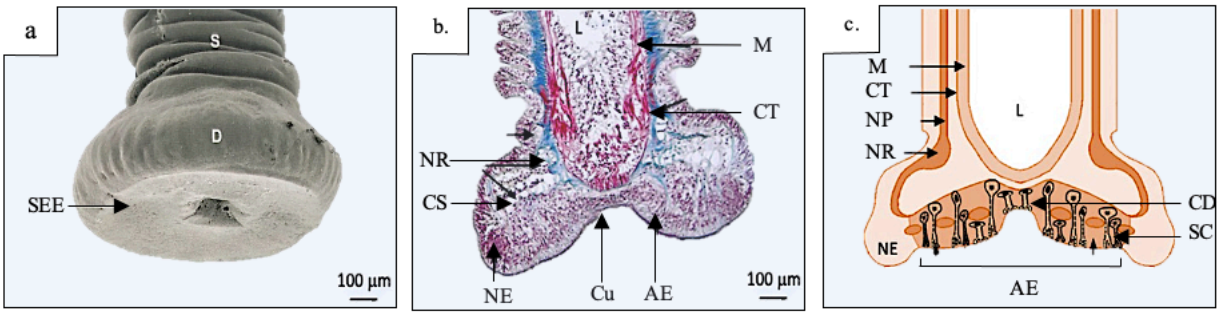

Figure 3 - Morphology and structure of the sea urchin *Paracentrotus lividus* tube foot | a. SEM photography of a disc-ending tube foot. **b.** Masson's trichrome staining of a disc-ending tube foot longitudinal section, distinguishing the myomesothelium (in red) from connective tissue (in blue). Epidermis is stained in pink. **c.** Schematic representation of a disc-ending tube foot longitudinal section, from a regular echinoid. **|** Abbreviations**:** AE, adhesive epidermis; CD, central depression; CS, calcareous skeleton; CT, connective tissue; Cu, cuticle; D, disc; L, lumen of the water-vascular system; M, myomesothelium; NE, non-adhesive epidermis; NP, nerve plexus; NR, nerve ring; S, stem; SC, secretory cells; SEE, sensory-secretory epidermis. Adapted from Matranga et al. 2005, Pjeta et al., 2020.

Myomesothelium comprises two main cell types, peritoneocytes and myocytes. Myocytes, due to their contractile activity, form the retractor muscle of the tube foot, enabling it to retract and extended. Peritoneocytes, monociliated cells situated apically in the epithelium, have phagocytic activity and dedifferentiation capacity during muscle regeneration. In an injury scenario, dedifferentiation is possible since both types of cells are successive stages of specialization of a single cell type, the epithelial cell of coeloms (García-Arrarás, 2010). Despite the absence of motor neuron-skeletal muscle junctions, studies have indicated a neural control of the contractile tissue through the release and diffusion of neurotransmitters (Flammang, 1995; Murray and García-Arrarás, 2004; Dolmatov et al., 2006; Elphick et al., 2015; Díaz-Balzac and Abreu-Arbelo, 2010; García-Arrarás, 2010; Kim et al., 2016).

Also under nervous system control, is the connective tissue, whose mechanical properties (extensibility, tensile strength, stiffness and toughness) can undergo reversible changes (Charlina et al., 2009; Ribeiro et al., 2011; Sugni et al., 2014; Motokawa and Fuchigami 2015; Mo et al., 2016). Being a mutable connective tissue (MCT), it deforms during tube foot protraction, flexion and retraction and it stiffs during attachment, allowing the tube foot to resist the hydrodynamic forces. It's composed by collagen fibers of varying sizes, conformation and spatial arrangement. Surrounding these collagen fibers, an elastomeric network of fibrillin microfibrils conserves the collagen fibrils organization when the tube feet is in motion. This allows the connective tissue to sustain the diameter of the tube foot, maintaining the hydrostatic pressure in the disc (Flammang, 1995; Santos and Flammang, 2005; Santos et al., 2005b). At the disc level, the connective tissue forms a circular plate, reinforcing the disc epidermis. It's known as terminal plate, having an asymmetric distribution throughout the disc. It forms a thinner layer in the center of the foot, while it encloses a

supportive calcified skeleton, in the periphery. This skeleton is made of two superposed structures, a distal rosette and a proximal frame, arranged in a circle around the lumen (Santos and Flammang, 2012). Both structures are connected to the muscular tissue previous described.

In general, the disc epidermis consists of four cell categories: support cells, sensory cells, non-ciliated adhesive secretory cells and ciliated de-adhesive secretory cells (Flammang et al., 1994). These epidermal cells usually occur in clusters, being separated by connective tissue protrusions (Figure 4 a.). The periphery of the disc, due to the absence of secretory cells, is called non-adhesive epidermis, and has a predominantly sensory role.

Secretory cells are generally flask-shaped, formed by an enlarged cell body and a long apical process that reaches the cuticle at the disc surface. In sea urchins, these processes are arranged in a tuft at the cell apex. The secreted granules show interspecific variations, depending only on the ultrastructure of their contents (Santos and Flammang, 2006). According to Santos et al. (2006), two broad groups of adhesive granules may be recognized in sea urchins. Bigger homogeneous electron-lucent granules (500 – 700 nm in diameter) in the central part of the disc and smaller heterogenous electron-dense granules (300 - 500 nm in diameter), in the remaining adhesive epidermis. So far only one species, *Paracentrotus lividus*, was shown to possess two types of adhesive granules (Figure 4 b – c.). Other investigated species possess only dense-cored adhesive granules. On the other hand, de-adhesive cells are filled with small homogeneous electron-dense secretory granules whose ultrastructure is remarkably constant in all the species (Santos and Flammang, 2006).

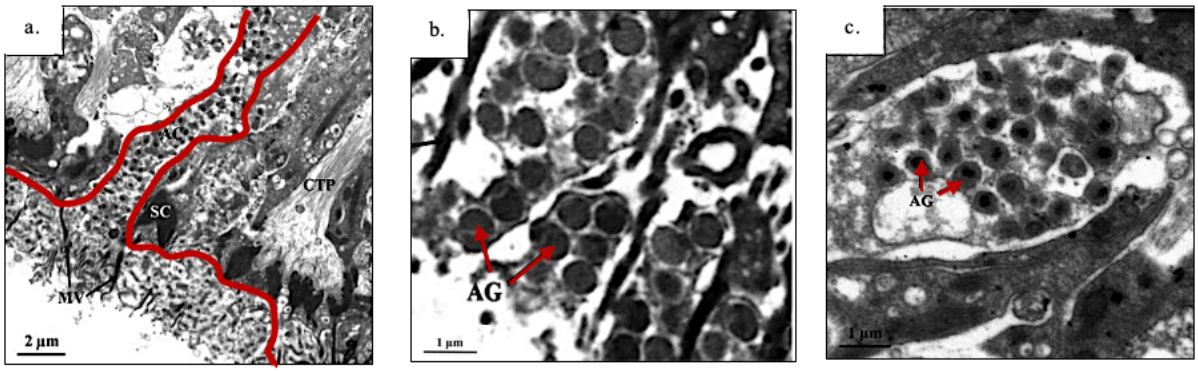

Figure 4 - Secretory granules ultrastructure in *Paracentrotus lividus* tube foot disc | a. SEM photography of a disc-ending tube foot longitudinal section. The tuft adhesive secretory cells, contoured in red, contain large spherical secretory granules in the cytoplasm. **b.** Adhesive granules close-up, in the central depression of the disc adhesive epidermis. The granules present a homogeneous electron-lucent appearance. **c.** Adhesive granules close-up, in the remaining adhesive epidermis of the disc. The granules present a heterogenous electron-dense appearance, consisting in a very electron-dense small core, surrounded by an electron-lucent ring-like. **|** Abbreviations: AC, adhesive secretory cell; AG, adhesive granules; CTP, connective tissue protrusion; MV, microvillar-like projection; SC, support cells; Adapted from Santos and Flammang, 2006.

These two cell types form a duo-glandular adhesion system, in which the adhesive secreted by the adhesive cells attaches the tube foot to the substrate and later on the tube foot is released enzymatically by the de-adhesive secretion, leaving a circular adhesive

footprint attached on the substrate (Kamino, 2008; Hennebert et al., 2011; Hennebert et al., 2012; Lengerer et al., 2018; Lengerer and Ladurner, 2018; Simão et al., 2020; Almeida et al., 2020).

1.2.1.2. Sea urchin adhesive footprint characterization

In both sea stars and sea urchins, the adhesive footprints have the same shape and diameter as the distal surface of the tube foot discs. Light microscopy (LM), scanning electron microscopy (SEM), transmission electron microscopy (TEM) and atomic force microscopy (AFM) studies have shown that the adhesive material in sea urchins always appears as a foam-like or sponge-like material made up of a meshwork of entangled globular nanostructures (Flammang, 2016; Hennebert et al., 2014). This structural organization results from the secretory cell apex tuft arrangement.

Biochemical composition of the sea urchin footprints has also been characterized. The first study on the sea urchin *Paracentrotus lividus*, by Santos and colleagues (2009), revealed a significant amount of inorganic residues (45.5%) and a considerably lower amount of proteins (6.4%), neutral sugars (1.2%) and lipids (2.5%).The obtained results were similar to the biochemical composition of sea star *Asterias rubens* footprints, reported by Flammang et al. (1998). Since the footprint material is highly insoluble, there was still a large portion (44.4%) to be characterized. In this unknown fraction, Santos et al. (2009) proposed the existence of amino sugars (e. g. N-*acetyl*-glucosamine*,* N-*acetyl*-galactosamine and sialic acid) and uronic acid, as already described in the sea star *A. rubens* (Flammang et al., 1998).

The protein moiety of *P. lividus* footprint shows a clear predominance of six amino acids, glycine (Gly), alanine (Ala), valine (Val), serine (Ser), threonine (Thr) and glutamate (Glx), that together constitute more than half of the total residues. It has also been reported to contain a higher amount of proline (Pro) and cysteine (Cys) than average eukaryotic proteins. These amino acids seem to have a crucial role in i) adhesion, since the identified charged and polar amino acids can establish hydrogen and ionic bonding or electrostatic interactions with different substratum and in ii) cohesion, where the cysteine residues could be involved in intermolecular disulfide bonds reinforcing the cohesive strength of the adhesive.

1.2.1.3. Proteins identification and role in sea urchin adhesion

The protein fraction has been the subject of several studies, that pin-pointed adhesion-related candidates. In *P. lividus*, proteome analysis of the tube foot disc and the adhesive secretion indicated 328 non-redundant disc-specific proteins of which 163 were highly overexpressed (Santos et al., 2009; Santos et al., 2013; Lebesgue et al., 2016). However, since there were no protein sequencing database of *P. lividus* tube feet available at the time,

the mass spectrometry-derived peptides were mapped to publicly available sea urchin protein databases. This approach only allowed the identification of highly conserved proteins. The only adhesion-specific protein detected by Santos and colleagues (2013) was *P. lividus* Nectin, a glycoprotein previously reported to be involved in *P. lividus* embryos substrate adhesion, during development (Matranga et al., 1992). This protein has 108.3 kDa, can form dimers, presents phosphorylated and glycosylated isoforms and contains six discoidin-like (DS) domains, that can bind to molecules bearing galactose and *N*-acetylglucosamine residues (Matranga et al., 1992; Santos et al., 2013; Toubarro et al., 2016; Sungjo Park et al., 2017). In adult *P. lividus* tube feet, two isoforms were reported (variant 1 and 2), differing in 15 amino acids. Both variants, possess the same structural motifs, being most likely the result of nucleotide substitutions (SNPs) during DNA replication due, for example, to high gene expression (Santos et al., 2009; Costa et al., 2010; Toubarro et al., 2016; Lebesgue et al., 2016). *P. lividus* Nectin is expressed in the disc adhesive epidermis, cuticle and adhesive footprint (Toubarro et al., 2016). Our lab recently provided additional evidences regarding Nectin adhesive and nano-mechanical properties, reporting the first successfully production of a sea urchin biomimetic recombinant adhesive protein (Batista et al., 2020).

Pjeta and colleagues (2020) recently sequenced and annotated a *P. lividus* tube feet-specific transcriptome. Combining transcriptomics, differential gene expression, re-mapping of proteomic data and *in situ* hybridization (ISH), the authors pin-pointed 16 adhesion-related transcripts (Nectin included), of which six had an orthologous sea star adhesion-related gene (Table 3) (Lengerer et al. 2019).

Table 3 – Molecular features of selected adhesion candidate genes identified the sea urchin *Paracentrotus lividus* | Abbreviations: A2M – alpha macroglobulin domain; C8 – cysteine-rich domain; DS – discoidin- like (F5/8 type C) domains; EGF – EGF-like calcium-binding domain; TIL – trypsin inhibitor-like; VWD – von Willebrand domain.

	Homology (identity)	Domains	Function
TR60905_c1_g1_i1	**Nectin** (99%) and Arub-27 (56.3%)	DS	Adhesive and/or cohesive protein
TR63383_c2_g1_i1	**Alpha-tectorin** (76.2%), Spf1 (50%), Arub-4, -10 and -25 (26.7%, 51.3% and 51.4%)	vWD, C8,CBD, TIL and EGF	Adhesive and/or cohesive protein
TR43200_c3_g1_i5	**Cephalochordate hypothetical protein** (62.5%) and Arub-11 (32.4%)	TIL	Cohesive protein
TR57217_c2_g1_i1	**Myeloperoxidase** (68.4%) and Arub 39.9%)	-----	Cohesive protein
TR63654_c4_g1_i1	**Neurogenic locus notch homologue protein** (77%), Arub-1, -6, -20 and -24 (40.6%, 56%, 46% and 34.6%)	C1r/C1s, Uegf, Bmp1 (CUB) and calcium-binding EGF	-----
TR61622_c8_g1_i2	**α-2-macroglobulin-like protein** (68.2%) and Arub-13 (35.8%)	A2M	Adhesive protein

These transcripts were identified as Nectin, alpha-tectorin, uncharacterized protein, myeloperoxidase, neurogenic locus notch homologue protein and alpha-macroglobulin.

Bioinformatic analysis showed that these transcripts present several domains which are recurrent in sea star and other marine adhesives (see 2.2. Glycosylation in non-echinoderms for further information), supporting the adhesive role of these novel sea urchin protein candidates.

Transcript TR60905_c1_g1_i1, showed a high similarity with Nectin (99% identity with variant 2). Discoidin-like domains (DS), present in Nectin, have also been described as one of the domains existent in Spf1, the first protein characterized in sea star *Asterias rubens* (Hennebert et al., 2014). Up to now, DS and galactose-binding lectin domains are considered the best candidates to promote interactions between Spf1 and the cuticular carbohydrate residues (Baumgartner et al., 1998; Tateno 2010). This large multimodular protein is conserved among distantly related sea stars, regardless of the habitat and tube feet morphotype, suggesting Spf1 role in sea star footprint cohesion (Lengerer et al. 2019). As such, Pjeta and colleagues (2020) hypothesized that Nectin is also a cohesive protein, binding to free or conjugated galactose and *N*-acetylglucosamine residues within the adhesive material and/or glycans at the disc cuticle. However, an adhesive role can't be discarded, since native Nectin is secreted into the adhesive footprint (Lebesgue et al., 2016) and recombinant Nectin has shown to retain adhesiveness (Batista et al., 2019).

Galactose-binding lectin domains were found in the TR63383_c2_g1_i1 transcript. It was identified as sea urchin alpha-tectorin, sharing partial sequence homologies with sea star Sfp1. Von Willebrand factor type D domains (vWD), cysteine-rich domain (C8), galactose-binding lectin domains (CTL), trypsin inhibitor-like cysteine rich domains (TIL) and EGF-like calcium binding domains (EGF) were described for this transcript and seem to be recurrent in other marine adhesive/cohesive proteins (e.g. sea stars and flatworms), being largely associated with protein- and carbohydrate-binding functions (Wunderer et al. 2019).

Transcript TR43200_c3_g1_i5 is homologous not only to a cephalochordate hypothetical protein, but also to the sea star Arub-11. All of these proteins possess trypsin inhibitor-like cysteine-rich domains (TIL) associated with footprint insolubility and cohesive strength. These particular domains typically contain ten cysteine residues that form five disulphide bonds, which is consistent with high cysteine levels reported for sea urchins and sea stars adhesive secretions (2.6% and 3.2%, respectively) (Santos et al., 2009; Flammang, 2016).

Transcript TR57217_c2_g1_i1, is similar to sea urchin myeloperoxidase, as well as sea star Arub-30. Peroxidases have been proposed to catalyze protein crosslinking within the adhesive, contributing to its high cohesive strength (Pjeta et al., 2020).

Transcript TR63654_c4_g1_i1, was identified as sea urchin neurogenic locus notch homologue protein, but also shares some homology with sea star Arub-1, -6, -20 and -24. These sea star transcripts are associated with calcium ion and protein binding abilities, complement C1r/C1s, Uegf, Bmp1 (CUB) and calcium-binding EGF-like domains, which have calcium ion and protein binding abilities.

Transcript TR61622_c8_g1_i2 has homology with sea urchin alpha-2-macroglobulin-like protein and sea star Arub-13. Alpha-2-macroglobulin-like proteins are usually extracellular and alpha macroglobulin domains (A2M) have been previously identified in barnacle cyprid larvae adhesive glycoproteins (SIPC and MULTIFUNCin) (Dreanno et al. 2006; Ferrier et al. 2016).

The identification of several proteins involved in sea urchins adhesives is further corroborated by the multi-proteinaceous nature of other reversible adhesives from sea stars (Hennebert et al., 2014) and flatworms (Wunderer et al., 2019).

These six transcripts exhibited an identical ISH expression pattern consistent with the location of the adhesive secretory cell bodies (Figure 5). All the transcripts were differentially expressed in the discs and could be found in the disc and adhesive secretion proteome datasets.

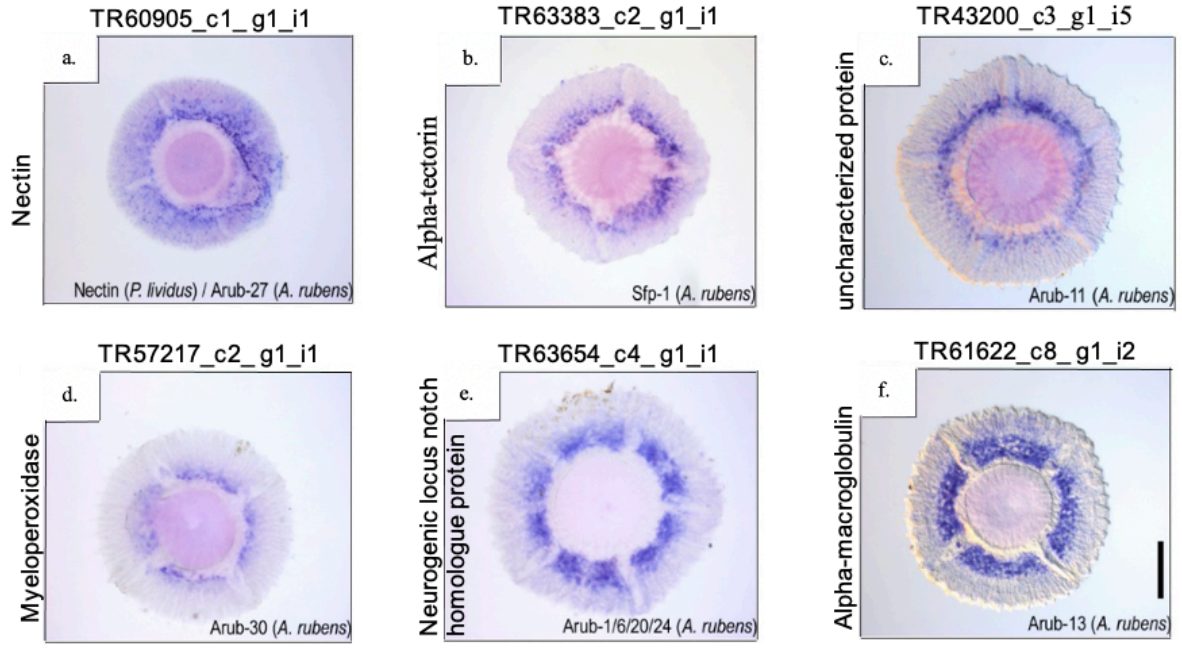

Figure 5 - *In situ* hybridisation expression patterns of selected adhesion candidate transcripts previously identified in the sea urchin *Paracentrotus lividus,* that have orthologous adhesion-related genes in the sea star *Asterias rubens* | Whole mount *in situ* hybridization, showing a pronounced ring-shaped labelling of the tube foot disc, consistent with the location of adhesive secretory cell bodies. Both the transcript (top part) and the respective BLAST hit for each transcript (left part) are shown in each image. Orthologues, identified in the sea star *Asterias rubens,* are shown on the bottom right of each image. Adapted from Pjeta et al. 2020

1.2.1.4. Glycans identification and role in sea urchin adhesion

Compared with the previously described protein fraction, the glycosidic fraction has received much less attention in *P. lividus*. Nevertheless, glycoproteins have been implicated in aquatic adhesion processes in a variety of organisms (see 2.2. Glycosylation in other marine organisms for further details).

The role of glycosylation in marine adhesives is still speculative, but has been proposed to increase conformational stability, enhance protein binding ability, and make proteins more resistant to degradation (Zhao et al., 2009; Roth et al., 2012; Wunderer et al., 2019). Yet, its already known that post-translational modifications (PTM) are responsible for the physico-chemical properties of the adhesive proteins and that among them, glycosylation leads to a higher degree of structural complexity (Nilsson, 2003; Sagert et al., 2006; Gabius et al., 2011; Hennebert et al., 2011; André et al., 2015). These molecular features directly impact several important characteristics of marine adhesives to act as an effectively holdfast, such as, the ability to display water from the substrate, spread, and rapidly form strong adhesive bonds with the surface; as well as, the ability to cure and resist microbial degradation (Kamino, 2008; Hennebert et al., 2011).

In a recent study, our lab focused in characterizing the glycans that compose sea urchin adhesives, complementing the earlier quantification of footprint neutral sugars performed by Santos and colleagues (2009). Using a battery of 22 lectins and three complementary assays (e.g lectin histochemistry, enzyme-linked lectin assay and lectin blotting), Simão et al. (2020) i) identified and localized glycans in *P. lividus* tube feet sections and in the adhesive footprint, proving the involvement of glycans in sea urchins adhesion, ii) quantified the glycan residues in the adhesive disc and ii) differentiated between free and conjugated glycans, attesting the existence of glycoproteins in sea urchins adhesives.

Simão and colleagues (2020) showed that N-acetylglucosamine (GlcNac) is present in *P. lividus* adhesive epidermis and footprint. It was identified in its simpler form by *Griffonia simplicifolia* lectin II (GSL II) and in a specific chitobiose arrangement (a dimer of β-1,4-linked glucosamine units), by *wheat* germ agglutinin (WGA), *Solanum tuberosum* lectin (STL) and *Lycopersicon esculetum* lectin (LEL) (see Table 4 for sugar specificities).

Table 4 – Lectins successfully bond to glycan residues in adhesive epidermis and footprint of *Paracentrotus lividus* | Glycans can bind covalently to different protein residues. While N-glycans attach to asparagine (Asn) residues by a N-glycosidic bond, O-glycans are linked to serine (Ser) and threonine (Thr) residues.

	Lectin	Sugar specificity	Glycosylation	Spatial localization
GSL II	*Griffonia simplicifolia* lectin II	α- and β- *N*-acetylglucosamine	N-glycan (Asn)	adhesive epidermis
WGA	wheat germ agglutinin	chitobiose (up to two units)		adhesive epiderms and cuticle
STL	*Solanum tuberosum* lectin	chitobiose (up to three units)		adhesive epidermis and cuticle (more intense in the central zone of the disc)
LEL	*Lycopersicon esculetum lectin*	chitobiose (up to four units)		ducts of adhesive cells (?)
SBA	soybean agglutinin	α- and β- *N*-acetylgalactosamine	O-glycan (Ser/Thr)	apex microvilosities and epidermal cells cytoplasm

Although, the above-mentioned lectins labelled specifically the adhesive epidermis, LEL produced a much more specific labelling than WGA and STL, staining what seems to be the adhesive granules inside the cell ducts, ending in apical tufts at the disc cuticle. LEL specifically labelled the outer ring of spherical structures, most likely corresponding to heterogeneous adhesive secretory granules previously described for *P. lividus* (see 2.1.1. Tube feet morphology and structure). These results combined with lectin blots, indicate the presence of a high molecular weight glycoprotein (> 180 kDa) with N-acetylglucosamine in the form of chitobiose [GlcNacβ(1,4)GlcNac], most likely 4 units, in the outer rim of the more abundant adhesive granules, as well as, in the less abundant homogenous adhesive granules. Due to its specific localization and the presence in the adhesive footprint, Simão et al. (2020) proposed this glycoprotein as the main component of *P. lividus* adhesive secretion.

Besides N-acetylglucosamine, Soybean agglutinin (SBA) which targets N-acetylgalactosamine, detected this glycan in the adhesive epidermis and in the footprint, being conjugated with two glycoproteins (apparent molecular weight of 72 and 135 kDa). However, its labelling seems to target microvilosities and the cytoplasm of abundant epidermal cells, most likely support cells. Despite not directly involved in adhesion, these proteins can still indirectly affect adhesion as shown in flatworms' reversible adhesion (Wunderer et al., 2019).

These results added new information to the duo-glandular model initially proposed by Flammang et al. (1995). It's now known that *P. lividus* adhesive secretions possesses glycoproteins with N-glycans and O-glycans, more specifically a large glycoprotein with N-acetylglucosamine oligomers and two smaller proteins with terminal N-acetylgalactosamine, as hypothesized by Santos et al. (2009). These results are further supported by the proteomic analysis performed by Lebesgue and colleagues (2016), where the authors reported the presence of highly expressed asparaginase-like proteins in the adhesive disc (Table 4) (Lebesgue et al., 2016). The later, are possible components of the de-adhesive secretion,

leading to the enzymatic detachment of the tube foot through deglycosylation of adhesive glycoproteins.

The model proposed by Simão and colleagues (2020) is in agreement with findings in sea stars. Hennebert and colleagues (2011) demonstrated the involvement of two large glycoproteins (210 and 290 kDa), containing N-acetylgalactosamine, N-acetylglucosamine, galactose, fucose and sialic acid.

Sugar moieties are present in the adhesive secretory cells and/or adhesive material of other reversibly attaching aquatic animals, not being restricted to Echinodermata.

1.2.2. Glycosylation in non-echinoderms adhesion

Besides Echinodermata, glycosylation has been reported in other aquatic organisms such as Platyhelminthes, Cnidaria, Mollusca and Chordata, being described as a high prevalent post-translational modification in aquatic adhesives, either permanent or reversible (Lengerer et al., 2006, 2014; Wunderer et al., 2019; Zeng et al., 2019).

Recent studies have identified adhesion-related transcripts and two large proteins involved in the flatworm *Macrostomum lignano* reversible adhesion (Pennati and Rothbächer 2014; Wasik et al., 2015; Lengerer et al., 2016; Lengerer et al., 2018; Wunderer et al., 2019; Wudarski et al., 2020). Mlig-ap1 and Mlig-ap2 were the first adhesive proteins described in this platyhelminth. Upon attachment, these proteins exhibit distinct spatial distribution within the footprint. While Mlig-ap2 is deposited in a ring-like organization at the outer margin, Mlig-ap1 accumulates mostly in the center of the adhesive granules. Knockdown experiments showed that despite the importance of both proteins in *M. lignano* adhesion, Mlig-ap1 alone is insufficient for attachment (Wunderer et al., 2019). Using double labeling (antibody and lectin staining) and pull-down experiments, Wunderer and colleagues (2019) showed that peanut agglutinin-lectin (PNA) that specifically targets Gal-β (1,3)-GalNac, is part of the Mlig-ap2.(Lengerer et al. 2016) The reversible adhesion of a *M. lignano* phylogenetically distant species, *Minona ileanae,* was analyzed by Pjeta and colleagues (2019). Know-down experiments showed that from the eight adhesion-related transcripts found in this study, seven (*M. ileanae adhesive protein 1-4* and *M. ileanae adhesive organ protein 1*) had a clear influence in the attachment phenotype, affecting adhesive granule morphology. A comparative analysis showed that Mile-ap1 has a high similarity to Mlig-ap1 and Spf1, due to the presence of protein domains such as C-type lectin domain (CTL), von Willebrand domain (vWD), C8-domain (C8) and trypsin inhibitor-like domain (TIL). In addition, multiple tandem repeats of calcium-dependent epidermal growth factor-like domains (EGF) were present, a characteristic of the fibrillin protein family. As for Mile-ap2, it could also be glycosylated as Mlig-ap2, since it contains a protein repeat unit with numerous threonine residues. However, since lectin labeling wasn't possible in adhesive glands whole mounts, the authors only demonstrated that

glucose/N-acetylglucosamine (labelled by PSA - *Pisum sativum* agglutinin, GSL II - *Griffonia (Bandeirara) simplicifolia* II) and galactose/N-acetylgalactosamine (PHA-E - *Phaseolus vulgaris* erythroagglutinin-lectin, PHA-L - *Phaseolus vulgaris* leucoagglutinin, PNA - Peanut agglutinin-lectin, GSL I - *Griffonia (Bandeirara) simplicifolia* I, ECL - *Erythrina cristagalli* lectin, VVL - *Vicia villosa* lectin, DBA - *Dolichos biflorus* agglutinin) are present in *M. ileanae* footprint (Pjeta et al. 2019).

Galactosyl (β-1,3) N-acetylgalactosamine residues are also involved in anemone *Exaiptasia pallida* protein based-adhesion (Clarke et al.,2020). These glycosylated proteins are present in the footprint meshwork and in the secretory cells of *E. pallida* pedal disc. Wheat germ agglutinin (WGA) which targets N-acetylglucosamine (GlcNac) was also reported in the footprint, due to putative mucocytes secretions. These results are supported by a prior transcriptomic study, where the upregulated genes described in the pedal disc indicate that glycosylation may be prevalent in the temporary adhesion of this species (Davey et al., 2019).

Consistently with the platyhelminths (*M. lignano* and *M. ileanae*) and anemones (*E. pallida*) findings, PNA has also been reported as a novel adhesion marker in the tunicate *Ciona intestinalis* larvae. Zeng and colleagues (2019) results have demonstrated the presence of galactosyl (β-1,3) N-acetylgalactosamine residues both in the adhesive secretory cells (i.e. collocytes) and in the proteinaceous footprint (Feoktistova et al., 2016; Zeng et al., 2019). In addition, this recent study, showed that besides the O-glycans already detected with PNA, sialylated N-glycans with terminal galactoses and N-acetylglucosamines are also part of the *C. intestinalis* adhesion.

Despite the well-known role of the amino acid 3,4-dihydroxyphenyl-$_L$-alanine (Dopa) in *Mytilus edulis*, recent studies have shown a possible involvement of glycoproteins in the establishment of mussels' adhesion (Patil et al., 2018). In *Perna viridis*, it was reported a *P. viridis* foot protein-1 (Pvfp-1), with a marked quinone-like redox cycling activity with a low Dopa content and with a significant glycan content, particularly mannose, N-acetylglucosamine and fucose (Zhao et al., 2009). Pvfp-1 adhesive and cohesive properties are accomplish by tryptophan glycosylation and hydroxylation (C^2-mannosyl-7-hydroxytryptophan – Man7-OHTrp) (Hwang et al., 2012; Park et al., 2019). Mussel foot protein 1 (Mfps 1), a Pvfp-1 analogous identified in *Mytilus edulis*, shares conservative structural elements (e.g Pro, Tyr, Dopa and Lys residues) with Pvfp-1, but did not shown similar glycosylation (Ohkawa et al., 2004; Sagert et al., 2006; Hwang et al., 2012; Lu et al., 2013; Park et al., 2019). Therefore, the role of glycans in Pvfp-1 adhesion is still speculative. It could be linked to protein stabilization, and/or intra and intermolecular hydrogen bonding (Toubarro et al., 2016; Shcherbakova et al., 2019).

From our knowledge, the already mentioned organisms use either reversible (e.g sea stars, sea urchins, barnacle larvae and flatworms) or permanent adhesion (e.g anemones, mussels and adult barnacles). A sub-type of reversible adhesion was identified in the limpet *Lottia limatula,* with a repeated transition between long-term adhesion and locomotive adhesion depending on the tide, also known as transitory adhesion. These limpets secrete two types of mucus, a non-adhesive and an adhesive mucus. The later, containing a higher protein and glycan content. α-Mannose and/or α-Fucose linked to N-acetylglucosamine in a chitobiose arrangement was reported in *L. limatula* adhesive secretion by Kang and colleagues (2020). The authors also identified novel adhesive proteins in limpets. Bioinformatic analysis demonstrated the existence of protein domains previous described for sea urchins, sea stars and flatworms, as von Willebrand factor type D, epidermal growth factors, scavenger receptor cysteine-rich C-type lectin-like, alpha-macroglobulin domain and galactose binding domain. Some proteins were homologous to fibrillin, alpha-tectorin, Mlig-ap1 and Spf1. All transcripts had glycosylation predicted sites and expression patterns compatible with location of secretory adhesive cells.

All these studies show that many known and/or candidate adhesive proteins are glycosylated or contain predicted glycosylation residues in their sequences (Figure 6). Although glycans role is still speculative, the growing availability of adhesive organs-specific databases (e.g. sea urchin tube feet transcriptome) conjugated with lectin assays and mass spectrometry can pave the way for a better understanding of the importance of glycoproteins in marine adhesion.

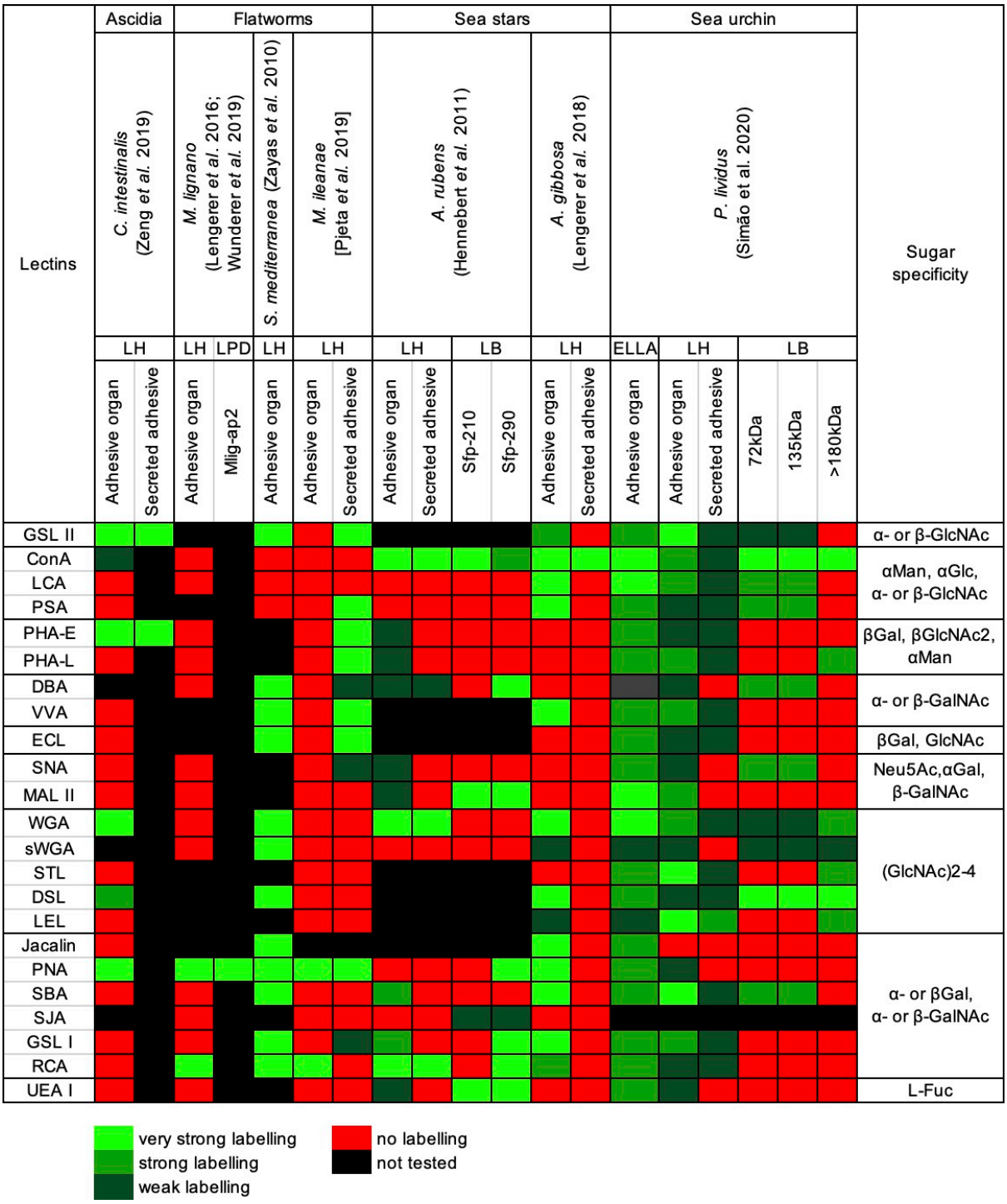

Figure 6 - Heat map of lectin-based glycan detection in temporary wet adhesives. | The rows display the lectins and the columns represent the tested organisms/techniques/type of samples. Very strong labelling is displayed in bright green, strong labelling in green, weak labelling in dark green and no labelling in dark red. The lectins that weren't tested are displayed in black. Abbreviations: ConA, Concavaline A; DBA, *Dolichos biflorus* agglutinin; DSL, *Datura stramonium* lectin; ECL, *Erythrina cristagalli* lectin; ELLA, enzyme-linked lectin assay; GSL I/II, *Griffonia simplicifolia* lectin I/II, LB, lectin blotting; LCA, *Lens culinaris* agglutinin; LEL, *Lycopersicon esculentum* lectin; LH, lectin histochemistry; LPD, lectin pull down; PHA-E/-L, *Phaseolus vulgaris* erythro / leuco agglutinin; MAL II, *Maackia amurensis* lectin II; PNA, Peanut agglutinin; PSA, *Pisum sativum* agglutinin; RCA, *Ricinus communis* agglutinin I; SBA Soybean agglutinin; SJA/SNA, *Sambucus nigra* agglutinin; STL, *Solanum tuberosum* lectin; UEA I, *Ulex europaeus* agglutinin I; sWGA, Succinylated wheat germ agglutinin; VVA, *Vicia villosa* agglutinin; WGA, Wheat germ agglutinin. Adapted from Simão et al., 2020

CHAPTER 2

RATIONALE AND AIMS

Bioadhesion is vital for many aquatic organisms, since it is through the production of adhesive secretions that these animals attach, move and feed in their habitats (Flammang et al., 2016). Currently, the best studied bioadhesives are from organisms that attach permanently (mussels, barnacles) or transitorily (limpets), while little is still known about reversible adhesion (sea urchins, sea stars).

In a recent publication, our lab focused on the characterization of the glycidic fraction of sea urchin adhesives (Simão et al., 2020), complementing Santos and colleagues (2009) results indicating the presence of neutral sugars in *P. lividus* adhesive material. Simão et al. (2020) i) identified and localized glycans in *P. lividus* tube feet sections and in the adhesive footprints, proving the involvement of glycans in sea urchins' adhesion, ii) quantified the glycan residues in the adhesive disc and ii) differentiated between free and conjugated glycans, attesting the existence of glycoproteins in sea urchins' adhesives. Simão et al. (2020) showed that glycoproteins with N-acetylglucosamine (GlcNac) residues are present in *P. lividus* adhesive epidermis and footprint. This glycan was identified in its simpler form by *Griffonia simplicifolia* lectin II (GSL II) and in a specific chitobiose arrangement (a dimer of β-1,4-linked glucosamine units), by *wheat* germ agglutinin (WGA), *Solanum tuberosum* lectin (STL) and *Lycopersicon esculetum* lectin (LEL). LEL staining was particularly interesting since it labelled what seems to be secretory granules, packed within the ducts of adhesive cells at the level of the disc cuticle.

Considering the above-mentioned data, the main aim of this thesis was to further investigate these *P. lividus* candidate adhesive/cohesive glycoproteins through:

- Lectin pulldowns, taking advantage of their specificities for different conjugated glycans;
- Identification of the pull-down glycoproteins by mass-spectrometry, making use of the recently published transcriptome specific for *P. lividus* adhesive organs;
- Select within the identified glycoproteins those that were previously pinpointed as putative adhesive candidates and perform an *in silico* analysis using bioinformatic tools to perform a detailed biochemical characterization.

CHAPTER 3

EXPERIMENTAL WORK

3.1. Glycoproteins extraction and enrichment

Glycans have been proposed to confer high resistance and cohesion to reversible adhesives (Flammang, 1995; Smith, 2016).

Glycoproteins bearing N-acetylglucosamine (GlcNacβ(1,4)GlcNac) and N-acetylgalactosamine (GalNAc) residues have been shown to be specifically expressed in *P. lividus* tube foot adhesive epidermis, being secreted into the adhesive footprint (Simão et al., 2020), being thus hypothesised as important for sea urchin reversible adhesion.

The first aim of this project was to successfully extract and produce enriched fractions of the above-mentioned glycoproteins using lectin pull-down experiments.

3.1.1. Glycoproteins extraction and enrichment

Sea urchins from the species *Paracentrotus lividus* (Lamarck, 1816) were collect during low tide at the west coast of Portugal, in Ericeira (Figure 7).

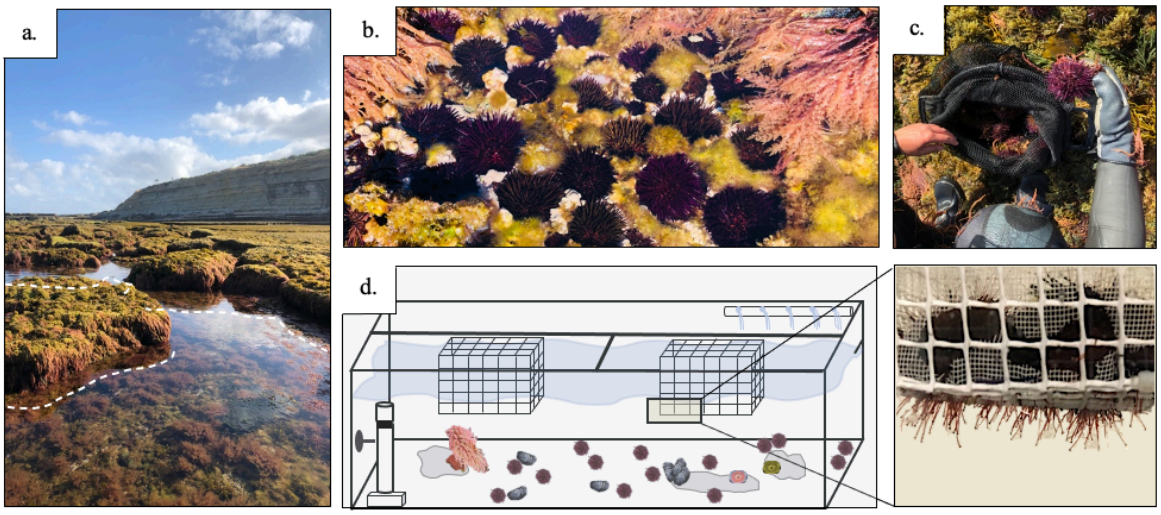

Figure 7 – *Paracentrotus lividus* natural and artificial environment | a. Praia do Matadouro, Ericeira, during low tide. *P. lividus* were collected in tide pools, delimited with a white dashed, and in the shore line. **b.** Sea urchins shallow depressions in coralline seaweeds to withstand the shore line hydrodynamics. **c.** Sea urchins collection and transportation. **d.** Representation of *P. lividus* artificial environment, recreated in laboratory. Aquarium housing sea stars, sea urchins, mussels and anemones. Sea stars were separated, being placed in the left basket, to avoid sea urchins' predation. Sea urchins were maintained in the right basket, without substrate, to prevent tube feet damage during detachment and handling.

Animals were maintained in an aquarium, under a controlled environment (Figure 7 d.). Temperature, salinity and pH were bi-weekly assessed. Nitrogen cycle was evaluated trough ammonia, nitrate and nitrite levels. Animals were weekly feed with corn and seaweeds.

3.1.2. Sample preparation

Oral tube feet, specialized for reversible adhesion, were collected from different animals to minimize individual variability.

Animals were placed upside down on small glass aquariums filled with artificial seawater. This induces tube feet stretching, facilitating their collection (Figure 8 a.).

Samples intended for protein extracts, were dissected to separate the adhesive discs from non-adhesive stems. Subsequently, samples were immediately stored at – 20ºC (Figure 8 c.).

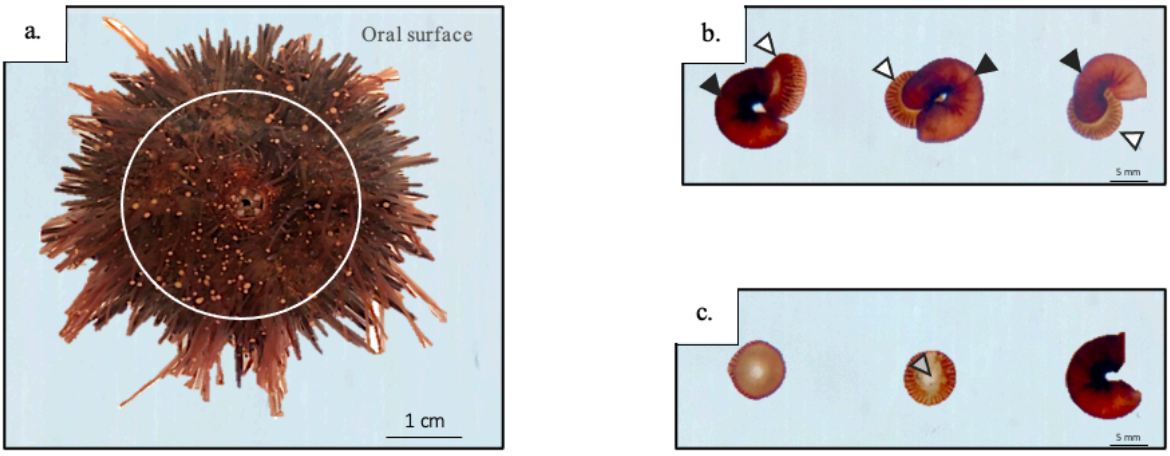

Figure 8 - Location and dissection of *Paracentrotus lividus* oral tube feet | a. Sea urchin oral surface, delimited with a white circumference. **b.** Dissected oral tube feet. The adhesive part of the tube foot, the disc, is identified with a white arrow. The non-adhesive part of the tube foot, the stem, is identified with a black arrow. **c.** Dissected oral tube feet, used for protein extracts, after tissue separation. Disc posterior view, identified with a grey arrow, indicates the region where the tissue was sectioned in order to separate adhesive discs from non-adhesive stems. Original artwork

3.1.3. Protein extracts

Proteins extracts were obtained combining (i) chemical (RIPA buffer) and (ii) mechanical (ball mill) lysis, to achieve a better protein extraction yield and reproducibility.

Prior to mechanical lysis, chemical tissue lysis was performed adding RIPA buffer to dissected discs (150 mM CaCl, 1.0% (v/v) Triton X-100, 0.5% (w/v) sodium deoxycholate, 0.1% (v/v) SDS, 50 mM Tris; pH 8.0), in a 1:2 proportion, which results in a successful disruption of cellular membranes. A cocktail of protease inhibitors (1:10 000) was added to this buffer to minimize proteolytic degradation of tube feet disc proteins. To proceed to mechanical lysis, samples containing 8 steel beads each (2 mm diameter, Retsch) were placed in a previously chilled Teflon chambers. The chambers were then placed in a ball mill (MM 400 Retsch) and set to 30 Hz for 10 minutes (Figure 9). The resulting homogenate was centrifuge at 14000 rpm (Hermle Z 323 K), for 10 minutes at 4ºC. The supernatant was recovered and preserved at – 20ºC.

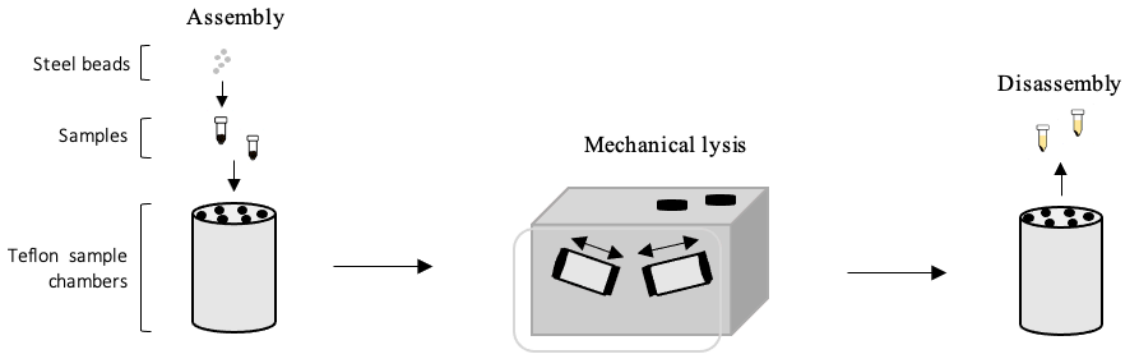

Figure 9 - Schematic representation of protein extracts procedure | Assembly. Samples in RIPA buffer and tubes containing eight steel balls each (2 mm diameter) were place in previously chilled Teflon sample chambers. **Mechanical lysis.** Teflon chambers were placed in a ball mill for 10 minutes at 30Hz. Teflon chambers movement is identified with black arrows. **Disassembly.** After mechanical lysis, samples, consisting of proteins suspended in RIPA buffer were recovered from the Teflon chambers and centrifuged. The *pellet* formed by disrupted tissue was discarded. (Original artwork)

3.1.4. Protein quantification

Protein quantification was assessed using Bradford assay. This colorimetric protein assay is based on the correlation between the absorbance at 595 nm and the amount of dye bounded to proteins in a sample, using a *standard* protein curve as reference (Noble and Bailey 2009).

The s*tandard* curve consisted of increasing amounts of Bovine serum albumin (BSA, Sigma; 0.05, 0.1, 0.2, 0.3, 0.4 and 0.5 μg/μl).

A 10 μl volume of each *standard* concentration and sample was add to a 96 wells microplate (Brand). Triplicates assured a mean absorbance value, minimizing the effect of possible micro pipetting errors. A 20 minutes incubation at room temperature (RT) was performed after the addiction of 200 μl Bradford reagent (Protein Assay Dye Reagent Concentrate, Bio-Rad) to each well used in the quantification. Absorbance at 595 nm was measure in a spectrophotometer (Bio Tek Synergy HT) after shacking the plate for 20 seconds.

Sample protein concentration was calculated using the *standard* curve as reference and the absorbance of the samples itself. For absorbance values outside the *standard* curve, it was not possible to calculate protein concentration. As such, samples with protein concentrations (i) higher than 0.5 μg/μl were diluted and (ii) lower than 0.05 μg/μl were concentrated (Figure 10).

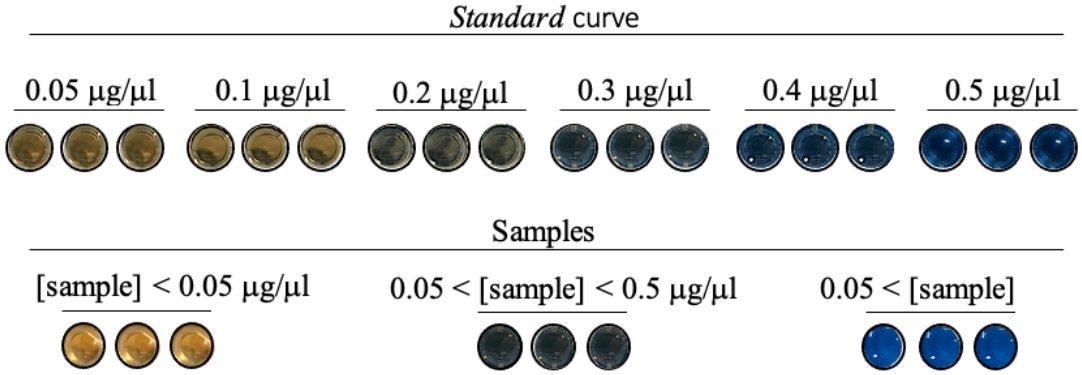

Figure 10 - Schematic representation of Bradford colorimetric protein assay | On top, coloured triplicates obtained with increasing concentrations of the reference protein BSA. At the bottom, examples of sample triplicates protein concentrations outside the *standard* curve that had to be either concentrated or diluted to fit the assay. Original artwork

3.1.5. Glycoproteins enrichment

Glycoproteins-enriched fractions were obtained through lectin pull-downs, based on the reversible and highly selective binding of lectins to mono- and oligosaccharides. As such, agarose beads bounded to 4 different lectins were used. Due to those lectin-glycan interactions, glycosylated and non-glycosylated proteins (or glycosylated proteins not recognized by the lectin) could be separated in different fractions. After selective binding to a given lectin, glycoproteins were dissociated from the lectin-bounded agarose beads using a mixture of competing sugars. Elution efficiency was assessed by boiling the remaining agarose beads.

Lectins affinity resins (Vector laboratories), consisting of lectins bounded with agarose-beads, had different binding capacities and substrates. (Table 5)

Table 5 – Lectin affinity resins binding capacity, detected mono- and oligosaccharides and eluting sugar solution | Abbreviations: LEL - *Lycopersicon esculetum* (tomato) lectin, SBA - *Soybean agglutinin,* WGA - *Wheat germ agglutinin,* GSLII - *Griffonia* (Bandeiraea) *simplicifolia* lectin II**,** GlcNac – N-acetylglucosamine; GalNac – N-acetylgalactosamine; NeuAc – sialic acid

Lectins' affinity resins	GSL II	WGA	LEL	SBA
Binding capacity	> 4.0 mg/ml	7.0 mg/ml	2.69 mg/ml	4.4 mg/ml
Glycans detected	GlcNAc	GlcNAc, GalNAc, NeuAc	GlcNAc, GalNAc	
Eluting sugar solution	N-acetylglucosamine or Chitin-binding lectins			Galactose- or GalNAc-binding lectins

Lectin-bounded resins were equilibrated with 1 ml of TBS-T supplemented with ions (20 mM Tris, 150 mM NaCl, 0.05% (v/v) Tween-20, 1 mM $CaCl_2$, 1 mM $MnCl_2$ pH 7.6) by continuous inversion (using a tube rotator), 4 times for 10 minutes. To prevent the loss of agarose beads, resins were centrifuged between washes at 8500 rpm, for 4 minutes at RT. The supernatants were discarded. (Figure 11 a.)

Equilibrated resins and samples were mix overnight at 4° C by continuous inversion (Figure 11 b.). The mixture was then centrifuged at 8500 rpm, for 4 minutes at 4°C. The supernatant, corresponding to the **unbound proteins (UB)**, was recovered for later analysis and preserved at -20°C. Lectin-bounded resins were then washed with 1 ml of TBS-T supplemented with ions (20 mM Tris, 150 mM NaCl, 0.05% (v/v) Tween-20, 1 mM $CaCl_2$, 1 mM $MnCl_2$ pH 7.6) 4 times, for 10 minutes by continuous inversion. Between washes, the mixture was centrifuged at 8500 rpm, for 4 minutes, at 4° C. The four supernatants, corresponding to the four **washing steps (W)** were recovered and preserved at -20°C for later analysis. Then, 200 µl of glycoprotein eluting solution (Vector laboratories, see Table 5) was added to the mixture (Figure 11 c.) and incubated for 60 minutes, at RT, with continuous inversion. The solution was then centrifuged at 8500 rpm, for 4 minutes, at 4°C and the supernatant, corresponding to the **eluted proteins (E)**, was recovered and stored at -20°C until later analysis. A second elution step was performed, as above described, and pooled with the first eluted proteins (E) fraction.

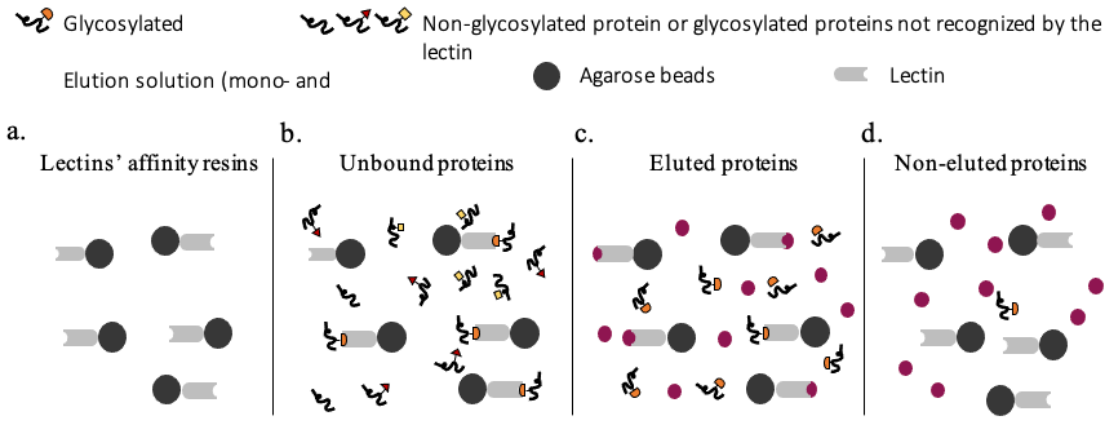

Figure 11 - Schematic representation of the glycoproteins pulldown procedure using lectin-bounded agarose beads | a. Lectins affinity resins formed by agarose beads (black) bound with specific lectins (grey). **b.** Lectin-coated agarose beads were incubated with tube feet disc protein extracts. Due to specific glycan/lectin interaction, only some glycosylated proteins (orange) bind to lectins, while non-glycosylated proteins or glycosylated proteins not recognized by the lectin (black, red and yellow figure) remain in the supernatant after centrifugation - *Unbound proteins fraction*. **c.** Glycoproteins are eluted using a solution rich in mono- and oligosaccharides (pink circles). Due to glycan competition, glycoprotein/lectin interaction is affected, glycoprotein dissociate from the lectin-bounded agarose beads and remain in the supernatant after centrifugation - *Eluted proteins fraction*. **d.** Elution efficiency was assessed by boiling the agarose beads in order to release glycans and glycoproteins that were not eluted in c. - *Non-eluted proteins fraction*. Original artwork

All the samples, except for non-eluted proteins (NE), were concentrated by precipitation (see section 3.1.6). **Non-eluted fraction (NE)** was only obtained later because it required boiling of the agarose beads with SDS-PAGE sample buffer (see section 3.1.7).

Results specificity was assessed by inhibited lectin-bounded agarose beads assays. Prior to overnight incubation, equilibrated resins were inhibited with a double elution step (400 µl x2 of eluting sugar solution) by inversion, during 2 hours at RT.

3.1.6. Protein precipitation

Protein precipitation was accomplished with trichloroacetic acid. This non-biocompatible precipitation method is based on solvation layer disruption by polar residues protonation. This interference in the hydrogen bonds between proteins hydrophobic surface and water molecules leads to protein insolubility (Sheehan, 2000; Koontz, 2014; Nerson and Cox, 2016). To minimize the risk of peptide bonds acid hydrolysis, residual acid is washed with acetone maintained at -20º C (Sheehan, 2000).

The precipitation solution (10% (w/v) TCA, 0.07% (v/v) β-mercaptoethanol in water) was added to unbound, washing and eluted fractions recovered during glycoproteins pull-downs. A 5 minutes vortex was performed to each supernatant, to mix. All samples were precipitated during 90 minutes at 4º C. Then, samples were centrifuged at 1000 rpm, during 20 minutes at 4ºC. All supernatants were discarded. Pellets were washed with 1 ml of cold washing solution (0.07% (v/v) β-mercaptoethanol in acetone). Each precipitated sample/washing solution was vortex for 5 minutes to mix. After mixture, samples were centrifuge at 10000 rpm, during 20 minutes at 4º C. A second and third wash were performed as described above. Pellets were dried overnight at 4º C to allow acetone evaporation.

3.1.7. Protein separation by gel electrophoresis (SDS-PAGE)

Protein separation was accomplished by Sodium dodecyl sulphate-polyacrylamide gel electrophoresis, also known as SDS-PAGE. This protein separation technique is based on proteins differential rates of migration, depending on their molecular weight, through a sieving matrix under the influence of an applied electrical field. Protein resolving does not depend on proteins native conformation due to the sodium dodecyl sulphate (SDS) added to the sample and running buffers. This detergent is responsible for the (i) denaturation of secondary and non-disulphide-linked tertiary structures, reducing proteins to their primary structure, (ii) coating of the proteins with a uniform negative charge, which covers the intrinsic charges of proteins R-groups and (iii) maintaining proteins linearized during the electrophoretic run (Brunelle, 2014). As such, SDS negatively charged proteins migrate, based on their molecular weight, to the positive anode.

Gel matrix was composed of an upper stacking gel at pH 6.8 and a lower resolving gel at pH 8.8, both buffered by Tris-HCl and made of acrylamide (acrylamide/bis-acrylamide 37.5:1, NZYTech). Stacking gel had lower acrylamide percentage (3.5 or 4%) than resolving (7.5 or 12.5%), allowing the proteins with different sizes to enter the resolving gel at the same time.

After casting, gels were placed inside an electrode assemble tank and afterwards, inside a tank (Figure 12). Both chambers were filled with Running Buffer 1x (25 mM Tris, 192 mM glycine, 0.1% (v/v) SDS, pH 8.3).

Prior to electrophoresis, previously precipitated samples (see section 3.1.6) and the remaining agarose beads, were mixed with sample buffer (62.5 mM Tris-HCl pH 6.8, 25% (v/v) glycerol, 2% (v/v) SDS, 5% (v/v) β-mercapthoetanol and 0.01% (w/v) bromophenol blue) and boiled for 5 minutes at 96^{o} C. Agarose beads required an extra 4 minutes centrifugation at 8500 rpm to obtain the supernatant (**non-eluted fraction - NE).**

In each gel, wells were loaded with 30 μl of UB, W1, W2, W3, W4, E and NE fractions. For posterior assessment of sample proteins molecular weight, 5 μl of molecular weight markers (NZYBlue Protein marker, NZYTech) were added to each gel. (Figure 12).

The run was performed in a mini-PROTEAN Tetra System (Bio-Rad) at 50V for maximum protein separation, increasing bands resolution. After SDS-PAGE, gels were either (i) stained with Coomassie Brilliant Blue R.250, for protein visualization (see section 3.1.8) or (ii) transferred to a PVDF membrane to assess for the presence of glycoproteins by lectin-blotting (see section 3.1.9).

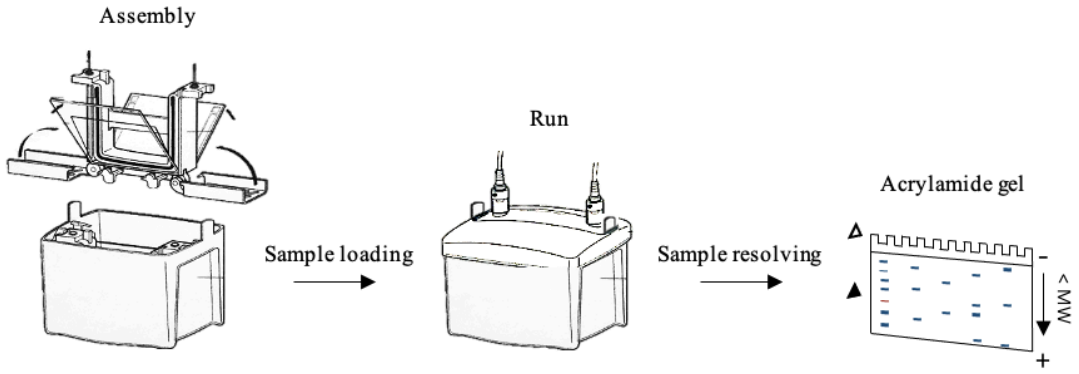

Figure 12 - Schematic representation of Sodium dodecyl sulphated-polyacrylamide gel electrophoresis (SDS-PAGE) | Assembly. Gels casted in glass plates were sealed in an electrode assemble tank which was then placed in a tank. **Sample loading.** 5 μl of molecular weight marker was added to the first well, followed by 30 μl of each fraction in the subsequent wells. The whole assembly was covered with Running Buffer 1x. **Run.** Application of an electrical field of 50 V, leading to proteins migration and separation, depending on their molecular weight. **Sample resolving.** Negatively charged proteins migrated towards the positive anode. Different molecular weights lead to differential migration. **Acrylamide gel**. Stacking gel, identified with a white arrow, allowed an evenly entrance of proteins with different molecular weights in the resolving gel, identified with a black arrow. Proteins migrate from the negative cathode (-) to the positive anode (+). Proteins with lower molecular weights migrated faster to the positive anode. Original artwork

3.1.8. Coomassie Brilliant Blue R-250 staining

Protein visualization was accomplished using Coomassie Brilliant Blue R-250 staining. In acidic conditions, the dye binds noncovalently to the amino and carboxyl protein groups through electrostatic attraction. These complex formation leads to a stabilization of the dye,

producing the blue colour (Goldring, 2018). The excess stain is eluted with solvent (Arndt et al., 2012).

After SDS-PAGE, the gel was incubated overnight at RT under mild agitation with staining solution (0.01% (w/v) Coomassie Brilliant Blue R-250, 40% (v/v) methanol, 10% (v/v) acetic acid). Then, the gel was carefully distained with a washing solution (40% (v/v) methanol, 10% (v/v) acetic acid) at RT under mild agitation.

3.1.9. Lectin-blotting

Lectin blotting is a modification of western blotting, using lectins instead of antibodies to detect proteins conjugated with specific glycans (Cao et al., 2013).

A specific visualization of glycoproteins was performed by (i) transferring the proteins separated by electrophoresis from the acrylamide gel to a polyvinylidene fluoride (PVDF) membrane and (ii) labelling glycoproteins with biotin-conjugated lectins that are subsequently recognized by a streptavidin-conjugated peroxidase, that later catalyses the oxidation of luminol by hydrogen peroxide (Figure 13).

Transfer to PVDF membrane is based on proteins migration to the positive anode, under the influence of an applied electrical field. Prior to the transfer, the membrane was activated for 10 minutes in methanol, at RT. After incubation, the membrane was equilibrated in transfer buffer (48 mM Tris, 39 mM glycine, 20% (v/v) methanol, 1.3 mM SDS pH 9.2). For protein transfer, the gel was concealed in a mounted slab and placed in a mini-trans-blot with a cooling unit and transfer buffer (48 mM Tris, 39 mM glycine, 20% (v/v) methanol, 1.3 mM SDS pH 9.2). After a 100V run for 65 minutes, the membrane was incubated with TBT-T-BSA (10 mM Tris-HCl, 150 mM NaCl, pH 8.0 0.1% (v/v) Tween-20, 3% (w/v) BSA) overnight at 4^{o} C, under mild agitation, to minimized unspecific binding. Then, the membrane was incubated with a lectin solution (1 μl/ml of biotinylated lectin in TBS-T-BSA-ions; Vector) during 90 minutes at RT, under mild agitation. Next, the membrane was washed 5 times with TBS-T (10 mM Tris-HCl, 150 mM NaCl, pH 8.0, 0.1% (v/v) Tween-20) for 10 minutes and incubated with HRP streptavidin solution (Vector) during 60 minutes at RT, under mild agitation. This last incubation was performed in the dark. Prior to detection by Enhanced chemiluminescence (ECL), 5 washes with TBS-T (10 mM Tris-HCl, 150 mM NaCl, pH 8.0, 0.1% (v/v) Tween-20) were done under mild agitation. The PVDF membrane was then incubated with hydrogen peroxide conjugated with luminol (ECL Prime Western Blotting Detection Reagent, Amersham GE). The image was captured using a CCD camera (Amersham Imager 680 RGB, GE Healthcare).

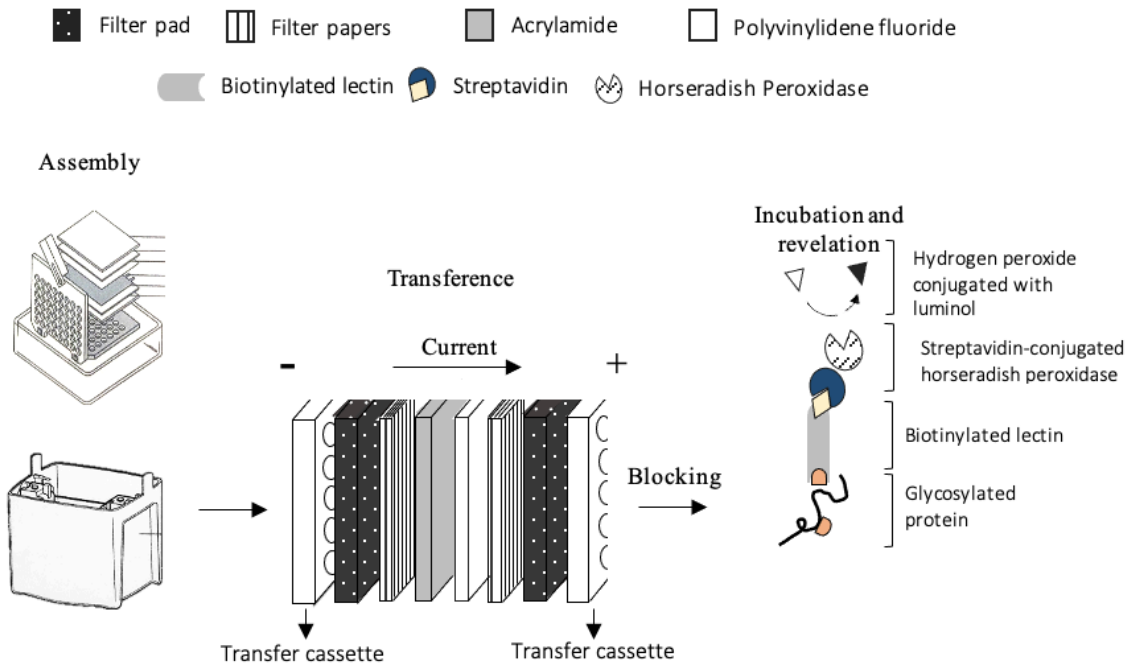

Figure 13 - Schematic representation of proteins transference to a polyvinylidene fluoride membrane | Assembly. The slab was mounted, from the negative cathode to the positive anode, with a filter pad, a filter paper, the acrylamide gel, a PVDF membrane, a filter paper and a filter pad. All the components were previously immersed in transfer buffer. **Protein transfer.** Application of an electrical field of 100 V for 65 minutes, leading to protein migration towards the positive anode. **Membrane Blocking.** PVDF membrane blocked with TBS-T-BSA to minimized unspecific binding during incubation. **Incubation and detection.** PVDF membrane was incubated 90 minutes with a lectin solution that recognizes specific glycoproteins, the later contains biotin that is detected by a streptavidin solution that in turn contains a horseradish peroxidase that catalyses the oxidation of luminol by hydrogen peroxide, yielding chemiluminescence that is detected by CCD camera. Original artwork

3.2. Glycoprotein identification and characterization

Previous proteomic studies only identified Nectin, as an adhesive protein due to the poor homologies with public protein databases. Recently, Pjeta et al. (2020) obtained the first transcriptome of *Paracentrotus lividus* adhesive organs, allowing adhesion specific proteins to be identified.

Based on this transcriptome, the second aim of this study was to identify novel candidate adhesive glycoproteins involved in *P. lividus* adhesion, using mass spectrometry. Only the eluted fractions were analysed to address this specific question.

Mass spectrometry was performed as a service, by the Centre for Proteome Research, Liverpool University.

3.2.1. Mass spectrometry

Mass-spectrometry measures the mass-to-charge ratio of ions. To assure technical and biological replicates, two eluted fractions for each tested lectin (8 samples in total) were analysed by mass spectrometry, each sample being composed of proteins extracted from 3 or more sea urchins recently collected from its natural environment at the same moment.

Samples were first bound to 10 µl of strataclean resin (Agilent), vortexed for 1 minute, centrifuged and the supernatant discarded. The resin was then washed three times with 40 µL 25 mM AmBic buffer and then digested on beads with 0.05 % RapiGest™ (w/v) for 10 minutes at 80℃, followed by reduction with 4 mM Dithiothreitol for 10 minutes at 60℃, alkylation with 14 mM Iodoacetamide for 30 minutes at room temperature, and finally digested with 0.5 µg of Trypsin in two steps (4 hours at 37℃, followed by overnight at 37℃ with agitation to keep beads suspended). Then, samples were acidified with 0.5 % Trifluoroacetic acid (v/v) for 45 minutes at 37ºC, centrifuged and 2.5 µl of clarified supernatant injected on column, ran on 50 minutes gradient on Q Exactive HF (Thermo). MS/MS data were searched for adhesive protein candidates against a database composed of the six open reading frames (ORFs) of *P. lividus* tube foot transcriptome using Mascot (version 2.7.0, Matrix Science). The peptide mass tolerance was set to 10 ppm, and fragment mass tolerance was set to 0.01 Da. Carbamidomethyl cysteine was set as a fixed modification, and oxidized methionine as variable modification. For all samples, candidate proteins with false discovery rates (FDRs) above 1% and only one unique peptide were excluded from subsequent analysis.

3.2.2. *In silico* analysis

Protein structure is influenced by a diversity of factors as primary amino acid sequence, structural units (e.g domains) and the establishment of intra and/or intermolecular bonds (Noble and Bailey, 2009). Since protein function is determined by their spatial conformation, an *in silico* analysis was performed to further characterize the adhesive protein candidates identified by mass spectrometry.

Various conserved domains have been described for marine adhesives proteins (see 1.1.2.1. Proteins identification and role in sea urchin adhesion), highlighting their importance in wet adhesion. To further characterize these domains in the putative adhesive proteins, their sequences were analysed using Basic Local Alignment Search Tool (BLAST) from National Center for Biotechnology Information (NCBI) and Universal Protein Resource (UniProt) datasets to identify regions of local similarity between sea urchin transcripts and known proteins. Then, the sequences were aligned using Cobalt Alignment Tool from NCBI. Domains prediction was performed using NCBI Conserved Domain Databases (Lu et al., 2020)and InterPro (Mitchell et al., 2019). The presence of a signal peptide, a feature of secreted proteins,

was predicted using SignalP 5.0 (Almagro et al., 2019). The amino acid composition, total number of charged residues, instability index, aliphatic index and GRAVY were predicted with ProtParam tool from Expasy. Theoretical isoelectric point and molecular weight of each protein were predicted using Compute pI/MW tool from Expasy. Putative N- and O- glycosylation sites were predicted using NetNGlyc 1.0 and NetOGlyc 4.0, and putative phosphorylation sites were predicted using NetPhos 3.1 (Buheitel and Stemmann, 2013) considerer threshold > 0.5). Protein three-dimensional structure was performed using RaptorX (Wang et al., 2018; Xu et al., 2019; Xu et al., 2020). Structural alignment, structure edition and protein visualization were performed with *UCSF Chimera* (Pettersen et al., 2004).

CHAPTER 4

RESULTS AND DISCUSSION

4.1. Glycoproteins purification

Glycoproteins enriched fractions were obtained through pull-down assays using four lectins with different glycan affinities (see section 3.1.5).

Since this protocol had never been used for sea urchin tube feet samples, it required several optimization steps (Table 6). Due to the differential binding capacity of the lectin-bound agarose beads (see Table 5 Experimental work), the lowest binding capacity of LEL-bound agarose beads (2.69 μg/μl) was used as a reference to determine the volume for the remaining lectins (GSL II, WGA and SBA). Proteins present in unbounded (**UB**), washed (**W**) and eluted (**E)** fractions were visualized with (i) Coomassie Brilliant Blue R-250 staining and (ii) lectin blotting, to detect the glycoproteins of interest. Both techniques were performed in the same conditions and at the same time, to obtain comparable results.

4.1.1. Pull-down assays

4.1.1.1 *Lycopersicon esculetum* (tomato) lectin pull down assay

Recently published research showed that *Lycopersicon esculetum* (tomato) lectin detects an intense protein band above 180 kDa in *P. lividus* tube feet discs, indicating that it contains several chitobiose units (GlcNac β(1,4) GlcNac) (Simão et al., 2020). Since LEL histochemistry labelling showed that this glycoprotein is spatially restricted to the adhesive epidermis, more specifically in the outer rim of the secretory granules, and is also secreted into the adhesive, it was proposed as an important glycoprotein for *P. lividus* adhesion.

To proceed to pull down assays optimization, different parameters were taken into account, such as (i) initial protein amount, needed for eluted proteins visualization with Coomassie Brilliant Blue R-250 staining, (ii) volume of lectin bounded agarose beads and eluting sugar solution, to maximize the retention of the glycoproteins of interest in the eluted (**E**) fraction and (iii) volume of sample buffer, necessary to detach the remaining glycoproteins from agarose beads in the non-eluted (**NE**) fraction (Table 6). Protein amount was calculated based on protein quantification values of several tube feet adhesive disc extracts that were performed throughout this study.

Table 6 – *Paracentrotus lividus* tube feet disc glycoproteins enrichment using LEL-bounded agarose beads pull-down assay. Tested conditions and results obtained during protocol optimization | a. Different initial protein concentrations were tested to establish a minimal protein amount to obtain visible protein bands with Coomassie Brilliant Blue R-250 staining. **b.** Protein precipitation was tested to obtain better protein band resolution and less smear in Coomassie Brilliant Blue R-250 stained gels. **c. d.** Various volumes of agarose beads, eluting sugar solution and sample buffer were tested to minimize the retention of the glycoproteins of interest in the unbound, washing and non-eluted fractions. The presence of glycoproteins only in the 1st washing step was considered as a null result (Supplementary Figure 2 - 4). Abbreviations: S - stacking gel, R – resolving gel, CS – Coomassie Brilliant Blue R-250 Staining, LB – Lectin-blotting.

		Protocol optimization for *Lycopersicon esculetum* (tomato)-bounded agarose beads											
		Tested conditions					Obtained results (visualized protein bands)					
		Protein amount	Acrylamide gels	Agarose beads	Elution sugar solution	Sample Buffer	Unbound protein fraction		Eluted protein fraction		Non-eluted protein fraction	
							CS	LB	CS	LB	CS	LB
Samples w/ precipitation	a.	555 µg	S: 4%; R: 12.5%	100 µl (269 µg)	100 µl	50 µl	> 25 kDa	---	> 48 kDa	> 75 kDa	---	---
		730 µg	S: 4%; R: 12.5%	100 µl (269 µg)	100 µl	50 µl	> 25 kDa	---	> 40 kDa	75 kDa, > 100 kDa	---	---
	b.	640 µg	S: 4%; R: 12.5%	100 µl (269 µg)	200 µl	100 µl	> 25 kDa	---	---	> 245 kDa	---	---
Precipitated samples		640 µg	S: 4%; R: 12.5%	100 µl (269 µg)	200 µl	100 µl	> 25 kDa	> 245 kDa	---	> 75 kDa	---	---
	c.	730 µg	S: 3.5%; R: 7.5%	200 µl (520 µg)	300 µl	60 µl	> 48 kDa	48 kDa, > 135 kDa	> 48 kDa	48 kDa, > 245 kDa	48 kDa	48 kDa, > 135 kDa
	d.	730 µg	S: 4%; R: 12.5%	334.57 µl (900 µg)	200 (x2) µl	100 µl	>17 kDa	> 100 kDa	> 17 kDa	> 245 kDa	---	> 245 kDa

First optimization (Table 6 a.) (Supplementary Figure 2) established a minimal initial protein amount needed for eluted proteins visualization with Coomassie Brilliant Blue R-250 staining. After testing two conditions (555 µg and 730 µg) it was concluded that the ideal minimal initial protein amount was 730 µg, since it allows the visualization of a higher number of protein bands (> 40 kDa) with Coomassie in the eluted fraction (**E**), some of which were simultaneously detected by LEL lectin blotting (> 75 kDa), corresponding to our glycoprotein of interest. However, protein bands resolution was low both in Coomassie stained gels and lectin blots.

To increase band resolution and remove interfering substances that can cause smear in SDS-PAGE, a second optimization step was performed by protein precipitation (Table 6 b.) (Supplementary Figure 3). Although, the initial protein amount (640 µg) was below the ideal amount set above (730 µg), the effect of protein precipitation was clear, since more protein bands were detected by LEL lectin blotting in the eluted fraction (E). The effect of doubling the eluting sugar solution volume was also tested (from 100 to 200 µl, Table 6 a. and b.), but no significant differences were observed.

We proceeded with a third step of optimization to combine the above mentioned minimal initial protein amount 730 µg, with a higher volume of agarose beads (from 100 to 200 µl) and a higher volume of eluting sugar solution (from 200 to 300 µl). (Table 6 c., Supplementary Figure 4). In addition, since previous results showed glycoproteins detected by LEL were above 75 kDa, the acrylamide concentration in the gels was also decreased to allow (i) better protein entrance in stacking gel (from 4 to 3.5%) and (ii) better protein separation in resolving gel (from 12.5 to 7.5%). The obtained results showed glycoproteins both in the unbound (**UB**) and non-eluted (**NE**) fractions, indicating that the agarose beads

and eluting sugar solution volumes used were still insufficient, since part of the glycoproteins of interest remained in these fractions (Supplementary Figure 4).

After several optimization steps, it was established that using 730 μg of disc protein extract, 334.57 μl of lectin coated agarose beads, 2 x 200 μl of eluting sugar elution and 100 μl of sample buffer, were the best conditions to obtain an enriched fraction of LEL-bound glycoproteins. The volume of agarose beads is limited by LEL binding capacity (2.69 mg/ml), therefore, the maximum amount of lectin that can be used is 900 μg, that for LEL corresponds to 334.57 μl. Glycoproteins elution was performed in two steps of 1h incubation with 200 μl of eluting sugar solution instead of one step of 1h incubation with 400 μl, because doubling the time maximized the elution efficiency in comparison with just doubling the volume. To evaluate these optimizations, it was considered the following factors (i) absence of protein bands in the non-eluted fraction (**NE**) in Coomassie staining and lectin blotting and (ii) lack of overlapping protein bands in unbound (**UB**) and eluted (**E**) fractions (Table 6, Figure 14).

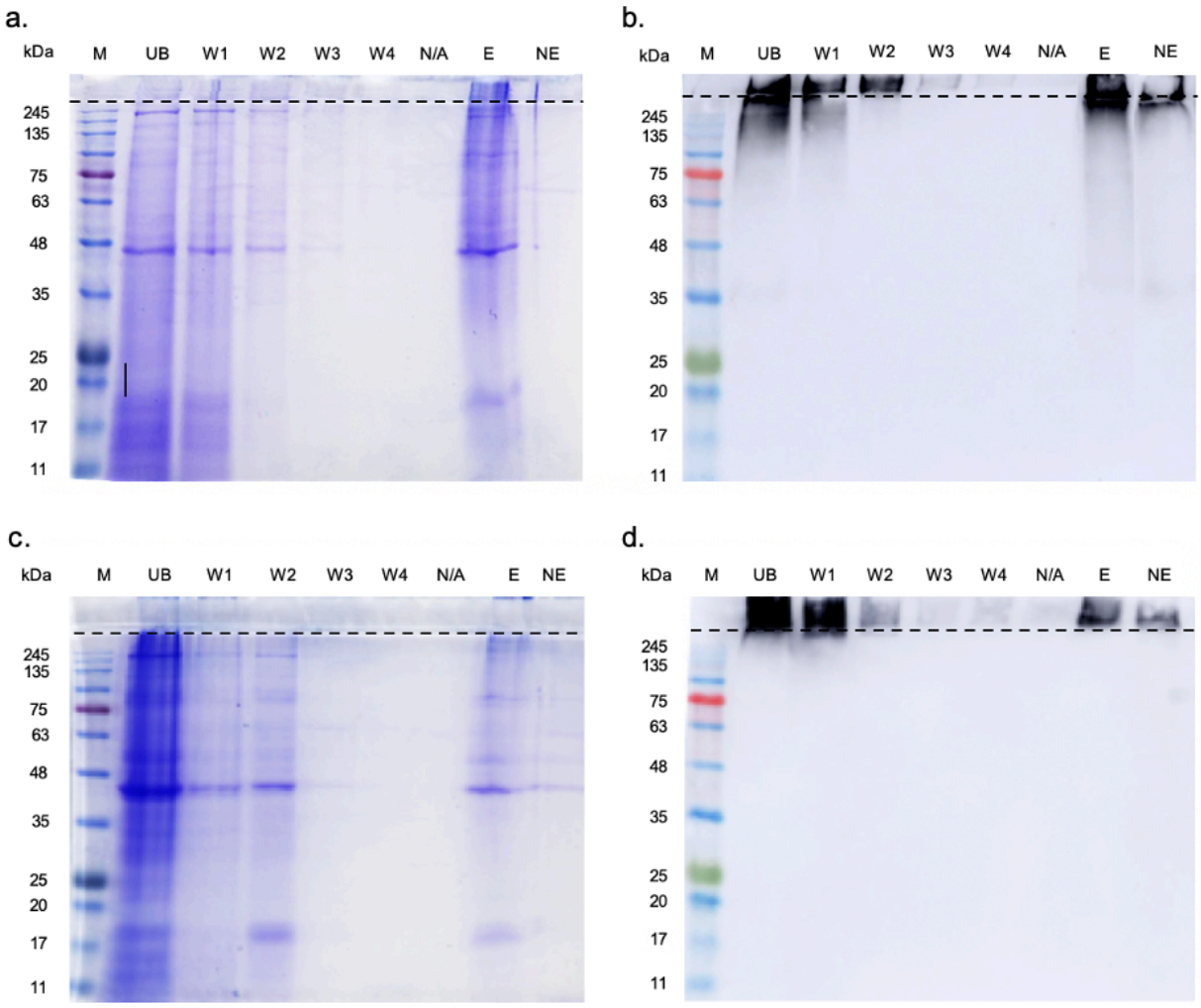

Figure 14 - Pull-down assay of glycoproteins from *Paracentrotus lividus* tube feet disc extracts using LEL-bounded agarose beads | One-dimensional gel electrophoresis protein profile (**a,c**) and corresponding lectin blot (**b,d**) using LEL-bounded agarose beads non-inhibited **(a,b)** and inhibited (**c,d)**. Abbreviations: E – eluted fraction; M - molecular weight markers; NE – non-eluted fraction; UB- unbound fraction; W1-4 – wash fractions. 31.8 seconds of exposure time. Dashed line indicates the separation between stacking and resolving gel.

With the above-mentioned conditions, it was possible to visualize with Coomassie staining, several well-resolved protein bands in the eluted fraction (**E**) with apparent molecular weights ranging from 17 to > 245 kDa (Figure 14 a.). Of these, only proteins above 245 kDa were detected by LEL using lectin-blotting (Figure 14 b.). These results confirm the presence of high-molecular glycoproteins with chitobiose residues, so large that they fail to enter the resolving gel, even using lower percentage of acrylamide in the gels (Supplementary Figure 4).

To access the specificity of the lectin/glycan interaction, LEL-bounded agarose beads were inhibited with 800 μl of the eluting sugar solution prior to incubation with protein extracts (twice the volume used to elute LEL-bound glycoproteins from non-inhibited beads). This resulted in a clear decrease in terms of protein amount and number of protein bands detected in the eluted (**E**) fraction of the inhibited Coomassie gel, in comparison with the non-inhibited one (Figure 14 a, c). The signal obtained in the blots in the eluted (**E**) fraction is also less intense with the inhibited beads (Figure 14 b, d). There are proteins in the Coomassie eluted fraction that aren't labelled by LEL in the blots (Figure 14), which might indicate that some non-specific binding to the beads still occurs, but there is a clear affinity for the glycans linked to larger proteins.

It must be also noted that both with non-inhibited and inhibited beads, some proteins were detected by LEL in the blots in the unbound (**UB**), 1st wash (**W1**) and 2^{sd} wash (**W2**) fractions. This is most reflected that a higher volume of beads would be needed to capture all LEL-specific glycoproteins present in the disc extract. The volume of eluting sugar solution allowed the release of a sufficient amount of glycoproteins to be detected in the Coomassie gels and lectin-blots, but still some glycoproteins persisted in the non-eluted (**NE**) fraction. This could indicate that a higher volume is needed or that some supernatant (eluted fraction) remained in tube with the beads.

4.1.1.2. *Wheat germ* agglutinin lectin pull down assays

WGA, which detects one or two chitobiose units, was previous reported to label the adhesive epidermis and cuticle in tube feet discs, as well as the adhesive footprints. In tube feet discs, it also detects glycoproteins with an apparent molecular weight of 35, 75, 135 and > 180 kDa.

Table 7 - *Paracentrotus lividus* tube feet disc glycoproteins enrichment using WGA-bounded agarose beads pull-down assay. Tested condition and results obtained during protocol optimization | a. b. Various volumes of agarose beads and sugar eluting solution were tested to maximize the pull-down of WGA-bounded glycoproteins. The presence of glycoproteins only in the 1st washing step was considered as a null result. Abbreviations: S - stacking gel, R – resolving gel, CS – Coomassie Brilliant Blue R-250 Staining, LB – Lectin-blotting.

	Wheat germ agglutinin-bounded agarose beads											
	Tested conditions					Obtained results (visualized protein bands)					
	Protein amount	Acrylamide gels	Agarose beads	Elution sugar solution	Sample Buffer	Unbound protein fraction		Eluted protein fraction		Non-eluted protein fraction	
						CS	LB	CS	LB	CS	LB
Precipitated samples	730 µg	S: 4%; R: 12.5%	128.57 µl (900 µg)	300 (x2) µl	100 µl	> 11kDa	---	> 11 kDa	35 kDa, 63 kDa, 75 kDa, > 245 kDa	> 11 kDa	35 kDa, 63 kDa, 75 kDa, > 245 kDa

For WGA-pull down assay, the same protein amount (730 µg) was used, but due to the different binding capacity (7 mg/ml) of WGA-bounded agarose beads, a volume of 128.57 µl was used to ensure the same 900 µg of lectin coated agarose beads. As for the remaining parameters, it was established that using 2 x 300 µl of eluting sugar elution and 100 µl of sample buffer, were the best conditions to obtain an enriched fraction of WGA-bound glycoproteins (Table 7).

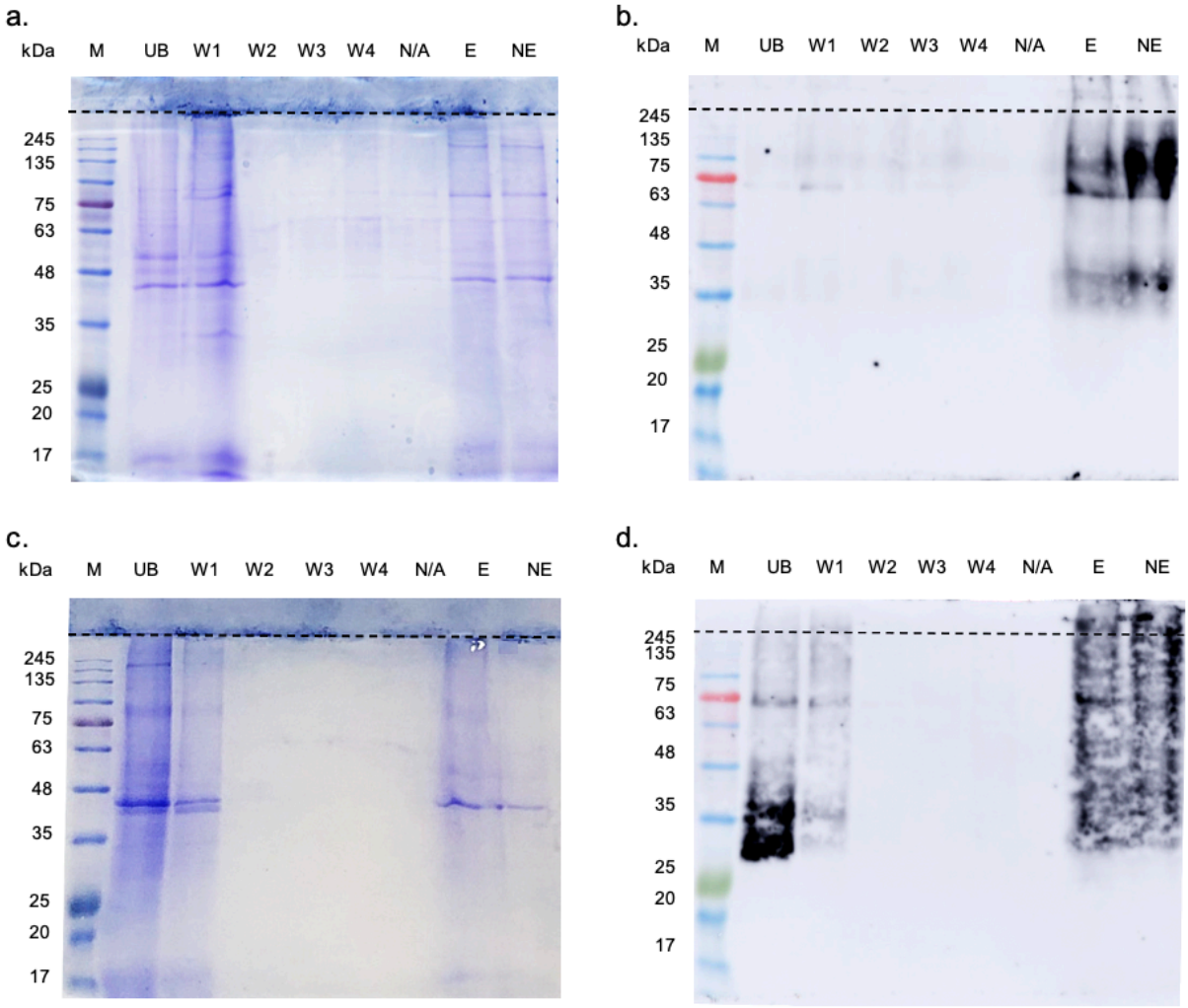

Figure 15 - Pull-down assay of glycoproteins from *Paracentrotus lividus* tube feet disc extracts using WGA-bounded agarose beads | One-dimensional gel electrophoresis protein profile (**a,c**) and corresponding lectin blot (**b,d**) using LEL-bounded agarose beads non-inhibited **(a,b)** and inhibited (**c,d)**. Abbreviations: E – eluted fraction; M - molecular weight markers; NE – non-eluted fraction; UB- unbound fraction; W1-4 – wash fractions. 24 exposition time. Dashed line indicates the separation between stacking and resolving gel.

With these conditions it was possible to visualized ten well-resolved protein bands in the eluted fraction (**E**), with an apparent molecular weight of 11, 30, 45, 55, 57, 60, 63, 100, 180 and 245 kDa (Figure 15 a.). Of these, only proteins above 30 kDa were detected with WGA lectin blotting, with an intense band at approximately 35, 63 and 75 kDa (Figure 15 b.). The non-eluted (**NE**) fraction presented the same bands, indicating the need for a higher volume of eluting sugar solution to release all WGA-bounded glycoproteins from the beads.

WGA inhibition was partially effective, demonstrated by the presence of several proteins in eluted (**E**) fraction, ranging from 30 to > 245 kDa in the Coomassie gels and blots (Figure 15 c, d). With the inhibited beads, several WGA labelled protein bands are visible in the blots (Figure 15 d) that were absent from the blots with non-inhibited beads (Figure 15 b), confirming there was some inhibition that prevented these proteins from attaching to the beads. However, the inhibition was not complete, allowing some glycoproteins, probably with many chitobiose residues, to attach to the beads in the eluted (**E**) and non-eluted (**NE**) fractions.

4.1.1.3. *Griffonia* (Bandeiraea) *simplicifolia* lectin II pull down assays

GSL II, which detects N-acetylglucosamine (GlcNAc) was previous described to detect glycoproteins in the tube feet discs, with apparent molecular weights of 72 and >180 kDa. GSLII labelled the disc cuticle and adhesive epidermis, as well as the secreted adhesive (Simão et al. 2020).

Table 8 - *Paracentrotus lividus* tube feet disc glycoproteins enrichment using GSL II-bounded agarose beads pull-down assay. Tested condition and results obtained during protocol optimization | a. b. Various volumes of agarose beads and sugar eluting solution were tested to maximize the pull-down of GSL II-bounded glycoprotein. The presence of glycoproteins only in the 1st washing step was considered as a null result. Abbreviations: S - stacking gel, R – resolving gel, CS – Coomassie Brilliant Blue R-250 Staining, LB – Lectin-blotting.

	Griffonia simplicifolia lectin-bounded agarose beads											
	Tested conditions					Obtained results (visualized protein bands)					
	Protein amount	Acrylamide gels	Agarose beads	Elution sugar solution	Sample Buffer	Unbound protein fraction		Eluted protein fraction		Non-eluted protein fraction	
						CS	LB	CS	LB	CS	LB
Precipitated samples	730 µg	S: 4%; R: 12.5%	225 µl (900 µg)	200 (x2) µl	100 µl	≥ 11 kDa	≥ 11 kDa	≥ 11 kDa	≥ 11 kDa	---	---

Due to its binding capacity (4 mg/ml), 900 µg of lectin coated agarose beads corresponded to 225 µl for GSL II. For GSL II pull down assays, we used (730 µg), 2 x 200 µl of eluting sugar elution and 100 µl of sample buffer, to obtain an enriched fraction of GSL II-bound glycoproteins (Table 8).

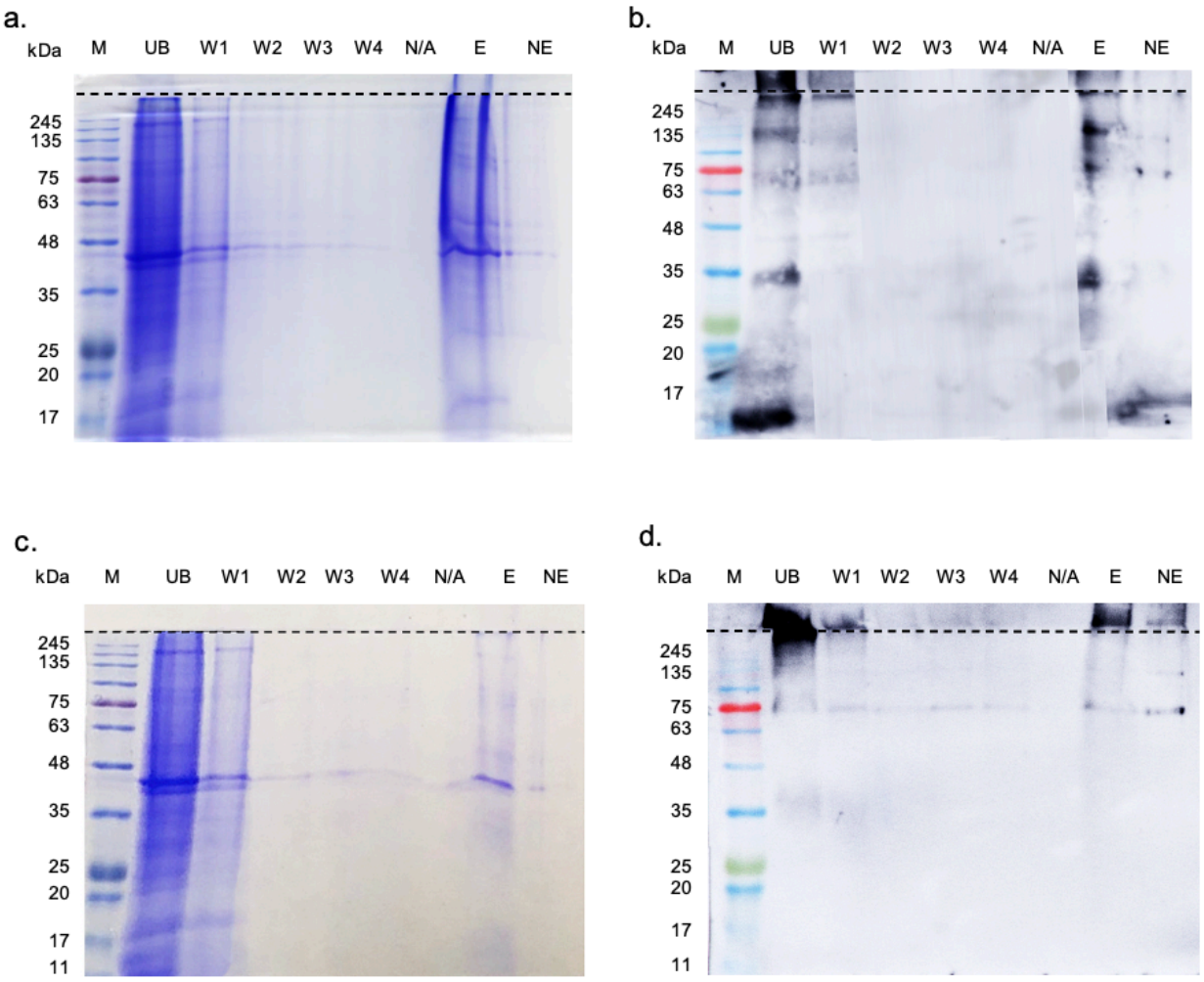

Figure 16 - Pull-down assay of glycoproteins from *Paracentrotus lividus* tube feet disc extracts using GSL-bounded agarose beads | One-dimensional gel electrophoresis protein profile (**a,c**) and corresponding lectin blot (**b,d**) of non-inhibited GSL-bounded agarose beads (**a,b**) and inhibited (**c,d**). Abbreviations: E – eluted fraction; M - molecular weight markers; NE – non-eluted fraction; UB- unbound fraction; W1-4 – wash fractions. 29 seconds exposition time. Dashed line indicates the separation between stacking and resolving gel.

With the above-mentioned conditions, it was possible to distinguish with Coomassie staining several protein bands in the eluted fraction (**E**) with apparent molecular weights ranging from 17 to > 245 kDa (Figure 16 a.). Of these, intense bands were detected by GSL II around 75, 135 and > 245 kDa (Figure 16 b). For this pull-down, almost no glycoproteins were detected in the non-eluted (**NE**) fraction in both the Coomassie and lectin-blot (Figure 16 a, b). However, GSL-II labelled proteins were visible in the unbound (**UB**) and 1st wash (**W1**) fractions, indicating that the volume of beads used was insufficient to capture all GSLII-specific glycoproteins (Figure 16 a, b).

As for the inhibition, it was quite efficient, since less GSL II labelled protein bands were detected in the eluted (**E**) fraction both in the Coomassie gel and the blot (Figure 16 c, d). Concordantly, less proteins were detected by GSL II in the unbound (**UB**), 1st wash (**W1**), and eluted (**E**) fractions in the blot with inhibited beads (Figure 16 d).

4.1.1.4. *Soybean* agglutinin lectin pull down assay

SBA was previously described to detect two glycoproteins in *P. lividus* tube feet discs, with an approximate molecular weight of 75 kDa and 135 kDa. This lectin, which detects N-acetylgalactosamine, labelled the adhesive footprint and the disc adhesive epidermis, targeting microvilosities and the cytoplasm of abundant epidermal cells, most likely support cells (Simão et al. 2020).

Table 9 – *Paracentrotus lividus* tube feet disc glycoproteins enrichment using SBA-bounded agarose beads pull-down assay. Tested conditions and results obtained during protocol optimization | a. b. Various volumes of agarose beads, sugar eluting solution and sample buffer were tested to maximize the pull-down of SBA-bounded glycoproteins. The presence of glycoproteins only the 1st washing step was considered as a null result. Abbreviations: S - stacking gel, R – resolving gel, CS – Coomassie Brilliant Blue R-250 Staining, LB – Lectin-blotting.

	***Soybean agglutinin* lectin-bounded agarose beads**											
	Tested conditions					**Obtained results (visualized protein bands)**					
	Protein amount	**Acrylamide gels**	**Agarose beads**	**Elution sugar solution**	**Sample Buffer**	**Unbound protein fraction**		**Eluted protein fraction**		**Non-eluted protein fraction**	
						CS	**LB**	**CS**	**LB**	**CS**	**LB**
Precipitated samples	730 µg	S: 4%; R: 12.5%	204.55 µl (900 µg)	200 (x2) µl	100 µl	≥ 11 kDa	≥ 11 kDa	≥ 45 kDa	40 kDa, 75 kDa, > 135 kDa	---	---

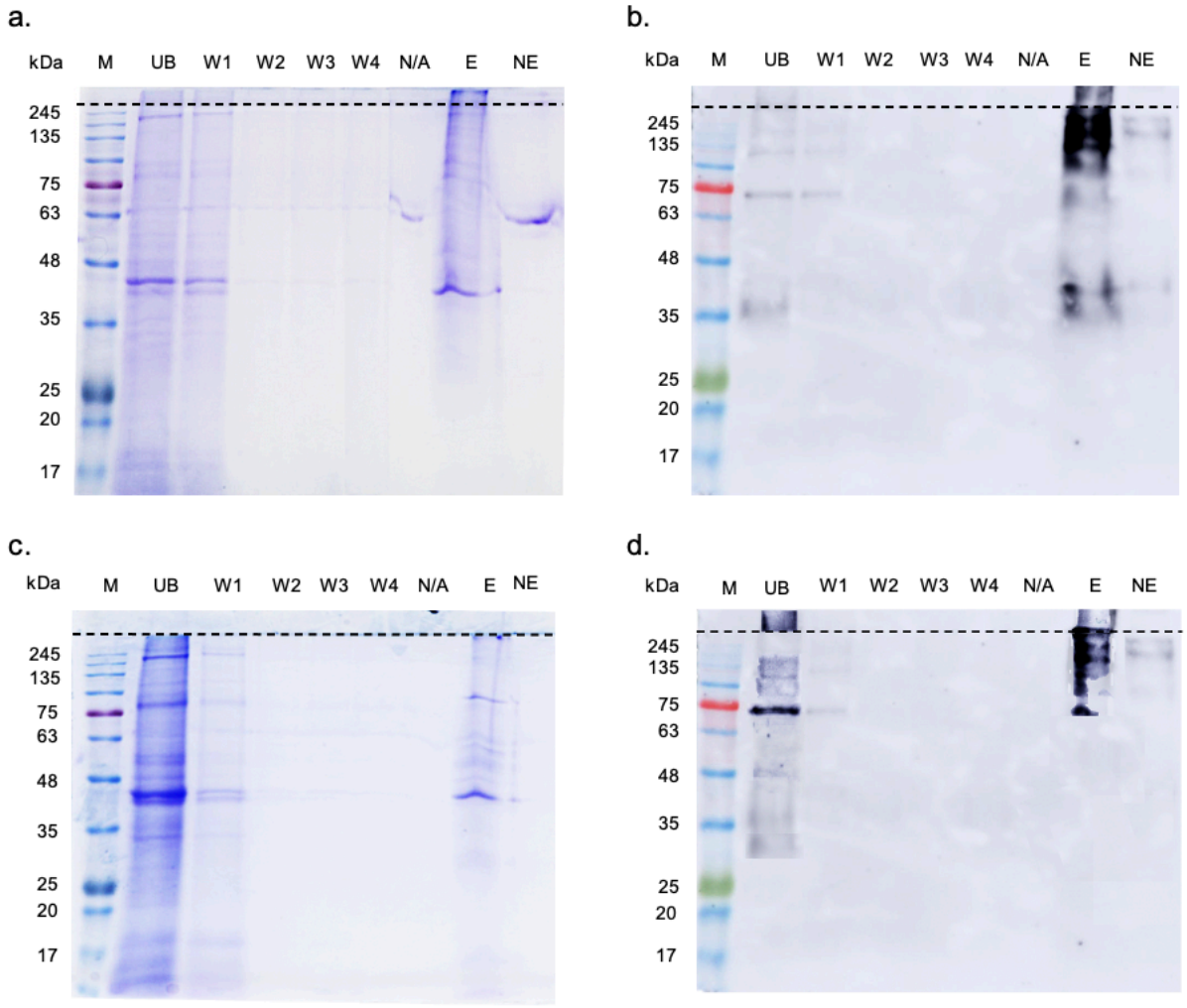

Figure 17 - Pull-down assay of glycoproteins from *Paracentrotus lividus* tube feet disc extracts using GSL-bounded agarose beads | One-dimensional gel electrophoresis protein profile (**a,c**) and corresponding lectin blot (**b,d**) of non-inhibited GSL-bounded agarose beads (**a,b**) and inhibited (**c,d**). Abbreviations: E – eluted fraction; M - molecular weight markers; NE – non-eluted fraction; UB- unbound fraction; W1-4 – wash fractions. 22.4 seconds exposition time. Dashed line indicates the separation between stacking and resolving gel.

The following condition were sufficient to effectively pull-down SBA-bound glycoproteins: 730 μg of protein extract, 204.55 μl of SBA coated agarose beads (binding capacity of 4.4 mg/ml), 2 x 200 μl of eluting sugar solution and 100 μl of sample buffer.

With the above-mentioned conditions, it was possible to visualize with Coomassie staining protein bands in the eluted fraction (**E**) with apparent molecular weights above 45 kDa (Figure 17 a.). Of these, SBA lectin blotting detected protein bands around 40, 75 and an intense band above 135 kDa and > 245 kDa. Despite the lower acrylamide percentage used, some glycoproteins of interest did not entirely enter the resolving gel, being retained in the stacking gel (Supplementary Figure 5).

The inhibition of SBA-coated agarose beads inhibited with 900 μl of eluting sugar solution, proved to be efficient, causing a decrease in the protein amount of the eluted I fraction in the Coomassie gels (Figure 17 a), as well as a lower number of glycoproteins detected by

SBA in the blots (Figure 17 b). Similarly, to WGA, inhibition of the beads increased the amount of proteins detected by SBA in the unbound (**UB**) fraction (Figure 15 d), indicating that they failed to bind to the agarose beads.

These results show that although we used three lectins that detect N-acetylglucosamine (GlcNac), they have different glycan specificities. GSL II, the less specific, detected the presence of GlcNac, whereas WGA and LEL detected GlcNac in a specific chitobiose arrangement (i. e. a dimer of β-1,4-linked glucosamine units). WGA detects up to two GlcNacβ(1,4)GlcNac units, while LEL can detect up to four chitobiose units.

GSL II pull-downs pin-pointed several glycoproteins containing GlcNac, with an approximate molecular weight of 75, 135 and >245kDa, thus expanding the number of previously reported glycoproteins (72 and >180kDa) (Simão et al., 2020). This can be due to the higher amount of protein used (47,02 μg of an enriched GlcNac-conjugated fraction instead of 20 μg adhesive disc protein extract used by Simão et al. 2020), a direct consequence of protein precipitation and pull-down enrichment. WGA detected glycoproteins with up to two units of chitobiose ranging from 35 to > 245 kDa. LEL detected glycoproteins with up to four units of chitobiose only above 135 kDa.

Our results show that GlcNac in its simple form, was the highest abundant glycan linked to disc proteins (the volume of GSL-bounded agarose beads was insufficient to pull-down all glycoproteins), followed by chitobiose up to two units (the volume of eluting sugar solution was insufficient to release all the glycoproteins pulled-down by WGA-bounded agarose beads) and then, chitobiose up to four units (LEL pulled down specifically a higher molecular weight protein). This is in agreement with (i) the inverse relation observed between protein bands and lectin specificity (Figure 14 – 16), and (ii) previous immunohistochemistry results showing that LEL produces the most specific labelling within the disc adhesive epidermis, targeting the secretory granules (Simão et al., 2020). Inhibition differences can be related with the capacity of the used sugar solution to inhibit the different lectins. Simão et al. (2020) reported full inhibition of WGA, partial inhibition of LEL and unsuccessful inhibition of GSL II and SBA using single sugars. In the present study, we used a mixture of several sugars indicated to elute glycoproteins from agarose-bound N-acetylglucosamine- or chitin-binding lectins and from agarose bound Galactose/GalNAc binding lectins. This might explain the improvement of inhibition of GSLII, LEL and SBA.

It should be stressed that despite their specificities, these three lectins (GSL II, WGA and LEL) pulled-down high molecular weight glycoproteins (>245kDa) that didn't enter the resolving gel, even decreasing the acrylamide concentration to 3.5 % and 7.5%, respectively, in the stacking and resolving gel (Supplementary Figure 4-5).

Recent studies with other aquatic animals, showed that (i) temporary adhesives are mixtures of several proteins; including (ii) large cohesive proteins and (iii) smaller adhesive proteins; some of which are (iv) glycoproteins that segregate in the outer rim of the adhesive secretory granules (Wunderer et al. 2019, Simão et al. 2020).

Spf1 (Uniprot X2KZ73), a major cohesive protein involved in footprint cohesion of the sea star *A. rubens*, has a calculated molecular mass of 428kDa (Hennebert et al. 2014). Large proteins that make the structural core of the adhesive footprint tend to be more conserved between closely related species, as demonstrated for the Class Asteroidea (Lengerer et al. 2019). However, new candidate adhesive proteins recently discovered (Pjeta et al. 2020) for the sea urchin *P. lividus*, are orthologs of sea star genes, which advocates for the conservation of large structural proteins in the temporary adhesives of Echinodermata. Similarly, in another Phylum, it was confirmed that temporary attachment of the flatworm *M. lignano* relies on two large proteins, the cohesive Mlig-ap1 (Uniprot A0A411ACX2) and the adhesive Mlig-ap2 (Uniprot A0A411ACY6), expressed in the adhesive cells. (Wunderer et al. 2019) Recently, these two proteins were found in another species of the same genus, *M. poznaniense* (Mpoz-ap1 and Mpoz-ap2) and in the more distant species *Minona ileanae* (Mile-ap3) sharing high sequence similarity (Davey et al. 2020). Therefore, it has been proposed that in large structural proteins the selection pressure is high for the conservation of functional domains, while in surface-binding proteins the relative amino acid composition is more important than the primary sequence (Lengerer et al. 2019; Davey et al. 2020).

The presence of glycoproteins segregated in the outer rim of secretory granules has been reported for the sea urchin *P. lividus* (Simão 2020), the flatworm *Macrostomum lignano* (Lengerer et al. 2016; Wunderer et al. 2019) and the sea star *Asterina gibbosa* (Lengerer et al. 2018). However, the attached glycan is quite variable: chitobiose in sea urchins (Simão et al. 2020), N-acetylgalactosamine, N-acetylglucosamine, galactose, fucose and sialic acid in sea stars (Sfp-210kDa, Sfp-290KDa) (Hennebert et al. 2011) and Gal-β(1–3)-GalNAc in flatworms (Mlig-ap2) (Wunderer et al. 2019).

SBA-pull downs have confirmed that sea urchin adhesive disc contain glycoproteins with N-acetylgalatosamine residues. However, unlike Simão et al. (2020) that only detected two glycoproteins at 72 and 135kDa, the present study revealed the presence of several high molecular weight glycoproteins > 135kDa in the eluted fraction. The recurrent labelling of these two glycoproteins (72 and 135kDa) with multiple lectins, targeting mainly the cytoplasm and microvilosities of abundant cells in the adhesive epidermis, led Simão and colleagues (2020) to hypothesize that they were components of support cells instead of secretory cells. Still, an indirect involvement in adhesion cannot be discarded since, the knock-down of a support-cell-specific protein in the flatworm *M. lignano*, produced a non-adhesive

phenotype, without influencing the production or secretion of the adhesive proteins (Wunderer et al. 2019).

Having verified that the obtained enriched fractions actually correspond to an affinity of the glycoproteins for the tested lectins, we proceeded with the identification by mass spectrometry of the proteins contained in each eluted fraction.

4.2. Glycoproteins identification by mass spectrometry

For proteomic analyses, proteins were extracted from two independent pull-downs for each of the four tested lectins. The protein contents of each pull-down were analysed by mass spectrometry and the obtained MS/MS data searched against the translated sea urchin tube foot transcriptome recently published by Pjeta et al (2020).

Computational analysis of the acquired MS/MS spectra showed a highest number of hits (i. e. 1250 proteins found in the sample) for GSL II, followed by WGA (1222 hits) and LEL (1189 hits), reinforcing the already mentioned increasing specificity of these lectins. A total hit of 1074 proteins were obtained for SBA. Of these, we only analysed hits with more than one unique peptide, since a higher number of peptides observed for a given protein increases the probability of identifying that protein correctly (Baldwin 2004; Tabb et al. 2013).

In accordance with Lebesgue et al. (2016), blasted proteins are involved in (i) cytoskeleton organization, (ii) metabolism, (iii) secretory pathways, (iv) transcription/translation processes and protein biosynthesis and (v) putative components of the adhesive secretions (Figure 18). However, despite the high number of protein hits, they correspond to a sub-set of the adhesive disc proteins, i.e. the glycoproteome due to the pull-downs procedures that capture only the protein that are bound to specific glycans. In fact, O-linked attachment of β-N-acetyl-glucosamine (O-GlcNAc) on serine and threonine residues of nuclear and cytoplasmic proteins has been reported as an important posttranslational modification, playing a key role in signal transduction pathways (Lima et al. 2009).

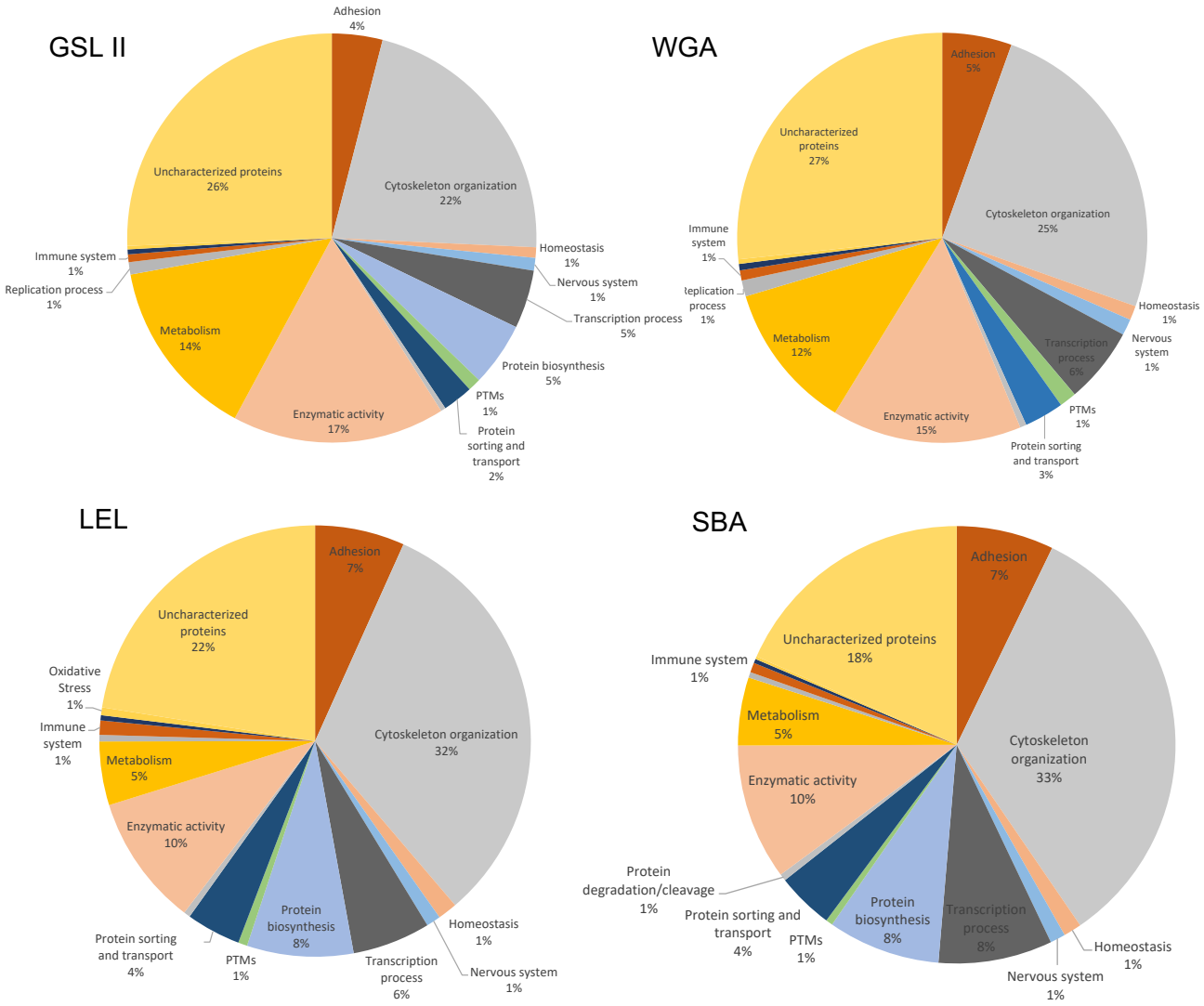

Figure 18 – GO annotation of *Paracentrotus lividus* pulldown proteins

To focus our analysis on potential cohesive/adhesive glycoproteins, we searched for the 16 candidate proteins proposed by Pjeta et al. (2020), that were selected based on their similar expression pattern consistent with the location of the adhesive cells, together with their putative functions based on the obtained BLAST hits and domain prediction. Within these, six candidate proteins were more promising since orthologous adhesion-related genes were found in the sea star *Asterias rubens*.

Of these 16 candidates, six were present in all of our samples: Nectin variant 2 precursor, alpha-2-macroglobulin-like protein 1, alpha-tectorin, myeloperoxidase and a uncharacterized protein LOC115927989 (Table 10). The sequence coverage and unique peptides were taken into consideration due to a peptide preferential ionization in MS/MS data (i. e. peptides derived from low abundance proteins are more difficult to detect, needing a higher number of fragment ion spectra to be acquire to increase identification coverage rate) (Eriksson and Fenyö, 2007; Huang et al., 2012).

Table 10 – Candidate adhesive proteins MS/MS and BLAST results | Abbreviations: COV: sequence coverage (%); MW: molecular weight (kDa); pI: isoelectric point

	Blast (Pjeta et al. 2020)	Our Blast	GSL II 1	GSL II 2	WGA 1	WGA 2	LEL 1	LEL 2	SBA 1	SBA 2	Unique peptides	MW	pI	Completeness sequence
			COV	COV	COV	COV	COV	COV	COV	COV				
TR60905_c1_g1_i1_5	Nectin variant 2 precursor [Paracentrotus lividus]	Nectin 2 [Paracentrotus lividus]	39	35	41	33,9	37	31	39	35	40	108,24	5.98	full length
TR63383_c2_g1_i1_5	PREDICTED: alpha-tectorin [Strongylocentrotus purpuratus]	Uncharacterized protein LOC100892803 [Strongylocentrotus purpuratus]	9	6	10	0,5	8	4	15	12	21	199.71	5.43	5' missing
TR46688_c0_g1_i1_6	PREDICTED: uncharacterized protein LOC100892803 [Strongylocentrotus purpuratus]		12	10,1	7	5,1	11	11	13	5	9	74.09	4.81	5' & 3' missing
TR57217_c2_g1_i1_5	PREDICTED: myeloperoxidase [Strongylocentrotus purpuratus]	myeloperoxidase [Strongylocentrotus purpuratus]	5	5	10,5	12,7	3,0	4	8	8	9	132.28	9.37	full length
TR61622_c8_g1_i2_4	PREDICTED: alpha-2-macroglobulin-like protein 1 isoform X1 [Strongylocentrotus purpuratus]	alpha-2-macroglobulin-like protein [Strongylocentrotus purpuratus]	10	10	10,6	9,8	11	10	14	11	29	157,63	5.15	full length
TR46467_c1_g1_i2_6	N/A	Uncharacterized protein LOC115927989 [Strongylocentrotus purpuratus]	25	x	24,6	x	14	25	19	27	8	43.6	8.65	full length

Of these, Nectin (TR60905_c1_g1_i1_5) was the first identified protein in every MS/MS spectrum, with the highest sequence coverage (31% up to 41%), with a total of 40 unique peptides (Supplementary Table 2). Our results indicate that it's a highly glycosylated protein (high coverage in each pulldown) containing GlcNac, chitobiose and GalNac residues (identification in the four lectin pulldowns).

A lower number of unique peptides was obtained for alpha-tectorin-like protein TR63383_c2_g1_i1_5 and TR46688_c0_g1_i1_6) and alpha-2-macroglobulin protein (TR61622_c8_g1_i2_4) (Supplementer Table 3-4). A lower sequence coverage indicates that these proteins can be large proteins, in which, few peptides are commonly ionized. While alpha-tectorin seems to have a higher number of quitobiose units (up to four units) and GalNac residues (lower coverage in WGA-bounded agarose beads pulldowns), alpha-2-macroglobulin appears to have a similar amount of different sugar residues (Table 10).

The lowest number of unique peptides (Supplementary Table 6 and 7) was registered for both uncharacterized protein LOC 115927989 and myeloperoxidase, most likely because they are poorly glycosylated proteins.

The new BLAST analysis allowed us to improve the annotation of these cohesive/adhesive candidate proteins. For instance, TR46688_c0_g1_i1_6 and TR63383_c2_c2_g1_i1_5, were previously identified as two different proteins, namely an uncharacterized protein LOC100892803 and an alpha-tectorin (Table 10). We found that these two transcripts correspond to two different parts of a large alpha-tectorin-like protein, homologous to an uncharacterized protein LOC100892803 from the sea urchin *Strongylocentrotus purpuratus*. TR46467_c1_g1_i2_6, formerly with no know homology, is now annotated as homologous to an uncharacterized protein LOC115927989 of *S. purpuratus*. In the following sub-chapters, the results obtained for these six adhesive protein candidates are discussed in more detail.

4.2.1. A third Nectin isoform is involved in *Paracentrotus lividus* adhesion and/or cohesion

Pjeta and colleagues (2020) selected transcript TR60905_c1_g1_i1_5, identified as Nectin variant 2, based on its over-expression at the adhesive disc relatively to the non-adhesive stem, its localization on the adhesive epidermis and footprint, and the presence of an orthologue gene in sea stars (Arub-27). This protein is so far the only confirmed adhesive protein in sea urchins, for which two variants have been already described (Matranga et al. 1992; Lebesgue et al., 2016; Toubarro et al., 2016).

It's a 108 kDa glycoprotein (Figure 14-17; Table 10) and can form dimers (Matranga et al 1989). We showed that it most likely contains chitobiose and GalNac residues. This in in agreement with previous reports of several glycosylated Nectin isoforms (Santos et al., 2013), but expands the current knowledge by revealing the type of residues involved in its glycosylation.

Protein identification showed that TR60905_c1_g1_i1_5 presents 99.1% similarity with Nectin variant 2 (Uniprot A0A182BBB6) and 98.4% with Nectin variant 1 (Uniprot Q70JA0), thus indicating that it might corresponds to a 3rd variant.

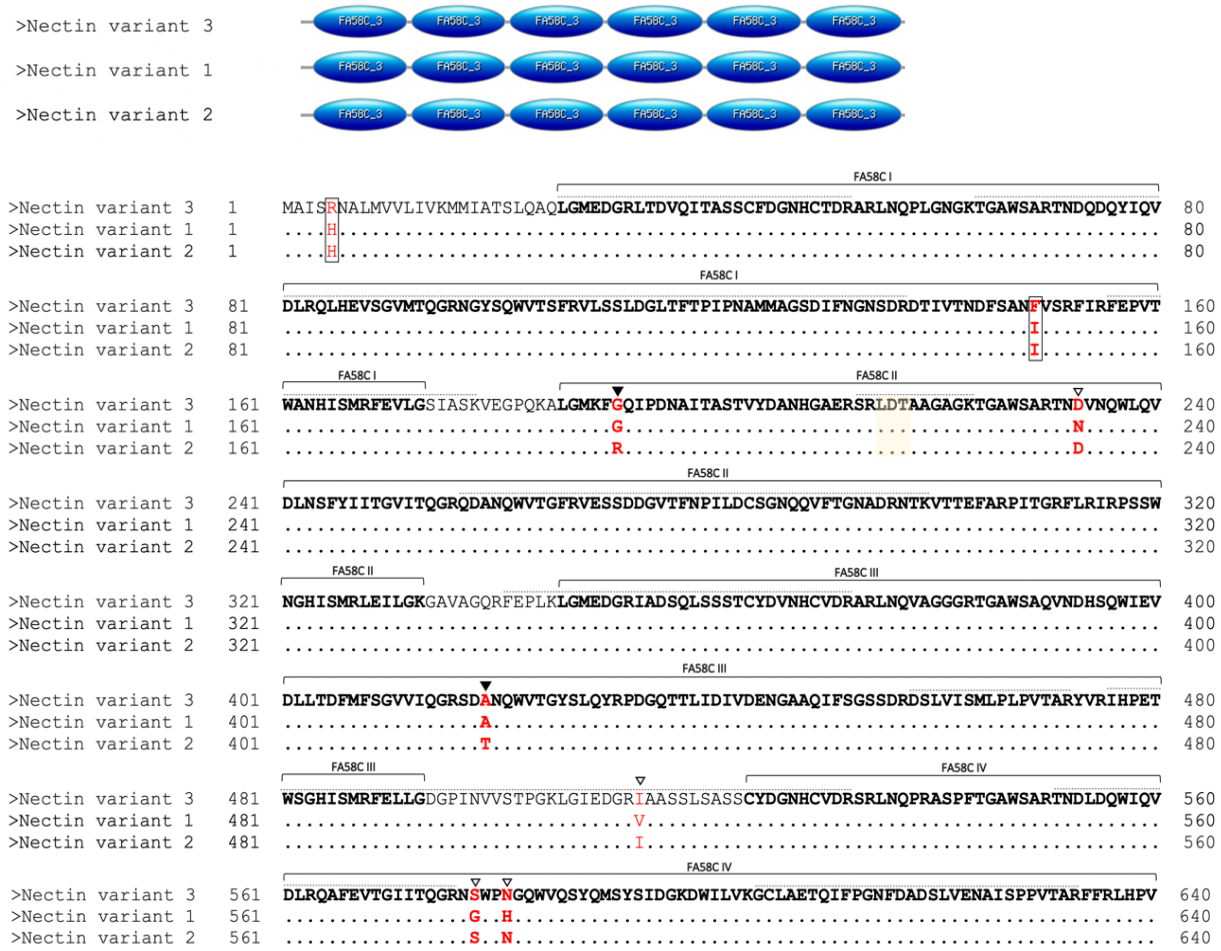

Figure 19 – Protein alignment of Nectin variants identified in adults *Paracentrotus lividus* tube feet | Nectin variant 1 [Uniprot Q70JA0] and Nectin variant 2 [Uniprot A0A182BBB6] were previously annotated by Matranga et al. 1989 and Toubarro et al. 2016. Amino acids in black and red, indicate, respectively, common and dissimilar residues between the three Nectin sequences. LDT, integrin binding site, is identified in yellow.

To confirm this possibility, we aligned the three sequences. Figure 19 shows (i) the amino acids discrepancies (pinpoint in red), (ii) the location of the FA58C domains (emphasized in bold) and (iii) the peptides identified by MS (dashed line over the amino acids). We found that transcript TR60905_c1_g1_i1_5 has higher similarity to variant 2, with only 8 amino acid substitutions, than variant 1 (13 amino acid substitutions). Between the three sequences 18 substitutions were detected, 16 of them within the domains. MS/MS analysis allowed us to confirm the existence of a 3rd variant of Nectin, confirming 7 of the 18 amino acid substitutions. A LDT sequence (Leu-Asp-Thr), at position 215-217 (Figure 19) proposed as an integrin receptor binding site by Costa et al. (2010), was present in all sequences,

All variants contain six tandemly repeated discoidin domains (FA58C), similar to C1/C2 domains present in the blood coagulation factors V and VII (Costa et al., 2010). These repeated domains were similar (46.7 up to 55% similarity), with some conserved amino acids. The modifications between variants occur near these conserved locations, with a maximum of ten amino acids apart, possibly impacting protein molecular features (Table 11), tertiary structure (Figure 20) and/or post-translational modifications (Figure 21).

Table 11 – Molecular features of Nectin variants identified in *Paracentrotus lividus* tube feet | Abbreviations: GRAVY: grand average of hydropathy; MW: molecular weight; pI: isoelectric point.

Seq ID	Amino acid composition (%)	Total number of negatively charged residues	Total number of positively charged residues	Instability index	Aliphatic index	GRAVY	MW	pI
Nectin variant 3	Ser (8.8%), Gly (8.3%), Ala (7.9%), Leu (7.6%), Thr (7.2%), Val (6.9%)	(Asp + Glu): 95	(Arg + Lys): 84	26.99 (stable)	81.08	-0.272	108,24	5,98
Variant 1	Ser (8.6%), Gly (8.4%), Ala (8.0%), Leu (7.6%), Thr (7.0%), Arg (6.8%)	96	85	28.01 (stable)	80.99	-0,283	108,25	6,01
Variant 2	Ser (8.8%),Gly (8.2%), Ala (7.9%), Leu (7.6%), Thr (7.2%), Val (6.8%)	96	84	27.80 (stable)	81.18	-0.284	108,35	5,95

In all variants, the most abundant amino acids are serine (Ser), glycine (Gly) and alanine (Ala). Total negative and positive charged residues were considered due to its impact on isoelectric point (pI) and GRAVY. Instability index refers to a protein *in vitro* stability,

indicating that Nectin is predicted to be stable. Aliphatic index is defined as the relative volume occupied by aliphatic side chains (alanine, valine, isoleucine and leucine), being possibly related with the structural stability of globular proteins. A high aliphatic index, as verified in the three variants, indicates that Nectin is thermo-stable over a wide temperature range. GRAVY depends on the hydropathy (either hydrophobicity or hydrophilicity) values of all amino acids present in the sequence. The three variants have a negative GRAVY, indicating that Nectin is a hydrophilic protein. The three variants have a theoretical pI around 6, indicating that Nectin is negatively charged upon secretion into seawater (pH = 8). Differential pH between the secretory granule and water has been proposed as a trigger for bioadhesive gelation (i. e. gel-transition) (Hennebert et al., 2014). Predicted molecular weight (approximately 108kDa) is in agreement with previous research (Costa et al., 2009, Santos et al., 2013, Lebesgue et al., 2016). All sequences are predicted to be secreted, with a likelihood of 0.9158 (variant 1), 0.9158 (variant 2) and 0.9181 (variant 3).

Having a highly similar amino acid composition (Table 11), 3D-structure prediction showed the impact of punctual amino acid modifications across the domains, since protein tertiary structure is determined by intramolecular noncovalent interactions, resultant from the distinctive chemical properties of amino acid side chains. Whereas hydrophilic amino acid side chains can interact with water, hydrophobic amino acid side chains tend to be in the interior of the protein (Dyson et al., 2006; Lodish, 2000)

Of the 18 substitutions observed (Figure 19), only five maintained their physicochemical properties, being considered as conservative (Supplementary Table 7). Due to hydropathicity differences, the observed amino acid modifications can lead to a spatial rearrangement of the domains in which they occur (Figure 20). Of note, only glycine/serine substitution occurred more than once (578th, 765th and 777th position). While serine is hydrophilic, glycine forms highly hydrophobic core. This substitution bias could be explained by a single point mutation in serine first codon position (in one of the two disjoint sets codifying for serine), leading to a glycine modification (Schwartz et al., 2019).

For each variant the following aspects were analysed: (i) secondary structure prediction, influencing the conformation acquired during protein folding, (ii) co-localization of non-conservative amino acids modifications, to access their effect on secondary and tertiary protein structures, (iii) domains and (iv) protein surface (Figure 21).

For the best of our knowledge, this is the first *P. lividus* adults tube feet Nectin 3D representation based on its actual protein scaffold. A previous representation (Costa et al. 2009) was generated by homology-based fold predictions, based on a medium-accuracy comparative model (30-50% sequence identity).

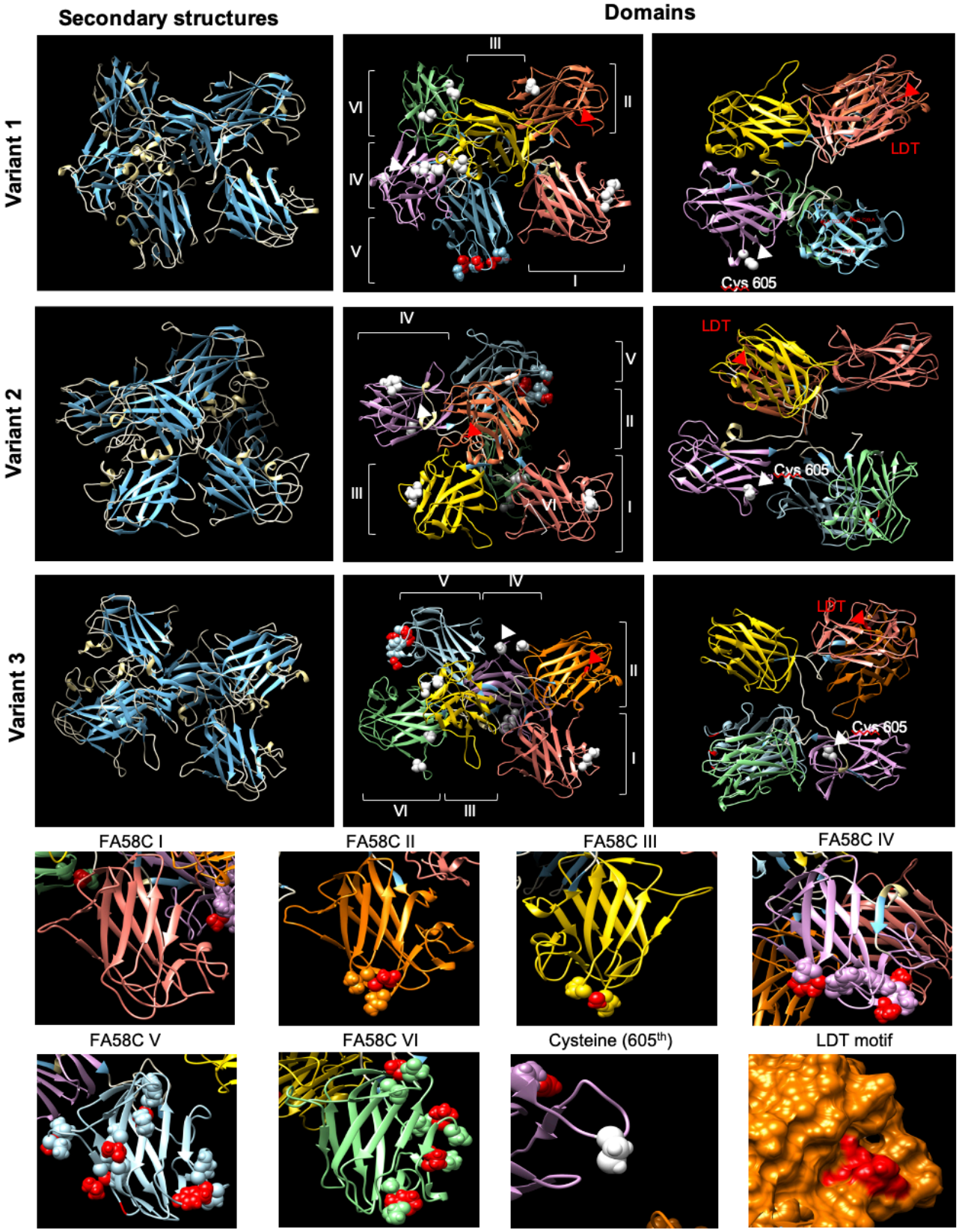

Figure 20 – Three-dimensional structural prediction of Nectin variants identified in *Paracentrotus lividus* tube feet | a. Nectin variant 1 **b.** Nectin variant 2 **c.** Nectin variant 3. | Legend: In the first column, secondary structures are identified in blue (β-sheets), in yellow (α helix) and in white (coiling structures). In the second column, the fixe domains are identified in pink (FA58C I), orange (FA58C II) yellow (FA58C III), purple (FA58C IV), blue (FA58C V) and green (FA58C VI). Cysteines are represented in white spheres and the LTD motif is identified in red. Third column presents all variants with FA58C I at the top right of each image. Small images, at the bottom of the panel, show in detail domains structure, cysteine proposed as responsible for Nectin homodimerization and LDT sequence location. Amino acids substitutions are identified in in red).

In a homology-based fold prediction, FA58C V was the only domain to present a jelly-roll β-sheet of five and three strands packed against each other (Costa et al., 2009). The authors also reported adjacent loops at the bottom of the *β*-barrel. We improved this prediction model, performing a structural analysis considering local environments created by the amino acid scaffold. This new analysis showed a similar jelly-roll *β*-sheet structural arrangement in all of the domains (Figure 20). These *β*-sheet rich structures observed in all variants (due to an amino acid preference) are a common feature of discoidin domains (FA58C) (Lefevre et al., 2020; Bhattacharjee and Biswas, 2010). For each domain, at the bottom of these structures, we also identified loop regions, which were proposed as membrane contact point, as in human coagulation factor V C2 domain (Costa et al., 2009).

With an irregular tertiary structure in C-like shape (Figure 20, 3rd column), each variant showed a different spatial organization regarding their domains (Figure 20, 2nd and 3rd column). These structural modifications could be due to the above-mentioned amino acid substitutions since the only unaltered domain (FA58C I) had conservative amino acid modifications.

The majority of the non-conservative modifications occur in the apex of the loops (Figure 20). For FA58C II, the substitution of a hydrophilic asparaginase (N233) by a hydrophobic aspartic acid (D233) lead to a different folding, in which this domain is buried in the interior of the protein in variant 2. Amino acid substitution in FA58C III is in agreement with this line of thought, since the substitution of a hydrophilic alanine (A419) by a hydrophilic threonine (T419) in the membrane contact point, didn't alter its spatial organization. It seems to be a controlled process. The fourth domain has amino acid substitutions in β-sheets involving threonine and serine modifications, being possibly implicated in post-translational modifications.

All variants have a low cysteine content (1.1%), with no cysteines in FA58C V, one in FA58C II, two in FA58C I and III and three in FA58C IV and VI. Based on their spatial distance shown in Figure 19, the predicted S-S bridges are FA58C I cys43-cys49, FA58C III cys363-cys369, FA58C IV cys523-cys529 and FA58C VI cys927-cys956. The remaining cysteines (FA58C II cys283, FA58C VI 927 and FA58C IV cys605) since they are spatially distant. These results are in agreement with the homology-based prediction made by Costa et al (2009). Being consistently in the outer surface in all variants (Figure 20), cysteine (605th) seems to be responsible for Nectin homodimerization. All proteins have a LDT (integrin binding) motif, in the second discoidin domain, at the protein surface. The presence of all these features, seems to indicate a preserved function between variants. Structural differences could be related with post-translational modifications (Figure 21).

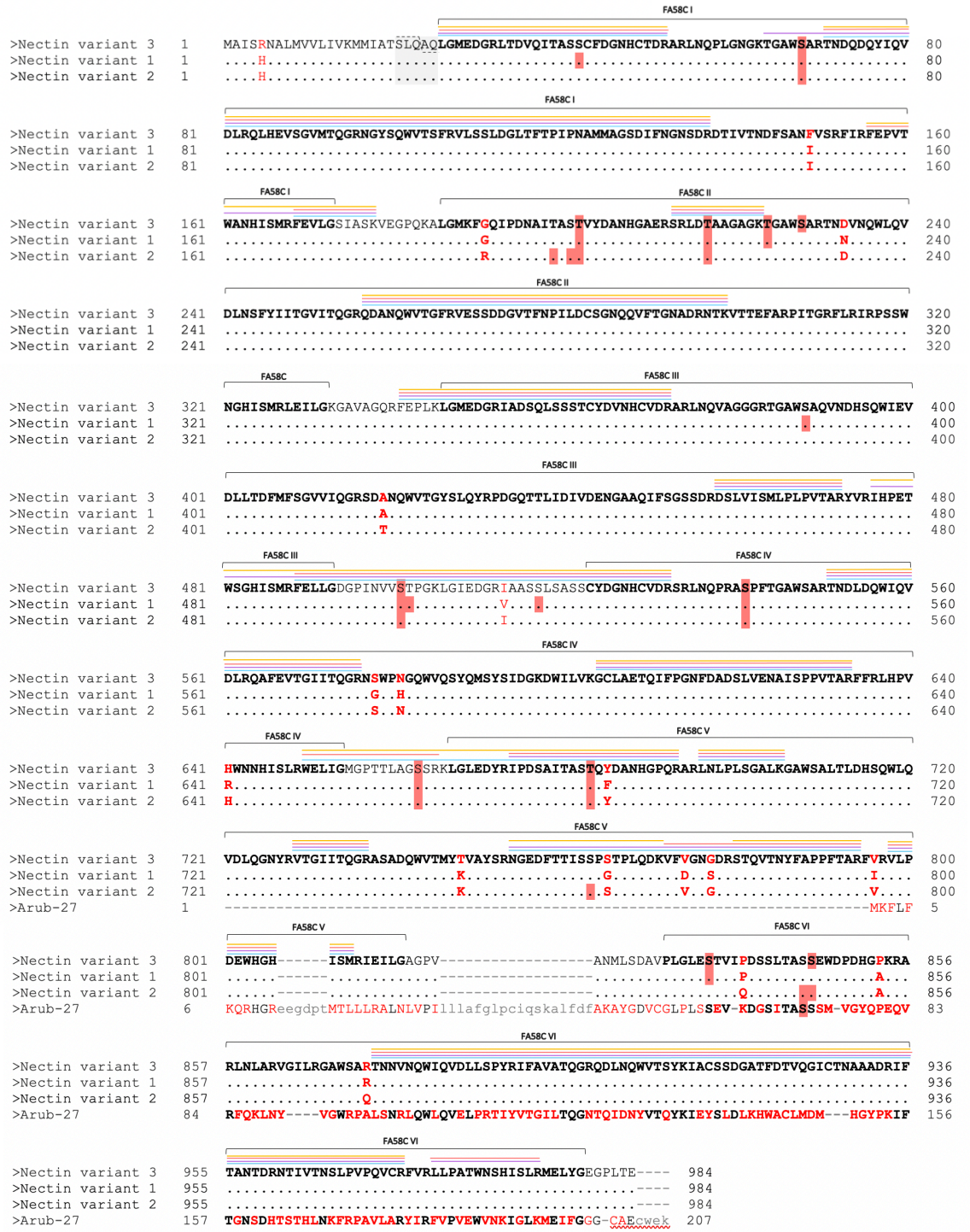

Figure 21 – N- and O-glycosylation prediction of aligned Nectin variants (*Paracentrotus lividus*) and Arub-27 (sea star *Asterias rubens*) | Nectin variant 1 [Uniprot Q70JA0] and Nectin variant 2 [Uniprot A0A182BBB6] were previously annotated by Matranga et al. 1989 and Toubarro et al. 2016. Arub-27 was previously annotated by Hennebert et al 2014. N-glycosylation sites are identified in purple, while O-glycosylation sites are in pink. Identified peptides by MS/MS, dashed over text, are identified in blue (GSL II), purple (LEL), pink (WGA) and orange (SBA).

According to prediction results (Figure 21), Nectin variants are O-glycosylated. However, our results, using N-glycan specific lectins, indicate that it also contains N-glycosylation. These different results could be due to the threshold used for the predictions (>

0.5, default threshold). Even considering only O-glycosylation, variants presented a different number of predicted glycosylated residues (four possible glycosylation sites were validated by MS/MS).

Adhesive protein variants have been reported in freshwater (Rees et al., 2019) and in marine (Floriolli et al., 2000; Lu et al., 2013; DeMartini et al., 2017; Anand and Vardhanan, 2020) mussels. Peroxidase variants, proposed as a crosslinking agent in marine adhesion, was also described in hydra temporary adhesion (Rodrigues et al., 2016).

Being a common phenomenon in underwater adhesion, nucleotide substitutions (SNPs) occurring during DNA replication due to high gene expression (Toubarro et al., 2016) seems improbable. The fact that the modifications occur in one nucleotide instead of a sequence portion, also discards RNA splicing. As such, we propose that Nectin variants result from RNA editing as a strategy to improve adhesion versatility, producing multiple forms of an adhesive protein that can be fine tunned to interact with surfaces with different chemical properties and conformations (Zhao et al., 2006; Stewart et al., 2011; Gantayet et al., 2014; Rees et al., 2019).

4.2.2. Alpha-2-macroglobulin-like protein is poorly glycosylated and can have an adhesive, structural or protective role in *P. lividus* adhesion

Based on its localization in the adhesive epidermis and the presence of an orthologue gene in sea stars (Arub-13), TR61622_c8_g1_i2_4 transcript was proposed as a candidate adhesive protein by Pjeta and colleagues (2020). Both pull-downs, MS data and *in silico* analysis shows alpha-2-macroglobulin is most likely a glycoprotein, containing chitobiose and GalNac residues (Figure 22). Protein identification indicated a 70.1% similarity with *Strongylocentrotus purpuratus* alpha-2-macroglobulin-like protein (NCBI XP_011676138.2). These two proteins presented interspecific amino acid differences, of which 62 substitutions were confirmed by mass-spectrometry.

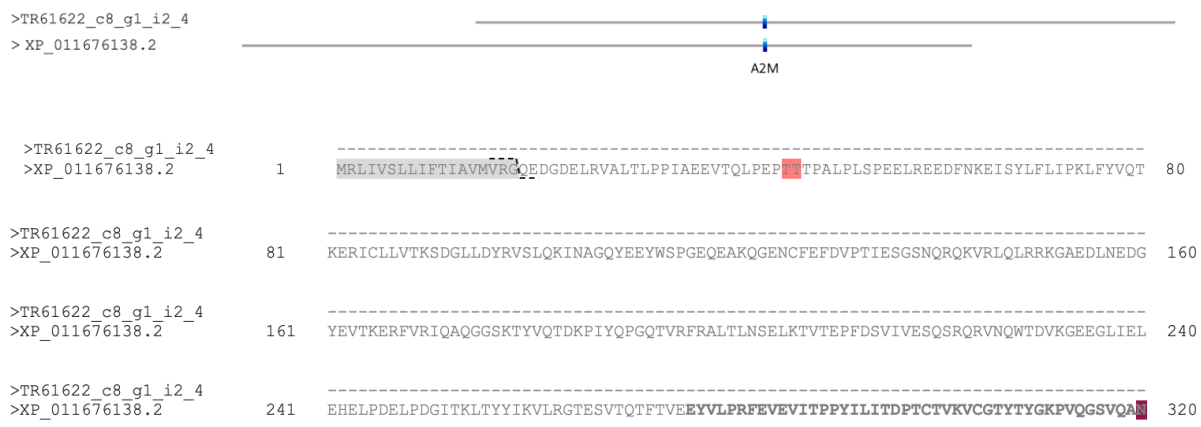

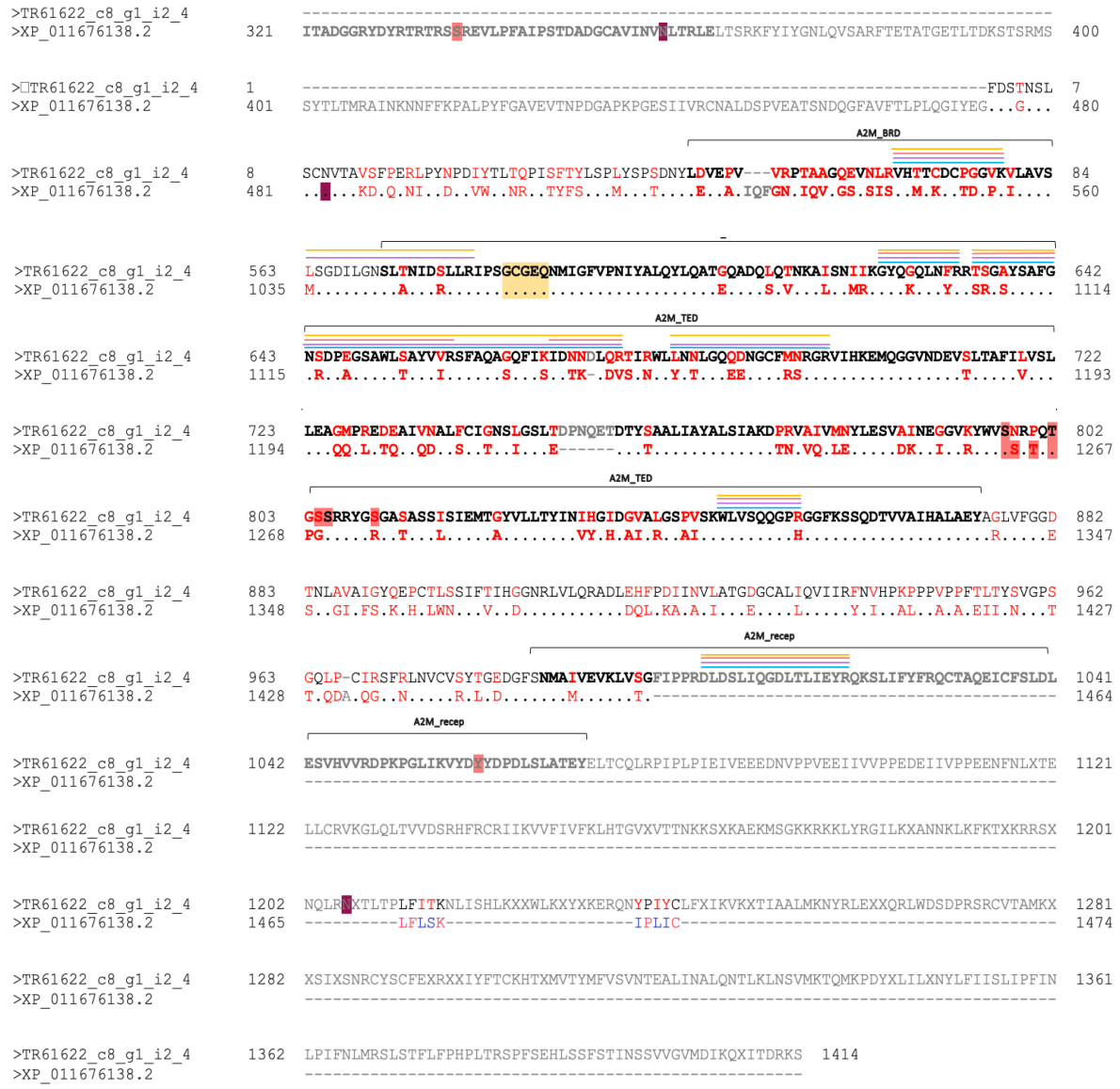

Figure 22 – Protein alignment alpha-2-macroglobulin like proteins of *Paracentrotus lividus* and *Strongylocentrotus purpuratus* | Amino acids in black and red, indicate, respectively, common and dissimilar residues between both sequences. N-glycosylation sites are identified with purple, while O-glycosylation sites are in pink. Highly cleaved site (GCGEQ) identified in yellow. Identified peptides by MS/MS, dashed over text, are identified in blue (GSL II), purple (LEL), pink (WGA) and orange (SBA).

The alignment of both sequences (Figure 22), allowed us to demonstrate that (i) the 5' end of TR61622_c8_g1_i2 transcript wasn't sequenced in the tube foot transcriptome and (ii) there's a possible interspecific difference regarding the size of these proteins (see Table 12). Interspecific sequence variation, was also observed in sea stars and barnacle candidate adhesive proteins (Jonker et al., 2014; He et al., 2018; Lengerer et al., 2019). It has been proposed that having an exact amino acid match might not be necessary, since functional conservation could be achieved through similar biochemical properties, like similar amino acid composition or post-translational modifications (e.g. glycosylation) rather than sequences similarity (Lengerer et al., 2019).

Both alpha-2-macroglobulin-like proteins, *S. purpuratus* have a predicted signal peptide with 18 residues (0.9939 likelihood, with a 0.9609 certain of cleavage site) while *P. lividus* transcript (TR61622_c8_g1_i2) does not (0.0587 likelihood) (Figure 22). Alpha-2-macroglobulin-like proteins are usually extracellular (Pjeta et al., 2020). As such, the absence of a signal peptide in *P. lividus* alpha-2-macroglobulin-like protein is more likely due to the incomplete transcript sequencing (5' end missing) and thus, it's possible that this protein is also routed to the secretory pathway.

Four different macroglobulin domains were predicted in both sequences: (i) alpha-2-macroglobulin bait region (A2M_BRD), (ii) alpha-2-macroglobulin (A2M), (iii) alpha-2-macroglobulin thiol ester-containing domain (A2M_TED) and (iv) alpha-2-macroglobulin receptor binding domain (A2M_recep). The first three domains are implicated in protease inhibition. While A2M is responsible for protease recognition, A2M_TED mediates the covalent binding between A2M protease complex thought the cleavage of a short highly conserved region (e. g. GCGEQ), present in all the aligned sequences, at the moment of protease binding (Figure 21). Bait region (A2M_BRD) is then cleaved, followed by a large conformational change that blocks the target protease within a cage-like complex, substantially decreasing access to protein substrates (Wong and Dessen 2014).

The identification of a alpha-macroglobulin-like protein which acts as a protease inhibitor, is in agreement with the enzymatic adhesion/de-adhesion model proposed for sea urchins (Lengerer and Ladurner 2018; Pjeta et al. 2020). Recent studies have identified a number of highly expressed proteases and glycosidases in *P. lividus* adhesive discs, which are believed to be putative de-adhesive proteins (Lebesgue et al., 2016). Having a protease inhibitor would provide control of the proteolytic action of the de-adhesive secretion and/or inactivate microbial proteases to protect the footprint from degradation.

Seq ID	Amino acid composition (%)	Total number of negatively charged residues	Total number of positively charged residues	Instability index	Aliphatic index	GRAVY	MW	pI
>TR61622_c8_g1_i2_4	Leu (9.2%), Val (7.9%), Ile (7.7%), Ser (7.2%), Gly (6.6%), Glu (6.5%)	(Asp+Glu): 159	(Arg + Lys): 123	unstable (44.82)	93.78	-0.054	> 157,63	5.15
>XP_011676138.2	Leu (8.4%), Val (8.1%), Ser (7.7%), Glu (7.5%), Thr (7.1%), Gly (6.8%)	(Asp+Glu): 185	(Arg + Lys): 126	unstable (42.19)	87.67	-0.186	163.53	4.79
>Arub-13	Val (9.2%), Ser (7.9%), Leu (7.5%), Glu (7.5%), Gly (6.8%), Thr (6.5%),	(Asp+Glu): 207	(Arg + Lys): 132	unstable (40.05)	85.38	-0.139	173.58	4.87

For all sequences the most abundant amino acids are leucine (Leu), valine (Val), serine (Ser), glycine (Gly) and glutamine (Glu). Instability index indicate alpha-macroglobulin like proteins as unstable. High aliphatic index, verified for all three sequences, indicates that they are thermo-stable over a wide temperature range. All sequences have a negative GRAVY, indicating that these alpha-macroglobulin like proteins as hydrophilic. The observed differences in this parameter are most likely a consequence of the incompleteness of *P. lividus*

transcript sequence. All proteins have a theoretical pI around 5, indicating that these alpha-2-macroglobulin is negatively charged upon secretion into seawater (pH = 8).

Regarding post-translational modifications, alpha-macroglobulin is predicted to be poorly glycosylated, with one N-glycosylation and five O-glycosylated sites predicted sites, none validated by MS/MS (Figure 22). Our results indicate that *P. lividus* alpha-2-macroglobulin most likely contains N-glycans (Table 10). In humans, alpha-2-macroglobulin has been shown to be N-glycosylated (Lin et al., 2012).

Alpha-macroglobulin like proteins have also been reported in other aquatic temporary attaching organisms, such as barnacle cyprids (SIPC), sea stars (Arub-13), limpets (P-vulgata-5) and ascidians larvae (H2Y2X2) (Dreanno et al., 2006; Lengerer et al., 2019; Liu et al., 2019; Kang et al., 2020) (Figure 23).

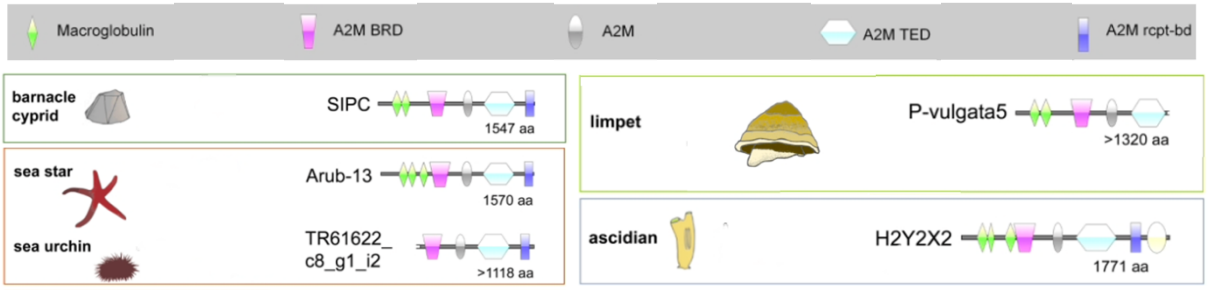

Figure 23 – Alpha-2-macroglobulin like proteins identified in barnacle cyprid, sea star, sea urchin, limpet and ascidian | Adapted from Davey et al. 202

The best studied alpha-macroglobulin-like adhesive protein, is the settlement-inducing protein complex (SIPC) secreted by barnacle cyprid larvae. Besides being used as a conspecific biochemical cue to induce the gregarious settlement of cyprids, it also functions as an adhesive protein (Rittschof and Cohen, 2004; Dreanno et al., 2006; Liang et al., 2019). Yorisue and colleagues (2012) proposed that SIPC might have evolved from alpha-2-macroglobulin by gene duplication, explaining the structural and sequence similarity between the two proteins. As above hypothesized, Domínguez-Pérez et al. (2020) also suggested a putative protective role for SIPC, maintaining the footprint integrity due to its protease inhibitor domains.

Alpha-2-macroglobulin-like protein can, therefore, have different functions in *P. lividus* adhesion. It could be a control mechanism to ensure the integrity of the adhesive secretion due to its inhibitory domains. Depending on further results, this glycoprotein can have a dual role as an adhesive role, as already proved in cyprids

4.2.3. Alpha-tectorin is heavily glycosylated and can be involved in cohesive/adhesive interactions with other components of *P. lividus* adhesive and/or of the disc cuticle

Alpha-tectorin was proposed by Pjeta and colleagues (2020) as an adhesive protein, sharing partial sequence homologies with sea star Spf1 (50% identity) and with Arub-4, -10 and -25 (26.7%, 51.3% and 51.4%, respectively). Spf1, from the sea star *Asterias rubens*, is a large protein of 426 kDa that displays specific protein-carbohydrate- and metal-binding domains that could contribute to the cohesion of the adhesive footprint as well as to adhesive interactions between the footprint and the cuticle covering the tube feet epithelium (Hennebert, et al. 2014).

We improved previous BLAST results (Pjeta et al. 2020), reporting a 77.1% (TR63383_c2_g1_i1) and 25.89% (TR46688_c0_g1_i1) similarity with sea urchin *Strongylocentrotus purpuratus* uncharacterized protein LOC100892803 (NCBI XP_030852014.1), an alpha-tectorin like protein. Protein alignment in Figure 24, shows that two transcripts can be assigned to different segments of an alpha-tectorin-like protein (named as consensus sequence in the alignment). These two proteins presented interspecific amino acid differences, of which 90 substitutions were confirmed by mass-spectrometry. This technique also validated 68 amino acids in the TR63383_c2_g1_i1_5 5' end. Spf1 was not sufficiently similar to both the uncharacterized protein (NCBI XP_030852014.1) and our consensus sequence (TR46688_c0_g1_i1_6 and TR63383_c2_g1_i1_5), being only evaluated regarding its molecular features (Table 13).

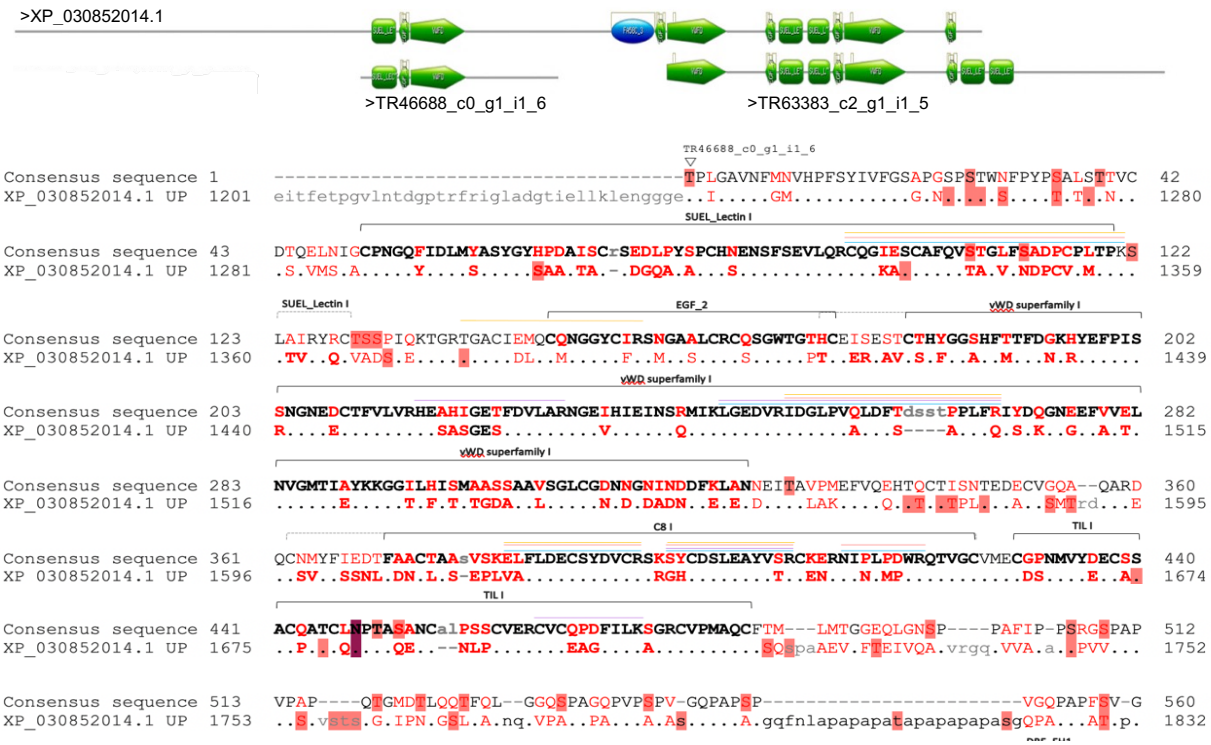

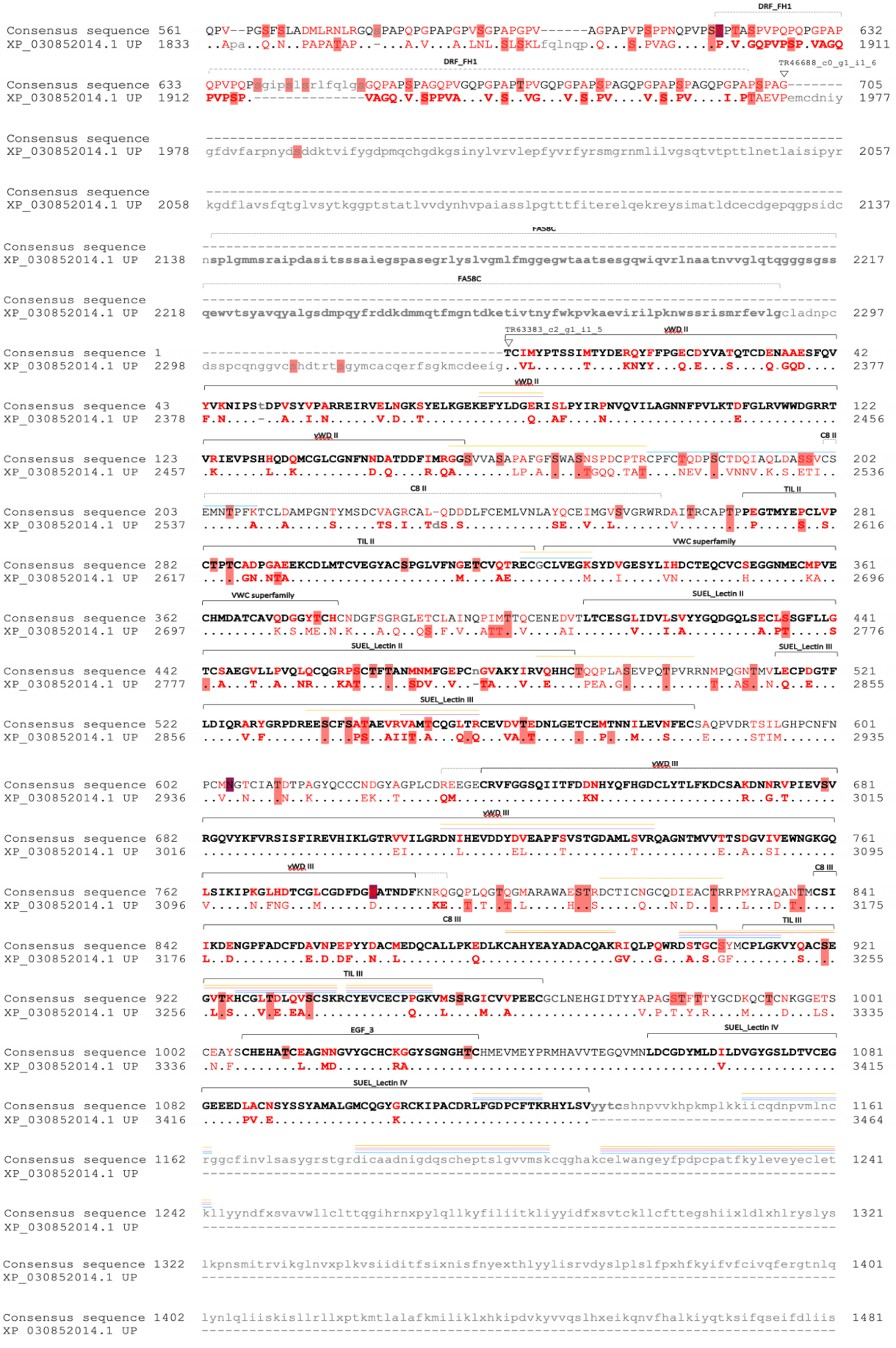
DRF_FH1
Consensus sequence 561 QPV--PGSFSLADMLRNLRGQSPAPQPGPAPGPVSGPAPGPV------AGPAPVPSPPNQPVPSLPTASPVPQPQPGPAP 632
XP_030852014.1 UP 1833 ..Apa..Q.N..PAPATAP..-...A.V...A.LNL.SLSKLfqlnqp.Q...S.PVAG....P.V.GQPVPSP.VAGQ 1911
DRF_FH1
TR46688_c0_g1_i1_6
Consensus sequence 633 QPVPQPSgipSlSrlfqlgSGQPAPSPAGQPVGQPGPAPTPVGQPGPAPSPAGQPGPAPSPAGQPGPAPSPAG------- 705
XP_030852014.1 UP 1912 PVPSP.----------VAGQ.V.SPPVA...V.S..VG...V.S.PV....V.S.PV....I.PTAEVPemcdniy 1977
Consensus sequence ---------- 2057
XP_030852014.1 UP 1978 gfdvfarpnydsddktvifygdpmqchgdkgsinylvrvlepfyvrfyrsmgrnmlilvgsqtvtpttlnetlaisipyr
Consensus sequence ---------- 2137
XP_030852014.1 UP 2058 kgdflavsfqtglvsytkggptstatlvvdynhvpaiasslpgtttfiterelqekreysimatldcecdgepqgpsidc
FA58C
Consensus sequence ---------- 2217
XP_030852014.1 UP 2138 nsplgmmsraipdasitsssaiegspasegrlyslvgmlfmggegwtaatsesgqwiqvrlnaatnvvglqtqgggsgss
FA58C
Consensus sequence ---------- 2297
XP_030852014.1 UP 2218 qewvtsyavqyalgsdmpqyfrddkdmmqtfmgntdketivtnyfwkpvkaevirilpknwssrismrfevlgcladnpc
TR63383_c2_g1_i1_5
vWD II
Consensus sequence 1 ----------TCIMYPTSSIMTYDERQYFFPGECDYVATQTCDENAAESFQV 42
XP_030852014.1 UP 2298 dsspcqnggvcshdtrtsgymcacqerfsgkmcdeeig..VL.....T....KNYY...Q.E...S....Q.GQD.... 2377
vWD II
Consensus sequence 43 YVKNIPStDPVSYVPARREIRVELNGKSYELKGEKEFYLDGERISLPYIRPNVQVILAGNNFPVLKTDFGLRVWWDGRRT 122
XP_030852014.1 UP 2378 F.N....-..A..I.N.....V.D..T.............Q..AF....N................E............ 2456
vWD II
C8 II
Consensus sequence 123 VRIEVPSHHQDQMCGLCGNFNNDATDDFIMRGGSVVASAPAFGFSWASNSPDCPTRCPFCTQDPSCTDQIAQLDASSVCS 202
XP_030852014.1 UP 2457 .K......L..K.........D.Q....R.QA.......LP.A....TGQQ.TAT....NEV..VNNV.K.S.ETI.. 2536
C8 II
TIL II
Consensus sequence 203 EMNTPFKTCLDAMPGNTYMSDCVAGRCAL-QDDDLFCEMLVNLAYQCEIMGVSVGRWRDAITRCAPTPPEGTMYEPCLVP 281
XP_030852014.1 UP 2537 ......A...A.....S.....TS.I..TdS.S...........SE..V..L.......V.....P.....S..S. 2616
TIL II
VWC superfamily
Consensus sequence 282 CTPTCADPGAEEKCDLMTCVEGYACSPGLVFNGETCVQTRECGCLVEGKSYDVGESYLIHDCTEQCVCSEGGNMECMPVE 361
XP_030852014.1 UP 2617 ....GN.NTA.....................M....AE.........M...I.....VN.........H.......KA.. 2696
VWC superfamily
SUEL_Lectin II
Consensus sequence 362 CHMDATCAVQDGGYTCHCNDGFSGRGLETCLAINQPIMTTQCENEDVTLTCESGLIDVLSVYYGQDGQLSECLSSGFLLG 441
XP_030852014.1 UP 2697 .........K.S.ME.N.K...A.Q..QS.F.V..ATT..V....AI.......V...I.A.........A.PT.....S 2776
SUEL_Lectin II
SUEL_Lectin III
Consensus sequence 442 TCSAEGVLLPVQLQCQGRPSCTFTANMNMFGEPCnGVAKYIRVQHHCTQQPLASEVPQTPVRRNMPQGNTMVLECPDGTF 521
XP_030852014.1 UP 2777 .A...T..A..NR...KAT.....SDV..V..-TA...V..E....PEA.G.....T..AS..N.Q..E... 2855
SUEL_Lectin III
Consensus sequence 522 LDIQRARYGRPDREESCFSATAEVRVAMTCQGLTRCEVDVTEDNLGETCEMTNNILEVNFECSAQPVDRTSILGHPCNFN 601
XP_030852014.1 UP 2856 .....V.F.....P.S..AIIT.A...Q.Q...VA.T.....P..M...S....E.....STIM..... 2935
vWD III
Consensus sequence 602 PCMNGTCIATDTPAGYQCCCNDGYAGPLCDREEGECRVFGGSQIITFDDNHYQFHGDCLYTLFKDCSAKDNNRVPIEVSV 681
XP_030852014.1 UP 2936 ..V..N....N..K......EK..T.....QM.................KN.................R..G.T..... 3015
vWD III
Consensus sequence 682 RGQVYKFVRSISFIREVHIKLGTRVVILGRDNIHEVDDYDVEAPFSVSTGDAMLSVRQAGNTMVVTTSDGVIVEWNGKGQ 761
XP_030852014.1 UP 3016 .....................EI.....L.....EL....T.....T.....E..A..SI..... 3095
vWD III
C8 III
Consensus sequence 762 LSIKIPKGLHDTCGLCGDFDGNATNDFKNRQGQPLQGTQGMARAWAESTRDCTICNGCQDIEACTRRPMYRAQANTMCSI 841
XP_030852014.1 UP 3096 V.....N.FNG...M......D.......KE..T.T..T.L.....H..S.....Q...N.D...L...D.T..... 3175
C8 III
TIL III
Consensus sequence 842 IKDENGPFADCFDAVNPEPYYDACMEDQCALLPKEDLKCAHYEAYADACQAKRIQLPQWRDSTGCSYMCPLGKVYQACSE 921
XP_030852014.1 UP 3176 L..D.........E.D.DF..N..L.........Q.................GV...G...A.S.GF.........S...... 3255
TIL III
Consensus sequence 922 GVTKHCGLTDLQVSCSKRCYEVCECPPGKVMSSRGICVVPEECGCLNEHGIDTYYAPAGSTFTTYGCDKQCTCNKGGETS 1001
XP_030852014.1 UP 3256 .L.S...V.E.EA.............Q...L....M..A.................V.P.T.Y.R....M....D...LS. 3335
EGF_3
SUEL_Lectin IV
Consensus sequence 1002 CEAYSCHEHATCEAGNNGVYGCHCKGGYSGNGHTCHMEVMEYPRMHAVVTEGQVMNLDCGDYMLDILDVGYGSLDTVCEG 1081
XP_030852014.1 UP 3336 .N.F.........L..MD.......RA.....................................V.............. 3415
SUEL_Lectin IV
Consensus sequence 1082 GEEEDLACNSYSSYAMALGMCQGYGRCKIPACDRLFGDPCFTKRHYLSVyytcshnpvvkhpkmplkkiicqdnpvmlnc 1161
XP_030852014.1 UP 3416 .....PV.E.............K.....----------3464
Consensus sequence 1162 rggcfinvlsasygrstgrdicaadnigdqscheptslgvvmskcqghakcelwangeyfpdpcpatfkyleveyeclet 1241
XP_030852014.1 UP ----------
Consensus sequence 1242 kllyyndfxsvavwllclttqgihrnxpylqllkyfiliitkliyyidfxsvtcklicfttegshiixldlxhlryslys 1321
XP_030852014.1 UP ----------
Consensus sequence 1322 lkpnsmitrvikglnvxplkvsiiditfsixnisfnyexthlyylisrvdyslplslfpxhfkyifvfcivqfergtnlq 1401
XP_030852014.1 UP ----------
Consensus sequence 1402 lynlqliiskisllrllxptkmtlalafkmiliklxhkipdvkyvvqslhxeikqnvfhalkiyqtksifqseifdliis 1481
XP_030852014.1 UP ----------

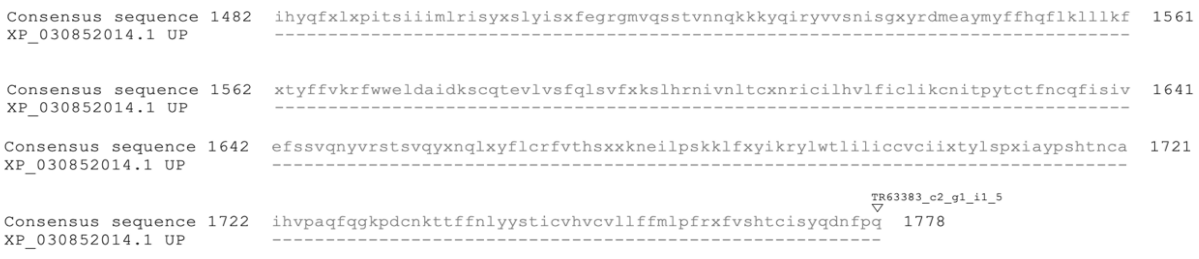

Figure 24 - Protein alignment of alpha-tectorin-like protein in *Paracentrotus lividus* and *Strongylocentrotus purpuratus* | Amino acids in black and red, indicate, respectively, common and dissimilar residues between both sequences. N-glycosylation sites are identified with purple, while O-glycosylation sites are in pink. Identified peptides by MS/MS, dashed over text, are identified in blue (GSL II), purple (LEL), pink (WGA) and orange (SBA).

As shown in Figure 24, *S. purpuratus* alpha-tectorin-like protein is a large multidomain protein (> 370kDa), which contains galactose-binding lectin domains (SUEL_Lectin), EGF-like domains, discoidin- like domains (FA58C), von Willebrand factor type D (vDW) and trypsin inhibitor-like cysteine rich domains (TIL) in a repeated pattern. This modular organization was also observed in alpha-tectorin like in *P. lividus* (>200 kDa).

These domains were also present in the sequences of adhesive proteins in sea stars (Spf1), flatworms (Mlig-ap1 and -2, Mile-ap1 and Mile-ap2a/b), limpets (P-vulgata_1, 2 and 4) and cnidaria, being associated with protein-protein, protein carbohydrate and protein-metal interactions (Pjeta et al., 2020). These binding functions can provide cohesive and adhesive interactions between alpha-tectorin and other glycans/proteins present either in the secreted adhesive and/or the outermost layer of the tube foot, the cuticle (Hennebert et al., 2014).

Predicted signal peptide was absent in the sequences of *S. purpuratus* (0.0011 likelihood) and *P. lividus* (0.0715 likelihood for TR46688_c0_g1_i1_6 and 0.0024 likelihood for TR63383_c2_g1_i1_5). Nevertheless, Spf1 (0.999 likelihood), Mlig-ap1 (0.9946 likelihood) and Mlig-ap2 (0.9919 likelihood) are predicted to be secreted. Since no start codon was found for none of the sea urchins sequences, we can't exclude the possibility that sea urchin alpha-tectorin might also be secreted.

Table 13 - Molecular features of sea urchin and sea star alpha-tectorin-like proteins | Abbreviations: GRAVY: grand average of hydropathy; MW: molecular weight; pI: isoelectric point.

Seq ID	Amino acid composition (%)	Total number of negatively charged residues	Total number of positively charged residues	Instability index	Aliphatic index	GRAVY	MW	pI
>TR46688_c0_g1_i1_6	Pro (13%), Ser (9.6%), Gly (9.4%), Ala (7.9%), Gln (6.2%), Val (5.8%)	(Asp+Glu): 59	(Arg + Lys): 34	unstable (74.36)	61.32	-0.272	74.09	4.81
>TR63383_c2_g1_i1_5	Leu (7.7%), Cys (7.1%), Val (6.6%), Gly (6.5%), Ser (6.4%), Thr (6.2%)	(Asp+Glu): 188	(Arg + Lys): 141	unstable (43.02)	76.72	-0.086	199.71	5.43
>XP_030852014.1	Gly (8.9%), Ser (8.0%), Ala (7.8%), Thr (7.2%), Pro (6.6%), Val (6.4%)	(Asp+Glu): 403	(Arg + Lys): 231	unstable (48.34)	64.83	-0.263	373.35	4.66
>Spf1	Gly (8.1%), Val (7.5%), Asp (7.2%), Glu (6.6%), Ala (6.2%), Ser (6.2%)	(Asp+Glu): 533	(Arg + Lys): 371	stable (36.80)	70.59	-0.328	428-25	4.92

Alpha-tectorin like proteins and Spf1 showed an amino acid bias towards glycine (Gly), serine (Ser) and alanine (Ala). Only Spf1 was predicted as stable, showing the lowest instability index (Table 13). All proteins have a negative GRAVY, indicating that they are highly

hydrophilic. All proteins have a theorical pI around 4.5 – 5, indicating that these alpha-tectorin like proteins are negatively charge upon secretion into seawater (pH = 8). All proteins have high molecular weights (>200 kDa). Alpha-tectorin like proteins are predicted to be highly glycosylated, containing both N- (most likely chitobiose units up to four units) and O- (GalNac residues) glycans (Figure 24, Table 10).

4.2.4. Myeloperoxidase is poorly glycosylated and can contribute to the cohesiveness of *P. lividus* adhesive secretion, catalysing protein crosslinking

Pjeta and colleagues (2020) proposed TR57217_c2_g1_i1 as a candidate adhesive protein, sharing 68.4% similarity with *S. purpuratus* myeloperoxidase (NCBI XP_787204.3). We confirmed this result (69% similarity), updating the accession number to XP_787204.4 (NCBI). These two proteins presented interspecific amino acid differences, of which, 53 differences were confirmed by mass-spectrometry (Figure 25).

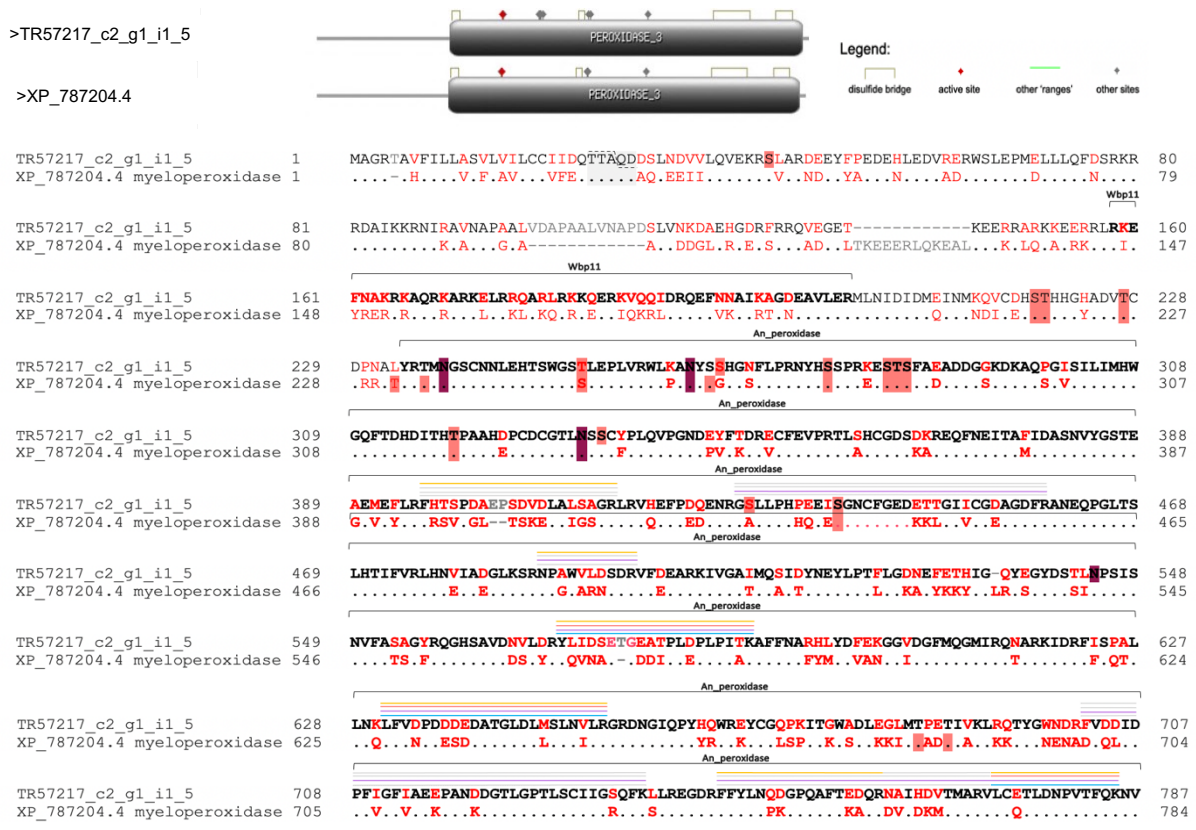

Figure 25 - Protein alignment of myeloperoxidase-like protein in *Paracentrotus lividus* and *Strongylocentrotus purpuratus* | Amino acids in black and red, indicate, respectively, common and dissimilar residues between both sequences. N-glycosylation sites are identified with purple, while O-glycosylation sites are in pink. Identified peptides by MS/MS, dashed over text, are identified in blue (GSL II), purple (LEL), pink (WGA) and orange (SBA).

As shown in Figure 25, myeloperoxidase has a twenty-eight amino acids signal peptide (0.962 likelihood, with a 0.8788 probability of cleavage site). It's a large protein, with an

approximate molecular weight of 94 kDa. Both sea urchin sequences presented a peroxidase domain. This is in agreement with previous reports of peroxidase-like enzymes being highly expressed in sea urchin tube foot discs (Lebesgue et al., 2016), in sea star adhesive secretion (Hennebert et al., 2015) and in cnidaria attachment basal area (Rodrigues et al., 2016). Peroxidases are believed to act as catalyzers of protein crosslinking, thus contributing to the high cohesive strength of wet adhesives (Pjeta et al. 2020). This enzyme is able to form four disulphide bridges (Figure 25), presenting a cysteine content of 3.3% (Table 17). This is in agreement with the reported insolubility of sea urchins and sea stars adhesive secretions, attributed to the presence of proteins with significant amounts of cysteine (2.6 and 3.2%, respectively) (Flammang et al., 2016).

Table 14 - Molecular features of sea urchin myeloperoxidase-like proteins | Abbreviations: GRAVY: grand average of hydropathy; MW: molecular weight; pI: isoelectric point.

Seq ID	Amino acid composition (%)	Total number of negatively charged residues	Total number of positively charged residues	Instability index	Aliphatic index	GRAVY	MW	pI
>TR57217_c2_g1_i1_5	Leu (9.3%), Ser (8.8%), Arg (8.2%), His (7.4%), Gln (5.5%), Val (5.3%)	(Asp+Glu): 87	(Arg + Lys): 130	unstable (46.85)	73.51	-0.51	94.02	4.94
>XP_787204.4	Leu (8.7%), Arg (8.4%), Ala (8.0%), Glu (7.3%), Asp (6.9%), Gly (6.5%),	(Asp+Glu): 117	(Arg + Lys): 120	unstable (41.56)	74.69	-0.621	93.86	7.98

Both sequences have leucine (Leu) and arginine (Arg) as two of the most abundant amino acids in their composition. The remaining amino acids differ, impacting the theorical isoelectric point, GRAVY and molecular weight. Both proteins were predicted as unstable (high instability index) but thermo-stable over a wide temperature range (high aliphatic index). All sequences have a negative GRAVY, indicating that they are hydrophilic. While *P. lividus* myeloperoxidase (TR57217_c2_g1_i1_5) has a theorical pI around 9, *S. purpuratus* myeloperoxidase is around 8, indicating that these proteins are differentially charged upon secretion into seawater (pH = 8). Both sequences have high molecular weight (>90 kDa). Myeloperoxidase is predicted to be poorly glycosylated, containing both N- and O-glycans (4 and 12 predicted glycosylation sites, respectively). In humans, myeloperoxidase is known to contain N-glycosylations and deglycosylation decreases its oxidation activity (Wang et al., 2018).

4.2.5. Uncharacterized protein involved in *P. lividus* adhesion

Based on its localization in the adhesive epidermis, Pjeta et al. (2020) selected TR46467_c1_g1_i2_6 as a candidate adhesive protein. However, like *P. lividus* MSP, this protein has no orthologue sequences in sea stars.

Our BLAST results showed that this transcript shares 38.31% similarity with *S. purpuratus* uncharacterized protein LOC115927989 (>XP_030850287.1). Both proteins presented interspecific amino acid differences, of which, 56 substitutions were confirmed by mass spectrometry (Figure 26).

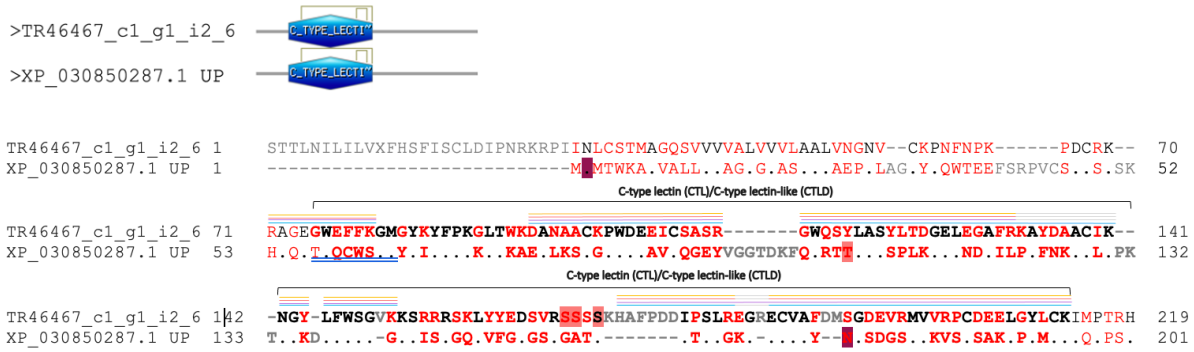

Figure 26 - Protein alignment of an uncharacterized protein of *Paracentrotus lividus* and *Strongylocentrotus purpuratus* | Amino acids in black and red, indicate, respectively, common and dissimilar residues between both sequences. N-glycosylation sites are identified with purple, while O-glycosylation sites are in pink. Identified peptides by MS/MS, dashed over text, are identified in blue (GSL II), purple (LEL), pink (WGA) and orange (SBA).

As shown in Figure 26, our transcript (TR46467_c1_g1_i2_6) has a twenty-nine amino acids signal peptide (0.9989 likelihood, with a 0.9520 probability of cleavage site), being most likely marked for the secretory pathway. Both uncharacterized proteins contain a C-type lectin (CTL) domain, a carbohydrate-recognition domain.

This domain is also present in the sequence of cohesive proteins in sea stars (Spf1) (Hennebert et al., 2012, Hennebert et al., 2014, Hennebert et al., 2015, Hennebert et al., 2018) and flatworms (Mlig-ap1) (Wunderer et al., 2019, Pjeta et al., 2020).

Being a secreted protein, apparently present in the adhesive secretory cells (Pjeta et al., 2020) and with a carbohydrate-recognition domain, it's a good candidate to promote interactions with the cuticular carbohydrate residues (i. e. in the fuzzy coat) (Hennebert et al., 2015).

Table 15 - Molecular features of sea urchin (*Paracentrotus lividus* and *Strongylocentrotus purpuratus*) uncharacterized protein | Abbreviations: GRAVY: grand average of hydropathy; MW: molecular weight; pI: isoelectric point.

seq ID	Amino acid composition (%)	Total number of negatively charged residues	Total number of positively charged residues	instability index	aliphatic index	GRAVY	MW	pI
>TR46467_c1_g1_i2_6	Ala (8.6%), Gly (8.1%), Lys (8.1%), Ser (8.15), Val (8.1%), Arg/Leu (7.0%)	(Asp+Glu): 22	(Arg+Lys): 28	unstable (48.82)	68.00	-0.368	20.82	8.86
>XP_030850287.1	Ala (10%), Gly (10%), Ser (10&), Lys (9%), Leu (8%), Pro/Val (5.5%)	(Asp+Glu): 16	(Arg+Lys): 22	stable (32.61)	66.57	-0.215	21.64	8.76

Main amino acid composition for both uncharacterized proteins were leucine (Leu), serine (Ser), alanine (Ala) and valine (Val). *P. lividus* uncharacterized protein was predicted as unstable, contrary to *S. purpuratus* uncharacterized protein (instability index). Both proteins were indicated as thermo-stable over a wide temperature range (high aliphatic index) and have a theoretical pI around 8.8, indicating that there are positively charge upon secretion into seawater (pH = 8) (Table 15).

Both TR46467_c1_g1_i1_6 and XP_030850287.1, contain a high cysteine content, having 14 (4.3%) and 10 cysteines (5%), respectively. Of these, four cysteine residues are highly conserved in the C-type lectin (CTL) domain, being involved in two disulfide bonds.

These results are consistent with high cysteine levels reported for sea urchins and sea stars adhesive secretions (2.6% and 3.2%, respectively) (Santos et al., 2009; Flammang, 2016).

Regarding PTMs, *P. lividus* uncharacterized protein is predicted to have only three linked O-glycans. This inconsistency with mass-spectrometry results (pull down by lectins that recognize N- and O-glycans) can be explained by the threshold used for *in silico* analysis.

4.3 Conclusions and future perspectives

With this thesis, our lab provided the further insights on five candidate adhesive/cohesive proteins involved in *Paracentrotus lividus* adhesion, through the characterization of their molecular features and conjugated glycans.

Up until now, Nectin was the only identified adhesive/cohesive protein in sea urchins (Lebesgue et al., 2016). Based on the recently published *P. lividus* tube foot specific transcriptome by Pjeta (2020), we report for the first time the identification of five adhesive/cohesive glycoproteins (Nectin variant 3, alpha--macroglobulin-like, alpha-tectorin-like, myeloperoxidase and an uncharacterized protein) in *P. lividus* adhesive discs. These candidate proteins are most likely conjugated with N-acetylglucosamine, a glycan previously shown to be present in the outer rim of the adhesive granules (Simão et al., 2020), expressed in the adhesive epidermis and secreted into the adhesive footprints (Pjeta et al., 2020), making these glycoproteins highly relevant for sea urchin adhesion.

Based on their sequences and domains, we can group the five protein candidates as follows: (i) two large negatively charge proteins (Nectin and alpha-tectorin) and a smaller positively charge protein (uncharacterized protein), with a probable adhesive and/or cohesive function, (ii) a alpha-macroglobulin enzyme, possibly promoting adhesion/cohesion or having a protective role and (iii) a peroxidase, most likely involved in protein crosslinking, contributing to the cohesiveness of the secreted adhesive (Table 16).

Table 16 – Glycosylated proteins candidates proposed as relevant for *Paracentrotus lividus* adhesion | Abbreviations: A2M, alpha macroglobulin domain; AE, adhesive epidermis; C8, cysteine-rich domain; CTL, C-type lectin domain; EGF, EGF-like calcium-binding domain; FA58C, discoidin domains; G, secretory granules; IHC, immunohistochemistry; ISH, *in situ* hybridization; MW: molecular weight; pI: isoelectric point; SUEL lectin, galactose-binding lectin domains; TIL, trypsin inhibitor-like; vWD, von Willebrand domain.

	Proteins pin pointed by ISH in Pjeta et al 2020 and by our work														
	sequence ID	location	Sequence completeness	Start/Stop codon	signal peptide	length	cysteine content	predicted glycosylation	predicted phosphorilation	predicted sulfation	conserved domains	homologous proteins of interest	unique peptides	MW	pI
TR60905_c1_g1_i1_5	nectin variant 3	AE (IHC, ISH), G (IHC)	full length	yes/yes	yes	984	1.1%	O, N	numerous	1	6x FA58C	nectin	40	108,24	5.98
TR61622_c8_g1_i2_4	α-macroglobulin like	AE (ISH)	5' missing	no/yes	no	1414	2.1%	O, N	numerous	2	A2M_N_2, A2M, A2M_2, A2M_recep	alpha-2-macroglobulin like protein 1, pregnancy zone protein	29	> 157,63	5.15
TR46688_c0_g1_i1_6	α-tectorin like		5' & 3' missing	no/no	no	705	5.1%	O, N	numerous	---	SUEL_Lectin x4, EGF, vWD x3, C8 x2, TIL x3	---	9	> 273.8	4.81
TR63383_c2_g1_i1_5			5' missing	no/yes	no	1778	7.1%	O, N	numerous	6		α-tectorin, Spf1	21		5.43
TR57217_c2_g1_i1_5	myeloperoxidase		full lenght	yes/yes	yes	829	3.3%	O, N	numerous	3	peroxidase	myeloperoxidase	9	94.02	4.94
TR46467_c1_g1_i2_6	uncharacterized protein		full length	yes/yes	yes	382	4.3%	O, N	numerous	---	CTL	---	8	20.82	8.86

This is in agreement with recent studies with other aquatic animals, showing that (i) temporary adhesives are mixtures of several proteins; including (ii) large cohesive proteins and (iii) smaller adhesive proteins; some of which are (iv) glycoproteins located in the outer rim of adhesive secretory granules (Wunderer et al., 2019, Simão et al., 2020).

Oppositely charged molecules, are also known to be involve in adhesion/deadhesion mechanisms in permanent (mussels and sandcastle worm) (Kim et al., 2016; Cui et al. ,2019) and in temporary adhesion (flatworms) (Wunderer et al., 2019). While a negatively charged

molecule serves as a releasing factor in flatworm *M. lignano* (due to adsorption to the positively charged Mlig-ap1 after secretion) (Wunderer et al., 2019), oppositely charged moleculas spontaneously condensated upon secretion by liquid-liquid phase separation in mussel and sandcastle adhesives, forming a coacervate phase (polymer-enriched) and a solvent phase (polymer depleted) (Sing, 2017; Dompé et al., 2020; Lebesgue et al., 2016). For *M. edulis* it was recently identified the first known naturally occurring self-coacervating adhesive protein in mussels (simple coacervation, with one colloidal solute) (Wei et al., 2014; Cui et al., 2017; Kaminker et al., 2017) as for *Phragmatopoma californica,* opposite charged proteins are needed to achieve a liquid-liquid phase separation, been separately secreted by two types of secretory cells (complex coacervation) (Stewart et al., 2011). The produced secretory granules are either homogeneous or heterogeneous, as reported in sea urchins (Flammang et al., 2016).

Coacervates have excellent transient physical properties for underwater adhesion as (i) higher density than water enabling surface wetting and (ii) low interfacial energy, allowing surface adsorption (Waite, 2017; Waite, 2019). It can also influence regulated secretion since electrostatic condensation of polyelectrolytic macromolecules into dense fluid granules allows the packaging and storing of large quantities of charged macromolecules.

The identification of oppositely charged adhesive/cohesive proteins (Nectin, α-tectorin and an uncharacterized protein) indicates a possible coacervation process, with more than two colloidal solutes, in *P. lividus* temporary adhesion. Their binding functions, promoting interactions with other glycans/proteins present either in the secreted adhesive and/or in the the disc cuticle (Hennebert et al., 2014) are due to their protein domains, associated with protein-protein, protein-carbohydrate and protein-metal interactions (Hennebert et al., 2015; Pjeta et al., 2020). High cysteine content of α-tectorin and uncharacterized protein, pinpoints the involvement of cysteine residues in intermolecular disulfide bonds reinforcing the cohesive strength of the adhesive (Santos and Flammang, 2006; Santos et al., 2009). Contrarily to DOPA-based adhesives, sea urchins crosslinking is promoted by peroxidases (myeloperoxidase). This liquid-to-solid maturation (e.g. mussels) promotes amyloid nanofiber formation for stronger adhesion, as already reported in sea urchins by Viana and Santos (2018), being possibly induced by a substantial pH differential between the regulated secretory system (pH = 6) and seawater (pH = 8), as well as changes of ionic composition (Stewart et al., 2017; Federle and Labonte, 2019).

Despite answering the main question proposed with this research project, the identification and characterization of some adhesion-related glycoproteins in *P. lividus* raised multiple questions, the first being the number of identified proteins. Due to incomplete databases regarding sea urchins, several proteins were identified as uncharacterized. To

address this question, further bioinformatic analyses (e.g. comparative analysis regarding domains or molecular features using principal component analysis) would be useful. The second question focus on model validation. Both knock out experiments and co-localized immunohistochemistry with specific antibodies would allow us to understand (i) if proteins are expressed by the same secretory adhesive cells, (iii) if these proteins are present in the adhesive granules and where in them and (iii) their direct or indirect impact on *P. lividus* adhesion. The last question addresses adhesive/cohesive properties of these proteins using recombinant protein expression, as performed by our group with Nectin variant 2 (Batista 2020). Validation of the adhesive properties of sea urchin inspired adhesive proteins can be achieved using self-assembled monolayers, ellipsometry, surface plasmon resonance and scanning probe microscopy.

As a follow up of the present thesis, it can be envisaged that further research in still needed to better characterize these five proposed sea urchin adhesive glycoproteins. Based on their sequences new antibodies can be produced to locate in more detail the expression of these glycoproteins (eg. immunogold transmission electron microscopy), followed by their purification by immune-affinity chromatography, and posterior identification of their glycosylation sites and attached glycan structures by mass spectrometry.

This basic research is important not only for a better understanding of sea urchin temporary adhesion but also for the development/improvement of medical adhesives, but also in tissue engineering (Choi Besim and Editors, n.d.) and drug delivering (Dutta and Das 2015; Müller et al. 2020). A better knowledge of these adhesive glycoproteins can contribute to identify common features in wet adhesives, highlighting key-elements that are important to mimic in bioinspired adhesives for biomedical application, but also to create a portfolio of diverse adhesive proteins with unique features to address a variety of clinical challenges.

Currently, the only marine organisms for which biomimetic recombinant adhesive proteins have been produced is still scarce (mussels - Hwang et al., 2005; sea urchins – Batista et al., 2020 and sea stars – Lefevre et al., 2020), and further investment and growth in the production of biomimetic adhesives is foreseen for years to come.

CHAPTER 5

REFERENCES

REFERENCES

Almagro Armenteros, José Juan, Konstantinos D. Tsirigos, Casper Kaae Sønderby, Thomas Nordahl Petersen, Ole Winther, Søren Brunak, Gunnar von Heijne, and Henrik Nielsen. 2019. "SignalP 5.0 Improves Signal Peptide Predictions Using Deep Neural Networks." *Nature Biotechnology* 37 (4): 420–23. https://doi.org/10.1038/s41587-019-0036-z.

Almeida, Mariana, Rui L. Reis, and Tiago H. Silva. 2020. "Marine Invertebrates Are a Source of Bioadhesives with Biomimetic Interest." *Materials Science and Engineering C* 108: 110467. https://doi.org/10.1016/j.msec.2019.110467.

Ameye, Laurent, René Hermann, Philippe Dubois, and Patrick Flammang. 2000. "Ultrastructure of the Echinoderm Cuticle after Fast-Freezing / Freeze Substitution and Conventional Chemical Fixations." *Microscopy Research and Technique* 48 (6): 385–93. https://doi.org/10.1002/(SICI)1097-0029(20000315)48:6<385::AID-JEMT8>3.0.CO;2-R.

Anand, P. P., and Y. Shibu Vardhanan. 2020. "Computational Modelling of Wet Adhesive Mussel Foot Proteins (Bivalvia): Insights into the Evolutionary Convolution in Diverse Perspectives." *Scientific Reports* 10 (1): 1–24. https://doi.org/10.1038/s41598-020-59169-y.

André, Sabine, Herbert Kaltner, Joachim C. Manning, Paul V. Murphy, and Hans Joachim Gabius. 2015. "Lectins: Getting Familiar with Translators of the Sugar Code." *Molecules* 20 (2): 1788–1823. https://doi.org/10.3390/molecules20021788.

Baldwin, Michael A. 2004. "Protein Identification by Mass Spectrometry: Issues to Be Considered." *Molecular and Cellular Proteomics* 3 (1): 1–9. https://doi.org/10.1074/mcp.R300012-MCP200.

Balkenende, Diederik W.R., Sally M. Winkler, and Phillip B. Messersmith. 2019. "Marine-Inspired Polymers in Medical Adhesion." *European Polymer Journal* 116 (January): 134–43. https://doi.org/10.1016/j.eurpolymj.2019.03.059.

Batista, Joana Domingues Leal. 2020. "Produção de Proteínas Recombinantes Inspiradas No Adesivo Do Ouriço Do Mar e Sua Adesão a Diferentes Substratos." Universidade de Lisboa.

Baumgartner, Stefan, Kay Hofmann, Ruth Chiquet-Ehrismann, and Philipp Bucher. 1998. "The Discoidin Domain Family Revisited: New Members from Prokaryotes and a Homology-Based Fold Prediction." *Protein Science* 7 (7): 1626–31. https://doi.org/10.1002/pro.5560070717.

Bhattacharjee, Nicholus, and Parbati Biswas. 2010. "Position-Specific Propensities of Amino Acids in the -Strand." *BMC Structural Biology* 10. https://doi.org/10.1186/1472-6807-10-29.

Buheitel, Johannes, and Olaf Stemmann. 2013. "Prophase Pathway-Dependent Removal of Cohesin from Human Chromosomes Requires Opening of the Smc3-Scc1 Gate." *EMBO Journal* 32 (5): 666–76. https://doi.org/10.1038/emboj.2013.7.

Burke, R D, L M Angerer, G W Humphrey, S Yaguchi, T Kiyama, S Liang, X Mu, et al. 2006. "A Genomic View of the Sea Urchin Nervous System" 300 (1): 434–60.

Cao, Jing, Shuzhen Guo, Ken Arai, Eng H. Lo, and Ming Ming Ning. 2013. "Studying Extracellular Signaling Utilizing a Glycoproteomic Approach: Lectin Blot Surveys, a First and Important Step." *Methods in Molecular Biology* 1013: 227–33. https://doi.org/10.1007/978-1-62703-426-5_15.

Carlos A. Díaz-Balzac, José E. Abreu-Arbelo, and José E. García-Arrarás. 2010. "Neuroanatomy of the Tube Feet and Tentacles in Holothuria Glaberrima (Holothuroidea, Echinodermata)." *Zoomorphology* 23 (1): 1–7. https://doi.org/10.1038/jid.2014.371.

Charlina, Natalia A, Igor Yu Dolmatov, and Iain C Wilkie. 2009. “Juxtaligamental System of the Disc and Oral Frame of the Ophiuroid Amphipholis Kochii (Echinodermata : Ophiuroidea) and Its Role in Autotomy. *Invertebrate Biology.* 128 (2): 145–56. http://doi.org/10.HH/j.1744-7410.2008.00160.x

Choi Besim, Andy H, and Ben-Nissan Editors. n.d. *Springer Series in Biomaterials Science and Engineering 14 Marine-Derived Biomaterials for Tissue Engineering Applications*. http://www.springer.com/series/10955.

Clarke, Jessica L., Peter A. Davey, and Nick Aldred. 2020. “Sea Anemones (Exaiptasia Pallida) Use a Secreted Adhesive and Complex Pedal Disc Morphology for Surface Attachment.” *BMC Zoology* 5 (1). https://doi.org/10.1186/s40850-020-00054-6.

Claudia Arndt, Stefanie Koristka, Anja Feldmann, Holger Bartsch, and Michael Bachmann. 2012. “Coomassie-Brilliant Blue Staining of Polyacrylamide Gels” 869: 465–69. https://doi.org/10.1007/978-1-61779-821-4.

Costa, Caterina, Carmela Cavalcante, Francesca Zito, Yukio Yokota, and Valeria Matranga. 2010. “Phylogenetic Analysis and Homology Modelling of Paracentrotus Lividus Nectin.” *Molecular Diversity* 14 (4): 653–65. https://doi.org/10.1007/s11030-009-9203-3.

Cui, Mengkui, Susu Ren, Shicao Wei, Chengjun Sun, and Chao Zhong. 2017. “Natural and Bio-Inspired Underwater Adhesives: Current Progress and New Perspectives.” *APL Materials* 5 (11). https://doi.org/10.1063/1.4985756.

Cui, Mengkui, Xinyu Wang, Bolin An, Chen Zhang, Xinrui Gui, Ke Li, Yingfeng Li, et al. 2019. “Exploiting Mammalian Low-Complexity Domains for Liquid-Liquid Phase Separation–Driven Underwater Adhesive Coatings.” *Science Advances* 5 (8): 1–13. https://doi.org/10.1126/sciadv.aax3155.

Davey, Peter A., Marcelo Rodrigues, Jessica L. Clarke, and Nick Aldred. 2019. “Transcriptional Characterisation of the Exaiptasia Pallida Pedal Disc.” *BMC Genomics* 20 (1): 1–15. https://doi.org/10.1186/s12864-019-5917-5.

Davey, Peter, Anne Marie Power, Romana Santos, Philip Bertemes, Peter Ladurner, Pawel Palmowski, Jessica Clarke, et al. 2020. “Omics-Based Molecular Analyses of Adhesion by Aquatic Invertebrates.”

DeMartini, Daniel G., John M. Errico, Sebastian Sjoestroem, April Fenster, and J. Herbert Waite. 2017. “A Cohort of New Adhesive Proteins Identified from Transcriptomic Analysis of Mussel Foot Glands.” *Journal of the Royal Society Interface* 14 (131). https://doi.org/10.1098/rsif.2017.0151.

Dinte, Elena, and Bianca Sylvester. 2018. “Adhesives: Applications and Recent Advances.” *Applied Adhesive Bonding in Science and Technology*. https://doi.org/10.5772/intechopen.71854.

Dolmatov, Igor Y., Vladimir S. Mashanov, and Olga R. Zueva. 2006. “Derivation of Muscles of the Aristotle’s Lantern from Coelomic Epithelia.” *Cell and Tissue Research* 327 (2): 371–84. https://doi.org/10.1007/s00441-006-0314-1.

Dompé, Marco, Francisco J. Cedano-Serrano, Mehdi Vahdati, Larissa van Westerveld, Dominique Hourdet, Costantino Creton, Jasper van der Gucht, Thomas Kodger, and Marleen Kamperman. 2020. “Underwater Adhesion of Multiresponsive Complex Coacervates.” *Advanced Materials Interfaces* 7 (4). https://doi.org/10.1002/admi.201901785.

Dreanno, Catherine, Kiyotaka Matsumura, Naoshi Dohmae, Koji Takio, Hiroshi Hirota, Richard R. Kirby, and Anthony S. Clare. 2006. “An A2-Macroglobulin-like Protein Is the Cue to Gregarious Settlement of the Barnacle Balanus Amphitrite.” *Proceedings of the National Academy of Sciences of the United States of America* 103 (39): 14396–401. https://doi.org/10.1073/pnas.0602763103.

Dutta, Lakshmi Priya, and Mahuya Das. 2015. “Coacervation—A Method for Drug Delivery,” *Advances of Medical Electronics.* 379–86. https://doi.org/10.1007/978-81-322-2256-9_35.

Elphick, Maurice R., Dean C. Semmens, Liisa M. Blowes, Judith Levine, Christopher J. Lowe, Maria I. Arnone, and Melody S. Clark. 2015. “Reconstructing SALMFamide Neuropeptide Precursor Evolution in the Phylum Echinodermata: Ophiuroid and Crinoid Sequence Data Provide New Insights.” *Frontiers in Endocrinology* 6 (FEB): 1–11. https://doi.org/10.3389/fendo.2015.00002.

Eriksson, Jan, and David Fenyö. 2007. “Improving the Success Rate of Proteome Analysis by Modeling Protein-Abundance Distributions and Experimental Designs.” *Nature Biotechnology* 25 (6): 651–55. https://doi.org/10.1038/nbt1315.

Favi, Pelagie M., Sijia Yi, Scott C. Lenaghan, Lijin Xia, and Mingjun Zhang. 2012. “Inspiration from the Natural World: From Bio-Adhesives to Bio-Inspired Adhesives.” *Journal of Adhesion Science and Technology* 28 (3–4): 290–319. https://doi.org/10.1080/01694243.2012.691809.

Federle, Walter, and David Labonte. 2019. “Dynamic Biological Adhesion: Mechanisms for Controlling Attachment during Locomotion.” *Philosophical Transactions of the Royal Society B: Biological Sciences* 374 (1784). https://doi.org/10.1098/rstb.2019.0199.

Feoktistova, Maria, Peter Geserick, and Martin Leverkus. 2016. “Crystal Violet Assay for Determining Viability of Cultured Cells.” *Cold Spring Harbor Protocols* 2016 (4): 343–46. https://doi.org/10.1101/pdb.prot087379.

Ferreira, P., António F.M. Silva, M. I. Pinto, and M. H. Gil. 2008. “Development of a Biodegradable Bioadhesive Containing Urethane Groups.” *Journal of Materials Science: Materials in Medicine* 19 (1): 111–20. https://doi.org/10.1007/s10856-007-3117-3.

Ferrier, Graham A., Steven J. Kim, Catherine S. Kaddis, Joseph A. Loo, Cheryl Ann Zimmer, and Richard K. Zimmer. 2016. “MULTIFUNCin: A Multifunctional Protein Cue Induces Habitat Selection by, and Predation on, Barnacles.” *Integrative and Comparative Biology* 56 (5): 901–13. https://doi.org/10.1093/icb/icw076.

Flammang, P., S. Demeulenaere, and M. Jangoux. 1994. “The Role of Podial Secretions in Adhesion in Two Species of Sea Stars (Echinodermata).” *The Biological Bulletin* 187 (1): 35–47. https://doi.org/10.2307/1542163.

Flammang, Patrick. 2016. “Adhesive Secretions in Echinoderms: A Review.” *Biological Adhesives, Second Edition*, 1–378. https://doi.org/10.1007/978-3-319-46082-6.

Flammang, Patrick, Alain Michel, Anne Van Cauwenberge, Henri Alexandre, and Michel Jangoux. 1998. “A Study of the Temporary Adhesion of the Podia in the Sea Star Asterias Rubens (Echinodermata, Asteroidea) through Their Footprints.” *Journal of Experimental Biology* 201 (16): 2383–95.

Floriolli, Renee Y., Johannes Von Langen, and J. Herbert Waite. 2000. “Marine Surfaces and the Expression of Specific Byssal Adhesive Protein Variants in Mytilus.” *Marine Biotechnology* 2 (4):

352–63. https://doi.org/10.1007/s101269900032.

Franco, Catarina Ferraz, Romana Santos, and Ana Varela Coelho. 2011. "Exploring the Proteome of an Echinoderm Nervous System: 2-DE of the Sea Star Radial Nerve Cord and the Synaptosomal Membranes Subproteome." *Proteomics* 11 (7): 1359–64. https://doi.org/10.1002/pmic.201000541.

Gabius, Hans Joachim, Sabine André, Jesús Jiménez-Barbero, Antonio Romero, and Dolores Solís. 2011. "From Lectin Structure to Functional Glycomics: Principles of the Sugar Code." *Trends in Biochemical Sciences* 36 (6): 298–313. https://doi.org/10.1016/j.tibs.2011.01.005.

Gantayet, Arpita, David J. Rees, and Eli D. Sone. 2014. "Novel Proteins Identified in the Insoluble Byssal Matrix of the Freshwater Zebra Mussel." *Marine Biotechnology* 16 (2): 144–55. https://doi.org/10.1007/s10126-013-9537-9.

García-Arrarás, José E. 2010. "Echinoderms Potential Model Systems for Studies on Muscle Regeneration" *Curr Pharm Des.* 16 (8): 942–55.

Ge, Liangpeng, and Shixuan Chen. 2020. "Recent Advances in Tissue Adhesives for Clinical Medicine," *Polymers*. 12, 939. doi:10.3390/polym12040939

Goldring, J. P.Dean. 2018. "The Roles of Acetic Acid and Methanol during Fixing and Staining Proteins in an SDS–Polyacrylamide Electrophoresis Gel." *Methods in Molecular Biology* 1853: 15–18. https://doi.org/10.1007/978-1-4939-8745-0_2.

Hennebert, Elise. 2010. "Adhesion Mechanisms Developed by Sea Stars: A Review of the Ultrastructure and Composition of Tube Feet and Their Secretion." *Biological Adhesive Systems*, 99–109. https://doi.org/10.1007/978-3-7091-0286-2_7.

Hennebert, Elise, Baptiste Leroy, Ruddy Wattiez, and Peter Ladurner. 2015. "An Integrated Transcriptomic and Proteomic Analysis of Sea Star Epidermal Secretions Identifies Proteins Involved in Defense and Adhesion." *Journal of Proteomics* 128: 83–91. https://doi.org/10.1016/j.jprot.2015.07.002.

Hennebert, Elise, Barbara Maldonado, Peter Ladurner, Patrick Flammang, and Patrick Flammang. 2015. "Experimental Strategies for the Identification and Characterization of Adhesive Proteins in Animals : A Review," *Interface Focus* 5: 20140064. http://dx.doi.org/10.1098/rsfs.2014.0064

Hennebert, Elise, Barbara Maldonado, Peter Ladurner, Patrick Flammang, and Romana Santos. 2014. "Experimental Strategies for the Identification and Characterization of Adhesive Proteins in Animals: A Review." *Interface Focus* 5 (1): 1–19. https://doi.org/10.1098/rsfs.2014.0064.

Hennebert, Elise, Romana Santos, and Patrick Flammang. 2012. "Echinoderms Don't Suck: Evidence against the Involvement of Suction in Tube Foot Attachment" *Zoosymposia* 7 (1): 25–32. https://doi.org/10.11646/zoosymposia.7.1.3.

Hennebert, Elise, Ruddy Wattiez, Mélanie Demeuldre, Peter Ladurner, Dong Soo Hwang, J. Herbert Waite, and Patrick Flammang. 2014. "Sea Star Tenacity Mediated by a Protein That Fragments, Then Aggregates." *Proceedings of the National Academy of Sciences of the United States of America* 111 (17): 6317–22. https://doi.org/10.1073/pnas.1400089111.

Hennebert, Elise, Ruddy Wattiez, and Patrick Flammang. 2011. "Characterisation of the Carbohydrate Fraction of the Temporary Adhesive Secreted by the Tube Feet of the Sea Star Asterias Rubens."

Marine Biotechnology 13 (3): 484–95. https://doi.org/10.1007/s10126-010-9319-6.

Holm, Eric R., Beatriz Orihuela, Christopher J. Kavanagh, and Daniel Rittschof. 2005. "Variation among Families for Characteristics of the Adhesive Plaque in the Barnacle Balanus Amphitrite." *Biofouling* 21 (2): 121–26. https://doi.org/10.1080/08927010512331344188.

Huang, Ting, Jingjing Wang, Weichuan Yu, and Zengyou He. 2012. "Protein Inference: A Review." *Briefings in Bioinformatics* 13 (5): 586–614. https://doi.org/10.1093/bib/bbs004.

Hwang, Dong Soo, Hongbo Zeng, Qingye Lu, Jacob Israelachvili, and J. Herbert Waite. 2012. "Adhesion Mechanism in a DOPA-Deficient Foot Protein from Green Mussels." *Soft Matter* 8 (20): 5640–48. https://doi.org/10.1039/c2sm25173f.

Jackson, Mark R. 2001. "Fibrin Sealants in Surgical Practice: An Overview." *American Journal of Surgery* 182 (2 SUPPL. 1). https://doi.org/10.1016/S0002-9610(01)00770-X.

Jain, Ritu, and Sarika Wairkar. 2019. "Recent Developments and Clinical Applications of Surgical Glues: An Overview." *International Journal of Biological Macromolecules* 137: 95–106. https://doi.org/10.1016/j.ijbiomac.2019.06.208.

Jaipan, Panupong, Alexander Nguyen, and Roger J. Narayan. 2017. "Gelatin-Based Hydrogels for Biomedical Applications." *MRS Communications* 7 (3): 416–26. https://doi.org/10.1557/mrc.2017.92.

Kaminker, Ilia, Wei Wei, Alex M. Schrader, Yeshayahu Talmon, Megan T. Valentine, Jacob N. Israelachvili, J. Herbert Waite, and Songi Han. 2017. "Simple Peptide Coacervates Adapted for Rapid Pressure-Sensitive Wet Adhesion." *Soft Matter* 13 (48): 9122–31. https://doi.org/10.1039/c7sm01915g.

Kamino, Kei. 2008. "Underwater Adhesive of Marine Organisms as the Vital Link between Biological Science and Material Science." *Marine Biotechnology* 10 (2): 111–21. https://doi.org/10.1007/s10126-007-9076-3.

Kang, Victor, Birgit Lengerer, Ruddy Wattiez, and Patrick Flammang. 2020. "Molecular Insights into the Powerful Mucus-Based Adhesion of Limpets (Patella Vulgata L.)." *Open Biology* 10 (6): 200019. https://doi.org/10.1098/rsob.200019.

Kim, Chan Hee, Eun Jung Kim, Hye Jin Go, Hye Young Oh, Ming Lin, Maurice R. Elphick, and Nam Gyu Park. 2016. "Identification of a Novel Starfish Neuropeptide That Acts as a Muscle Relaxant." *Journal of Neurochemistry* 137 (1): 33–45. https://doi.org/10.1111/jnc.13543.

Kim, Sangsik, Jun Huang, Yongjin Lee, Sandipan Dutta, Hee Young Yoo, Young Mee Jung, Yongseok Jho, Hongbo Zeng, and Dong Soo Hwang. 2016. "Complexation and Coacervation of Like-Charged Polyelectrolytes Inspired by Mussels." *Proceedings of the National Academy of Sciences of the United States of America* 113 (7): E847–53. https://doi.org/10.1073/pnas.1521521113.

Koontz, Laura. 2014. "TCA Precipitation." *Methods in Enzymology* 541: 3–10. https://doi.org/10.1016/B978-0-12-420119-4.00001-X.

Lebesgue, Nicolas, Gonçalo da Costa, Raquel Mesquita Ribeiro, Cristina Ribeiro-Silva, Gabriel G. Martins, Valeria Matranga, Arjen Scholten, Carlos Cordeiro, Albert J.R. Heck, and Romana Santos. 2016. "Deciphering the Molecular Mechanisms Underlying Sea Urchin Reversible Adhesion: A Quantitative Proteomics Approach." *Journal of Proteomics* 138: 61–71.

https://doi.org/10.1016/j.jprot.2016.02.026.

Lee, Bruce. P.; P.B. Messersmith, J. N. Israelachvili and J. H Waite. 2011. “Mussel-Inspired Adhesives and Coatings.” *Annual Review of Materials Research* 41: 99–132. https://doi.org/10.1146/annurev-matsci-062910-100429.Mussel-Inspired.

Lefevre, Mathilde, Patrick Flammang, A. Sesilja Aranko, Markus B. Linder, Thomas Scheibel, Martin Humenik, Maxime Leclercq, et al. 2020. “Sea Star-Inspired Recombinant Adhesive Proteins Self-Assemble and Adsorb on Surfaces in Aqueous Environments to Form Cytocompatible Coatings.” *Acta Biomaterialia* 112: 62–74. https://doi.org/10.1016/j.actbio.2020.05.036.

Lengerer, Birgit, Morgane Algrain, Mathilde Lefevre, Jérôme Delroisse, Elise Hennebert, and Patrick Flammang. 2019. “Interspecies Comparison of Sea Star Adhesive Proteins.” *Philosophical Transactions of the Royal Society B: Biological Sciences* 374 (1784): 1–8. https://doi.org/10.1098/rstb.2019.0195.

Lengerer, Birgit, Marie Bonneel, Mathilde Lefevre, Elise Hennebert, Philippe Leclère, Emmanuel Gosselin, Peter Ladurner, and Patrick Flammang. 2018. “The Structural and Chemical Basis of Temporary Adhesion in the Sea Star Asterina Gibbosa.” *Beilstein Journal of Nanotechnology* 9 (1): 2071–86. https://doi.org/10.3762/bjnano.9.196.

Lengerer, Birgit, Elise Hennebert, Patrick Flammang, Willi Salvenmoser, and Peter Ladurner. 2016. “Adhesive Organ Regeneration in Macrostomum Lignano.” *BMC Developmental Biology* 16 (1). https://doi.org/10.1186/s12861-016-0121-1.

Lengerer, Birgit, and Peter Ladurner. 2018. “Properties of Temporary Adhesion Systems of Marine and Freshwater Organisms.” *Journal of Experimental Biology* 221 (16). https://doi.org/10.1242/jeb.182717.

Lengerer, Birgit, Robert Pjeta, Julia Wunderer, Marcelo Rodrigues, Roberto Arbore, Lukas Schärer, Eugene Berezikov, et al. 2014. “Biological Adhesion of the Flatworm Macrostomum Lignano Relies on a Duo-Gland System and Is Mediated by a Cell Type-Specific Intermediate Filament Protein.” *Frontiers in Zoology* 11 (1): 1–15. https://doi.org/10.1186/1742-9994-11-12.

Lengerer, Birgit, Julia Wunderer, Robert Pjeta, Giada Carta, Damian Kao, Aziz Aboobaker, Christian Beisel, Eugene Berezikov, Willi Salvenmoser, and Peter Ladurner. 2018. “Organ Specific Gene Expression in the Regenerating Tail of Macrostomum Lignano.” *Developmental Biology* 433 (2): 448–60. https://doi.org/10.1016/j.ydbio.2017.07.021.

Lew, Wesley K, and Fred A Weaver. 2008. “Clinical Use of Topical Thrombin as a Surgical Hemostat” 2 (4): 593–99.

Liang, Chao, Jack Strickland, Zonghuang Ye, Wenjian Wu, Biru Hu, and Dan Rittschof. 2019. “Biochemistry of Barnacle Adhesion: An Updated Review.” *Frontiers in Marine Science* 6 (September): 1–20. https://doi.org/10.3389/fmars.2019.00565.

Lima, Victor V., Christiné S. Rigsby, David M. Hardy, R. Clinton Webb, and Rita C. Tostes. 2009. “O-GlcNAcylation: A Novel Post-Translational Mechanism to Alter Vascular Cellular Signaling in Health and Disease: Focus on Hypertension.” *Journal of the American Society of Hypertension* 3 (6): 374–87. https://doi.org/10.1016/j.jash.2009.09.004.

Lin, Zhenxin, Andy Lo, Diane M. Simeone, Mack T. Ruffin, and David M. Lubman. 2012. “An N-

Glycosylation Analysis of Human Alpha-2-Macroglobulin Using an Integrated Approach." *Journal of Proteomics and Bioinformatics* 5 (5): 127–34. https://doi.org/10.4172/jpb.1000224.

Lu, Qingye, Eric Danner, J. Herbert Waite, Jacob N. Israelachvili, Hongbo Zeng, and Dong Soo Hwang. 2013. "Adhesion of Mussel Foot Proteins to Different Substrate Surfaces." *Journal of the Royal Society Interface* 10 (79). https://doi.org/10.1098/rsif.2012.0759.

Lu, Shennan, Jiyao Wang, Farideh Chitsaz, Myra K. Derbyshire, Renata C. Geer, Noreen R. Gonzales, Marc Gwadz, et al. 2020. "CDD/SPARCLE: The Conserved Domain Database in 2020." *Nucleic Acids Research* 48 (D1): D265–68. https://doi.org/10.1093/nar/gkz991.

Matranga, Valeria. 2005. *Echinodermata*. Germany: Springer.

Matranga, Valeria, Daniela Di Ferrol, Francesca Zito, Melchiorre Cervello, and Eizo Nakano. 1992. "A New Extracellular Matrix Protein of the Sea Urchin Embryo with Properties of a Substrate Adhesion Molecule." *Roux's Archives of Developmental Biology* 201 (3): 173–78. https://doi.org/10.1007/BF00188716.

Mitchell, Alex L., Teresa K. Attwood, Patricia C. Babbitt, Matthias Blum, Peer Bork, Alan Bridge, Shoshana D. Brown, et al. 2019. "InterPro in 2019: Improving Coverage, Classification and Access to Protein Sequence Annotations." *Nucleic Acids Research* 47 (D1): D351–60. https://doi.org/10.1093/nar/gky1100.

Mo, Jingyi, Sylvain F. Prévost, Liisa M. Blowes, Michaela Egertová, Nicholas J. Terrill, Wen Wang, Maurice R. Elphick, and Himadri S. Gupta. 2016. "Interfibrillar Stiffening of Echinoderm Mutable Collagenous Tissue Demonstrated at the Nanoscale." *Proceedings of the National Academy of Sciences of the United States of America* 113 (42): E6362–71. https://doi.org/10.1073/pnas.1609341113.

Modjarrad, Kayvon, and Sina Ebnesajjad. 2013. "Handbook of Polymer Applications in Medicine and Medical Devices." In *Handbook of Polymer Applications in Medicine and Medical Devices*, 103. USA: Elsevier Inc.

Motokawa, Tatsuo, and Yoshiro Fuchigami. 2015. "Coordination between Catch Connective Tissue and Muscles through Nerves in the Spine Joint of the Sea Urchin Diadema Setosum." *Journal of Experimental Biology* 218 (5): 703–10. https://doi.org/10.1242/jeb.115972.

Müller, Werner E.G., Emad Tolba, Shunfeng Wang, Meik Neufurth, Ingo Lieberwirth, Maximilian Ackermann, Heinz C. Schröder, and Xiaohong Wang. 2020. "Nanoparticle-Directed and Ionically Forced Polyphosphate Coacervation: A Versatile and Reversible Core–Shell System for Drug Delivery." *Scientific Reports* 10 (1): 1–16. https://doi.org/10.1038/s41598-020-73100-5.

Murray, Gisela, and José E. García-Arrarás. 2004. "Myogenesis during Holothurian Intestinal Regeneration." *Cell and Tissue Research* 318 (3): 515–24. https://doi.org/10.1007/s00441-004-0978-3.

Navinkumar J Patil, Paola Gabriela Vinueza Naranjo, Bruno Zappone. 2018. "Wet Adhesive Properties of Asian Green Mussel (Perna Viridis) Foot Protein Pvfp-5 : An Underwater Adhesive Primer. no. April 2019.

Nerson, D. L. & Cox, M. M. 2016. *Lehninger Principles of Biochemistry*. New York: Macmillan Higher Education.

Nilsson, Carol L. 2003. “Lectins: Proteins That Interpret the Sugar Code.” *Analytical Chemistry* 75 (15): 348–53. https://doi.org/10.1021/ac031373w.

Noble, James E., and Marc J.A. Bailey. 2009. *Chapter 8 Quantitation of Protein*. *Methods in Enzymology*. 1st ed. Vol. 463. Elsevier Inc. https://doi.org/10.1016/S0076-6879(09)63008-1.

O’Rorke, Richard D., Oleksandr Pokholenko, Feng Gao, Ting Cheng, Ankur Shah, Vishal Mogal, and Terry W.J. Steele. 2017. “Addressing Unmet Clinical Needs with UV Bioadhesives.” *Biomacromolecules* 18 (3): 674–82. https://doi.org/10.1021/acs.biomac.6b01743.

Ohkawa, Kousaku, Ayako Nishida, Hiroyuki Yamamoto, and J. Herbert Waite. 2004. “A Glycosylated Byssal Precursor Protein from the Green Mussel Perna Viridis with Modified Dopa Side-Chains.” *Biofouling* 20 (2): 101–15. https://doi.org/10.1080/08927010410001681246.

Palacio, Manuel L.B., and Bharat Bhushan. 2012. “Research Article: Bioadhesion: A Review of Concepts and Applications.” *Philosophical Transactions of the Royal Society A: Mathematical, Physical and Engineering Sciences* 370 (1967): 2321–47. https://doi.org/10.1098/rsta.2011.0483.

Pandey, Nikhil, Luis F. Soto-Garcia, Jun Liao, Philippe Zimmern, Kytai T. Nguyen, and Yi Hong. 2020. “Mussel-Inspired Bioadhesives in Healthcare: Design Parameters, Current Trends, and Future Perspectives.” *Biomaterials Science* 8 (5): 1240–55. https://doi.org/10.1039/c9bm01848d.

Park, Sohee, Sangsik Kim, Yongseok Jho, and Dong Soo Hwang. 2019. “Cation-ΠInteractions and Their Contribution to Mussel Underwater Adhesion Studied Using a Surface Forces Apparatus: A Mini-Review.” *Langmuir* 35 (48): 16002–12. https://doi.org/10.1021/acs.langmuir.9b01976.

Park, Sungjo, D. Kent Arrell, Santiago Reyes, Enoch Y. Park, and Andre Terzic. 2017. “Conventional and Unconventional Secretory Proteins Expressed with Silkworm Bombyxin Signal Peptide Display Functional Fidelity.” *Scientific Reports* 7 (1): 1–8. https://doi.org/10.1038/s41598-017-14833-8.

Pennati, Roberta, and Ute Rothbächer. 2014. “Bioadhesion in Ascidians: A Developmental and Functional Genomics Perspective.” *Interface Focus* 5 (1): 1–10. https://doi.org/10.1098/rsfs.2014.0061.

Pettersen, Eric F., Thomas D. Goddard, Conrad C. Huang, Gregory S. Couch, Daniel M. Greenblatt, Elaine C. Meng, and Thomas E. Ferrin. 2004. “UCSF Chimera--a Visualization System for Exploratory Research and Analysis.” *Journal of Computational Chemistry* 25 (13): 1605–12. https://doi.org/10.1002/jcc.20084.

Pjeta, Robert, Herbert Lindner, Leopold Kremser, Willi Salvenmoser, Daniel Sobral, Peter Ladurner, and Romana Santos. 2020. “Integrative Transcriptome and Proteome Analysis of the Tube Foot and Adhesive Secretions of the Sea Urchin Paracentrotus Lividus.” *International Journal of Molecular Sciences* 21 (3). https://doi.org/10.3390/ijms21030946.

Pjeta, Robert, Julia Wunderer, Philip Bertemes, Teresa Hofer, Willi Salvenmoser, Birgit Lengerer, Stefan Coassin, et al. 2019. “Temporary Adhesion of the Proseriate Flatworm Minona Ileanae.” *Philosophical Transactions of the Royal Society B: Biological Sciences* 374 (1784). https://doi.org/10.1098/rstb.2019.0194.

Qi Guo, Jingsi Chen, Jilei Wang, hongbo Zeng, Jing Yu. 2020. “Recent Progress in Synthesis and Application of Mussel-Inspired Adhesives.” https://doi.org/10.1039/C9NR09780E.

Quan, Wei Yan, Zhang Hu, Hua Zhong Liu, Qian Qian Ouyang, Dong Ying Zhang, Si Dong Li, Pu Wang Li, and Zi Ming Yang. 2019. “Mussel-Inspired Catechol-Functionalized Hydrogels and Their Medical Applications.” *Molecules* 24 (14): 1–27. https://doi.org/10.3390/molecules24142586.

Rathi, Sneha, Raju Saka, Abraham J. Domb, and Wahid Khan. 2019. “Protein-Based Bioadhesives and Bioglues.” *Polymers for Advanced Technologies* 30 (2): 217–34. https://doi.org/10.1002/pat.4465.

Reece, T Brett, Thomas S Maxey, and Irving L Kron. 2001. “A Prospectus on Tissue Adhesives” *The American Journal of Surgery.* 182: 40–44.

Rees, David J., Arash Hanifi, Angelico Obille, Robert Alexander, and Eli D. Sone. 2019. “Fingerprinting of Proteins That Mediate Quagga Mussel Adhesion Using a De Novo Assembled Foot Transcriptome.” *Scientific Reports* 9 (1): 1–14. https://doi.org/10.1038/s41598-019-41976-7.

Ribeiro, Ana R., Alice Barbaglio, Cristiano D. Benedetto, Cristina C. Ribeiro, Iain C. Wilkie, Maria D.C. Carnevali, and Mário A. Barbosa. 2011. “New Insights into Mutable Collagenous Tissue: Correlations between the Microstructure and Mechanical State of a Sea-Urchin Ligament.” *PLoS ONE* 6 (9): 1–10. https://doi.org/10.1371/journal.pone.0024822.

Richter, Katharina, and Ingo Grunwald. 2018. *Katharina Richter, Ingo Grunwald, and Janek von Byern 54 Contents*.

Rittschof, Dan, and Jonathan H. Cohen. 2004. “Crustacean Peptide and Peptide-like Pheromones and Kairomones.” *Peptides* 25 (9): 1503–16. https://doi.org/10.1016/j.peptides.2003.10.024.

Rodrigues, Marcelo, Philippe Leclère, Patrick Flammang, Michael W. Hess, Willi Salvenmoser, Bert Hobmayer, and Peter Ladurner. 2016. “The Cellular Basis of Bioadhesion of the Freshwater Polyp Hydra.” *BMC Zoology* 1 (1): 1–15. https://doi.org/10.1186/s40850-016-0005-7.

Rodrigues, Marcelo, Thomas Ostermann, Leopold Kremeser, Herbert Lindner, Christian Beisel, Eugene Berezikov, Bert Hobmayer, and Peter Ladurner. 2016. “Profiling of Adhesive-Related Genes in the Freshwater Cnidarian Hydra Magnipapillata by Transcriptomics and Proteomics.” *Biofouling* 32 (9): 1115–29. https://doi.org/10.1080/08927014.2016.1233325.

Roth, Ziv, Galit Yehezkel, and Isam Khalaila. 2012. “Identification and Quantification of Protein Glycosylation.” *International Journal of Carbohydrate Chemistry* 2012: 1–10. https://doi.org/10.1155/2012/640923.

Sagert, Jason, Chengjun Sun, and J. Herbert waite. 2006. “Chemical Subtleties of Mussel and Polychaete Holdfasts.” *Biological Adhesives*, 125–43. https://doi.org/10.1007/978-3-540-31049-5_7.

Sanders, Lindsey, and Jiro Nagatomi. 2014. “Clinical Applications of Surgical Adhesives and Sealants.” *Critical Reviews in Biomedical Engineering* 42 (3–4): 271–92. https://doi.org/10.1615/CritRevBiomedEng.2014011676.

Santos, R., G. da Costa, C. Franco, P. Gomes-Alves, P. Flammang, and A. V. Coelho. 2009. “First Insights into the Biochemistry of Tube Foot Adhesive from the Sea Urchin Paracentrotus Lividus (Echinoidea, Echinodermata).” *Marine Biotechnology* 11 (6): 686–98. https://doi.org/10.1007/s10126-009-9182-5.

Santos, Romana, Ângela Barreto, Catarina Franco, and Ana Varela Coelho. 2013a. “Mapping Sea Urchins Tube Feet Proteome - A Unique Hydraulic Mechano-Sensory Adhesive Organ.” *Journal*

of Proteomics 79: 100–113. https://doi.org/10.1016/j.jprot.2012.12.004.

Santos, Romana, and Patrick Flammang. 2005. “Morphometry and Mechanical Design of Tube Foot Stems in Sea Urchins: A Comparative Study.” *Journal of Experimental Marine Biology and Ecology* 315 (2): 211–23. https://doi.org/10.1016/j.jembe.2004.09.016.

Santos, Romana, and Patrick Flammang. 2006. “Morphology and Tenacity of the Tube Foot Disc of Three Common European Sea Urchin Species: A Comparative Study.” *Biofouling* 22 (3): 173–86. https://doi.org/10.1080/08927010600743449.

Santos, Romana, and Patrick Flammang. 2008. “Estimation of the Attachment Strength of the Shingle Sea Urchin, Colobocentrotus Atratus, and Comparison with Three Sympatric Echinoids.” *Marine Biology* 154 (1): 37–49. https://doi.org/10.1007/s00227-007-0895-6.

Santos, Romana, and Patrick Flammang. 2012. “Is the Adhesive Material Secreted by Sea Urchin Tube Feet Species-Specific?” *Journal of Morphology* 273 (1): 40–48. https://doi.org/10.1002/jmor.11004.

Santos, Romana, Delphine Haesaerts, Michel Jangoux, and Patrick Flammang. 2005a. “Comparative Histological and Immunohistochemical Study of Sea Star Tube Feet (Echinodermata, Asteroidea).” *Journal of Morphology* 263 (3): 259–69. https://doi.org/10.1002/jmor.10187.

Santos, Romana, Delphine Haesaerts, Michel Jangoux, and Patrick Flammang. 2005b. “The Tube Feet of Sea Urchins and Sea Stars Contain Functionally Different Mutable Collagenous Tissues.” *Journal of Experimental Biology* 208 (12): 2277–88. https://doi.org/10.1242/jeb.01641.

Schwartz, Gregory W., Tair Shauli, Michal Linial, and Uri Hershberg. 2019. “Serine Substitutions Are Linked to Codon Usage and Differ for Variable and Conserved Protein Regions.” *Scientific Reports* 9 (1): 1–9. https://doi.org/10.1038/s41598-019-53452-3.

Shcherbakova, Aleksandra, Matthias Preller, Manuel H. Taft, Jordi Pujols, Salvador Ventura, Birgit Tiemann, Falk F.R. Buettner, and Hans Bakker. 2019. “C-Mannosylation Supports Folding and Enhances Stability of Thrombospondin Repeats.” *ELife* 8. https://doi.org/10.7554/eLife.52978.

Sheehan, David. 2000. “Physical Biochemistry: Principles and Applications.” *Polymer News* 25 (11): 364. https://doi.org/10.5816/blackscholar.43.3.0099.

Simão, Mariana. 2020. “Characterization of the Glycans Involved in Sea Urchin Paracentrotus Lividus Reversible Adhesion.” *Encyclopedic Dictionary of Genetics, Genomics and Proteomics*. https://doi.org/10.1002/0471684228.egp09104.

Sing, Charles E. 2017. “Development of the Modern Theory of Polymeric Complex Coacervation.” *Advances in Colloid and Interface Science* 239: 2–16. https://doi.org/10.1016/j.cis.2016.04.004.

Smith, Andrew M. 2016. “Biological Adhesives, Second Edition.” *Biological Adhesives, Second Edition*, 1–378. https://doi.org/10.1007/978-3-319-46082-6.

Spotnitz, William D., and Sandra Burks. 2008. “Hemostats, Sealants, and Adhesives: Components of the Surgical Toolbox.” *Transfusion* 48 (7): 1502–16. https://doi.org/10.1111/j.1537-2995.2008.01703.x.

Stewart, Russell J., Todd C. Ransom, and Vladimir Hlady. 2011. “Natural Underwater Adhesives.” *Journal of Polymer Science, Part B: Polymer Physics* 49 (11): 757–71. https://doi.org/10.1002/polb.22256.

Stewart, Russell J., Ching Shuen Wang, In Taek Song, and Joshua P. Jones. 2017. "The Role of Coacervation and Phase Transitions in the Sandcastle Worm Adhesive System." *Advances in Colloid and Interface Science* 239: 88–96. https://doi.org/10.1016/j.cis.2016.06.008.

Stewart, Russell J, Ching Shuen Wang, and Hui Shao. 2011. "Complex Coacervates as a Foundation for Synthetic Underwater Adhesives." *Advances in Colloid and Interface Science* 167 (1–2): 85–93. https://doi.org/10.1016/j.cis.2010.10.009.

Sugni, Michela, Dario Fassini, Alice Barbaglio, Anna Biressi, Cristiano Di Benedetto, Serena Tricarico, Francesco Bonasoro, Iain C. Wilkie, and Maria Daniela Candia Carnevali. 2014. "Comparing Dynamic Connective Tissue in Echinoderms and Sponges: Morphological and Mechanical Aspects and Environmental Sensitivity." *Marine Environmental Research* 93: 123–32. https://doi.org/10.1016/j.marenvres.2013.07.010.

Tabb, David L, David B Friedman, and Amy-Joan L Ham. 2013. "Tandem Mass Spectra." *Proteomics* 10 (1): 267–72. https://doi.org/10.1038/nprot.2006.330.Verification.

Tateno, Hiroaki. 2010. "SUEL-Related Lectins, a Lectin Family Widely Distributed throughout Organisms." *Bioscience, Biotechnology and Biochemistry* 74 (6): 1141–44. https://doi.org/10.1271/bbb.100086.

Toubarro, Duarte, Analuce Gouveia, Raquel Mesquita Ribeiro, Nélson Simões, Gonçalo da Costa, Carlos Cordeiro, and Romana Santos. 2016a. "Cloning, Characterization, and Expression Levels of the Nectin Gene from the Tube Feet of the Sea Urchin Paracentrotus Lividus." *Marine Biotechnology* 18 (3): 372–83. https://doi.org/10.1007/s10126-016-9698-4.

Toubarro, Duarte, Analuce Gouveia, Raquel Mesquita Ribeiro, Nélson Simões, Gonçalo da Costa, Carlos Cordeiro, and Romana Santos. 2016b. "Cloning, Characterization, and Expression Levels of the Nectin Gene from the Tube Feet of the Sea Urchin Paracentrotus Lividus." *Marine Biotechnology* 18 (3): 372–83. https://doi.org/10.1007/s10126-016-9698-4.

Vernengo, Andrea J. 2016. "Adhesive Materials for Biomedical Applications." *Adhesives - Applications and Properties*. https://doi.org/10.5772/64958.

Viana, Ana S, and Romana Santos. 2018. "Nanoscale Characterization of the Temporary Adhesive of the Sea Urchin Paracentrotus Lividus." *Beilstein Journal of Nanotechnology* 9: 2277–86.

Waite, J. H. 2002. "Adhesion à La Moule." *Biochemistry* 1180: 1172–80. https://doi.org/https://doi.org/10.1093/icb/42.6.1172.

Waite, J. Herbert. 2017. "Mussel Adhesion - Essential Footwork." *Journal of Experimental Biology* 220 (4): 517–30. https://doi.org/10.1242/jeb.134056.

Waite, J. Herbet. 2019. "Translational Bioadhesion Research Embracing Biology without Tokenism." *Philosophical Transactions of the Royal Society A: Mathematical, Physical and Engineering Sciences* 377 (2138): 9–11. https://doi.org/10.1098/rsta.2018.0266.

Wang, Jia, Jian Nan Li, Zhao Cui, and Ming Hui Zhao. 2018. "Deglycosylation Influences the Oxidation Activity and Antigenicity of Myeloperoxidase." *Nephrology* 23 (1): 46–52. https://doi.org/10.1111/nep.12926.

Wasik, Kaja, James Gurtowski, Xin Zhou, Olivia Mendivil Ramos, M. Joaquina Delás, Giorgia Battistoni, Osama El Demerdash, et al. 2015. "Genome and Transcriptome of the Regeneration-Competent

Flatworm, Macrostomum Lignano." *Proceedings of the National Academy of Sciences of the United States of America* 112 (40): 12462–67. https://doi.org/10.1073/pnas.1516718112.

Wei, Wei, Yerpeng Tan, Nadine R. Martinez Rodriguez, Jing Yu, Jacob N. Israelachvili, and J. Herbert Waite. 2014. "A Mussel-Derived One Component Adhesive Coacervate." *Acta Biomaterialia* 10 (4): 1663–70. https://doi.org/10.1016/j.actbio.2013.09.007.

Weisel, By John W. 2005. "FIBRINOGEN AND FIBRIN A Bstract Fibrinogen Is a Large , Complex , Fibrous Glycoprotein with Three Pairs of I . I Ntroduction Fibrinogen Is a Fi Brous Protein That Was Fi Rst Classi Fi Ed with Keratin , ˚ Repeat in Wide-Angle X-Ray" 70 (04): 247–99. https://doi.org/10.1016/S0065-3233(04)70008-X.

Wong, Steve G., and Andréa Dessen. 2014. "Structure of a Bacterial A2-Macroglobulin Reveals Mimicry of Eukaryotic Innate Immunity." *Nature Communications* 5: 1–9. https://doi.org/10.1038/ncomms5917.

Wudarski, Jakub, Bernhard Egger, Steven A. Ramm, Lukas Schärer, Peter Ladurner, Kira S. Zadesenets, Nikolay B. Rubtsov, Stijn Mouton, and Eugene Berezikov. 2020. "The Free-Living Flatworm Macrostomum Lignano." *EvoDevo* 11 (1): 1–8. https://doi.org/10.1186/s13227-020-00150-1.

Wunderer, Julia, Birgit Lengerer, Robert Pjeta, Philip Bertemes, Leopold Kremser, Herbert Lindner, Thomas Ederth, et al. 2019. "A Mechanism for Temporary Bioadhesion." *Proceedings of the National Academy of Sciences of the United States of America* 116 (10): 4297–4306. https://doi.org/10.1073/pnas.1814230116.

Xu, Kaige, Yuqing Liu, Shousan Bu, Tianyi Wu, Qiang Chang, Gurankit Singh, Xiaojian Cao, et al. 2017. "Egg Albumen as a Fast and Strong Medical Adhesive Glue." *Advanced Healthcare Materials* 6 (19): 1–10. https://doi.org/10.1002/adhm.201700132.

Zeng, Fan, Julia Wunderer, Willi Salvenmoser, Michael W. Hess, Peter Ladurner, and Ute Rothbächer. 2019. "Papillae Revisited and the Nature of the Adhesive Secreting Collocytes." *Developmental Biology* 448 (2): 183–98. https://doi.org/10.1016/j.ydbio.2018.11.012.

Zhao, Hua, Nicholas B. Robertson, Scott A. Jewhurst, and J. Herbert Waite. 2006. "Probing the Adhesive Footprints of Mytilus Californianus Byssus." *Journal of Biological Chemistry* 281 (16): 11090–96. https://doi.org/10.1074/jbc.M510792200.

Zhao, Hua, Jason Sagert, Dong Soo Hwang, and J. Herbert Waite. 2009. "Glycosylated Hydroxytryptophan in a Mussel Adhesive Protein from Perna Viridis." *Journal of Biological Chemistry* 284 (35): 23344–52. https://doi.org/10.1074/jbc.M109.022517.

Zhu, Wenzhen, Yon Jin Chuah, and Dong An Wang. 2018. "Bioadhesives for Internal Medical Applications: A Review." *Acta Biomaterialia* 74 (April): 1–16. https://doi.org/10.1016/j.actbio.2018.04.034.

Zueva, Olga, Maleana Khoury, Thomas Heinzeller, Daria Mashanova, and Vladimir Mashanov. 2018. "The Complex Simplicity of the Brittle Star Nervous System." *Frontiers in Zoology* 15 (1): 1–26. https://doi.org/10.1186/s12983-017-0247-4.

CHAPTER 6

SUPPLEMENTARY DATA

Supplementary Table 1 – Adhesion strength measured for single tube feet of sea stars and sea urchins on various smooth substrata | Abbreviations: PMMA: poly(methylmetacrylate); PP: polypropylene; PS polystyrene. Adapted from Flammang 2016.

Species	Substratum	Tenacity (MPa)	References
Asteroids			
Asterias rubens	Glass	0.20–0.24	Flammang and Walker (1997) and Hennebert et al. (2010)
	PMMA	0.18	Santos et al. (2005a)
Asterias vulgaris	Glass	0.17	Paine (1926)
Marthasterias glacialis	Glass	0.43	Hennebert et al. (2010)
Echinoids			
Arbacia lixula	Glass	0.09	Santos and Flammang (2006)
Colobocentrotus atratus	PMMA	0.54	Santos and Flammang (2008)
Echinometra mathaei	PMMA	0.22	Santos and Flammang (2008)
Heterocentrotus trigonarius	PMMA	0.25	Santos and Flammang (2008)
Paracentrotus lividus	Glass	0.29-0.31	Santos and Flammang (2006)
	PMMA	0.34	Santos et al. (2005a); Santos and Flammang (2006)
	PP	0.14-0.17	Santos et al. (2005a); Santos and Flammang (2006)
	PS	0.29	Santos and Flammang (2006)
Sphaerechinus granularis	Glass	0.20	Santos and Flammang (2006)
Stomopneustes variolaris	PMMA	0.21	Santos and Flammang (2006)

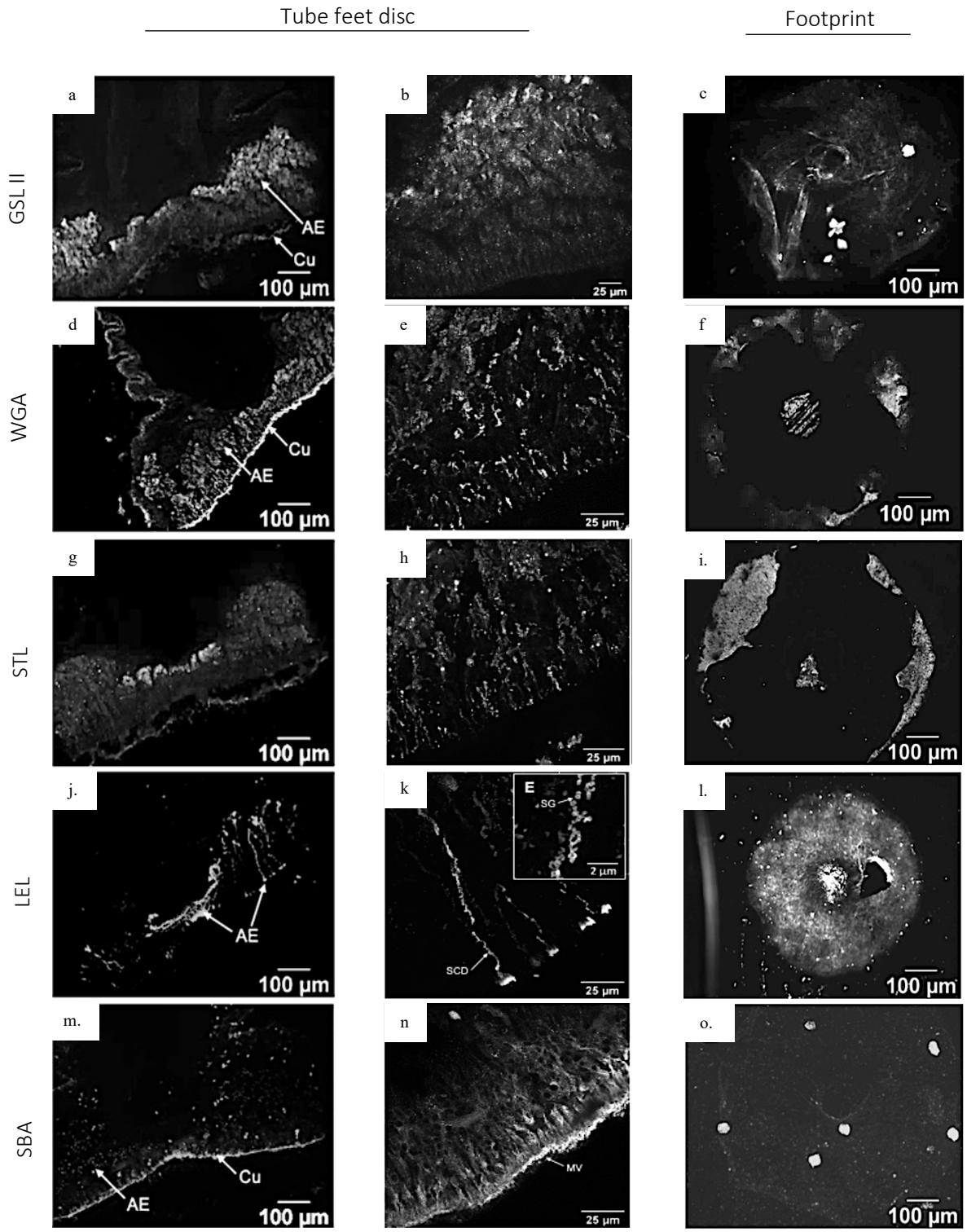

Supplementary Figure 1 – Sea urchin *Paracentrotus lividus* adhesive and tube feet sections labelling with GSL II, WGA, STL, LEL and SBA | The disc surface is oriented downwards towards the right in all the pictures. Detection of N-acetylglucosamine in the simple (GSL II) and chitobiose (WGA, STL, LEL) form and N-acetylgalactosamine (SBA). Abbreviations: GSL II, *Griffonia simplicifolia* lectin II; LEL, *Lycopersicon esculentum* lectin; SBA, *Soybean* agglutinin; STL, *Solanum tuberosum* lectin; WGA, *Wheat germ* agglutinin. A close up of the adhesive epidermis labelling is in the center column to a detail representation of the cellular structures stained.

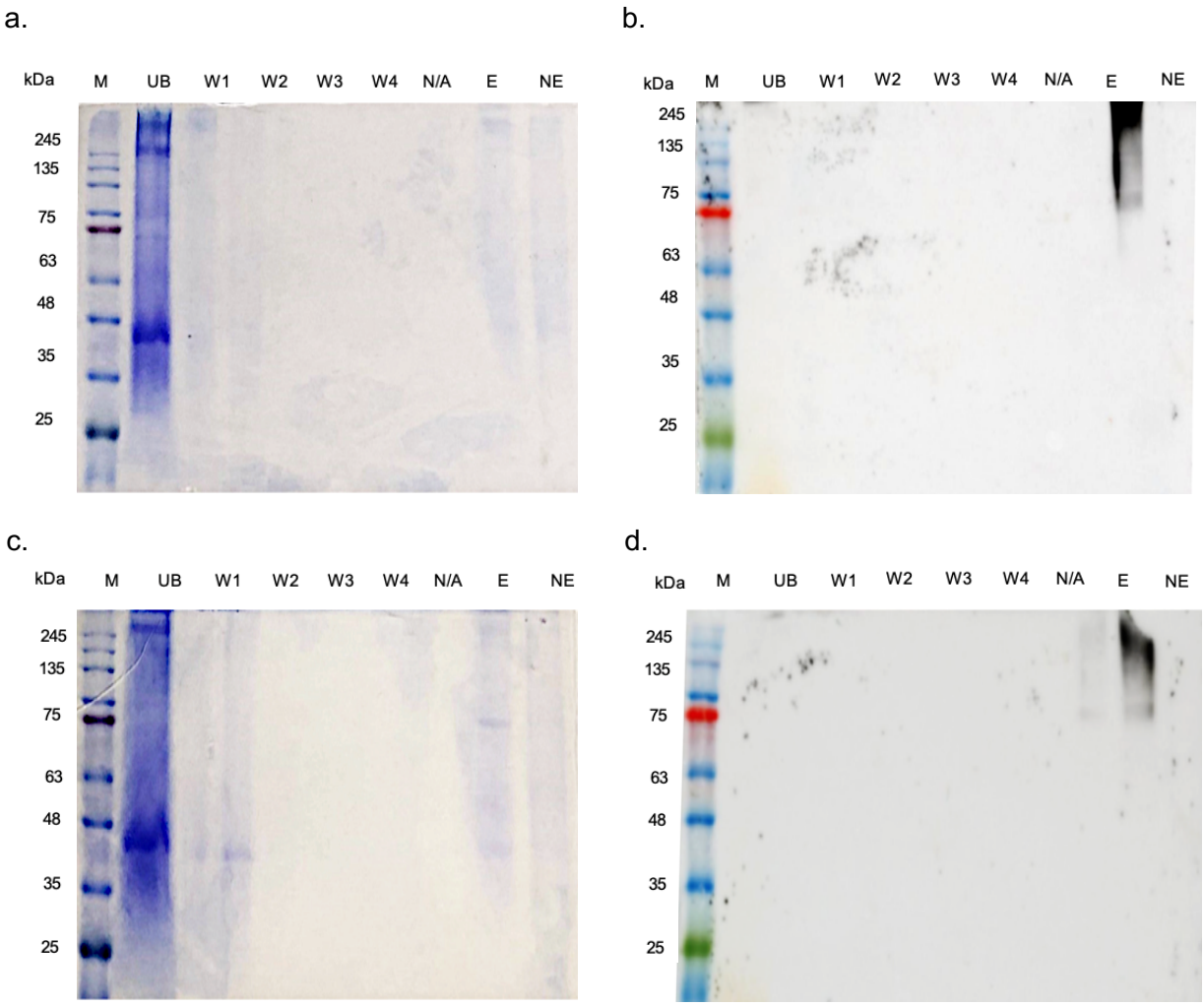

Supplementary Figure 2 - Pulldown assay (first optimization) of glycoproteins from *Paracentrotus lividus* tube feet disc extracts using LEL-bounded agarose beads | One-dimensional gel electrophoresis protein profile (**a,c**) and corresponding lectin blot (**b,d**) using 550 μg **(a,b)** and 730 μg (**c,d) of protein amount**. Abbreviations: E – eluted fraction; M - molecular weight markers; NE – non-eluted fraction; UB- unbound fraction; W1-4 – wash fractions. 6.9 seconds of exposure time.

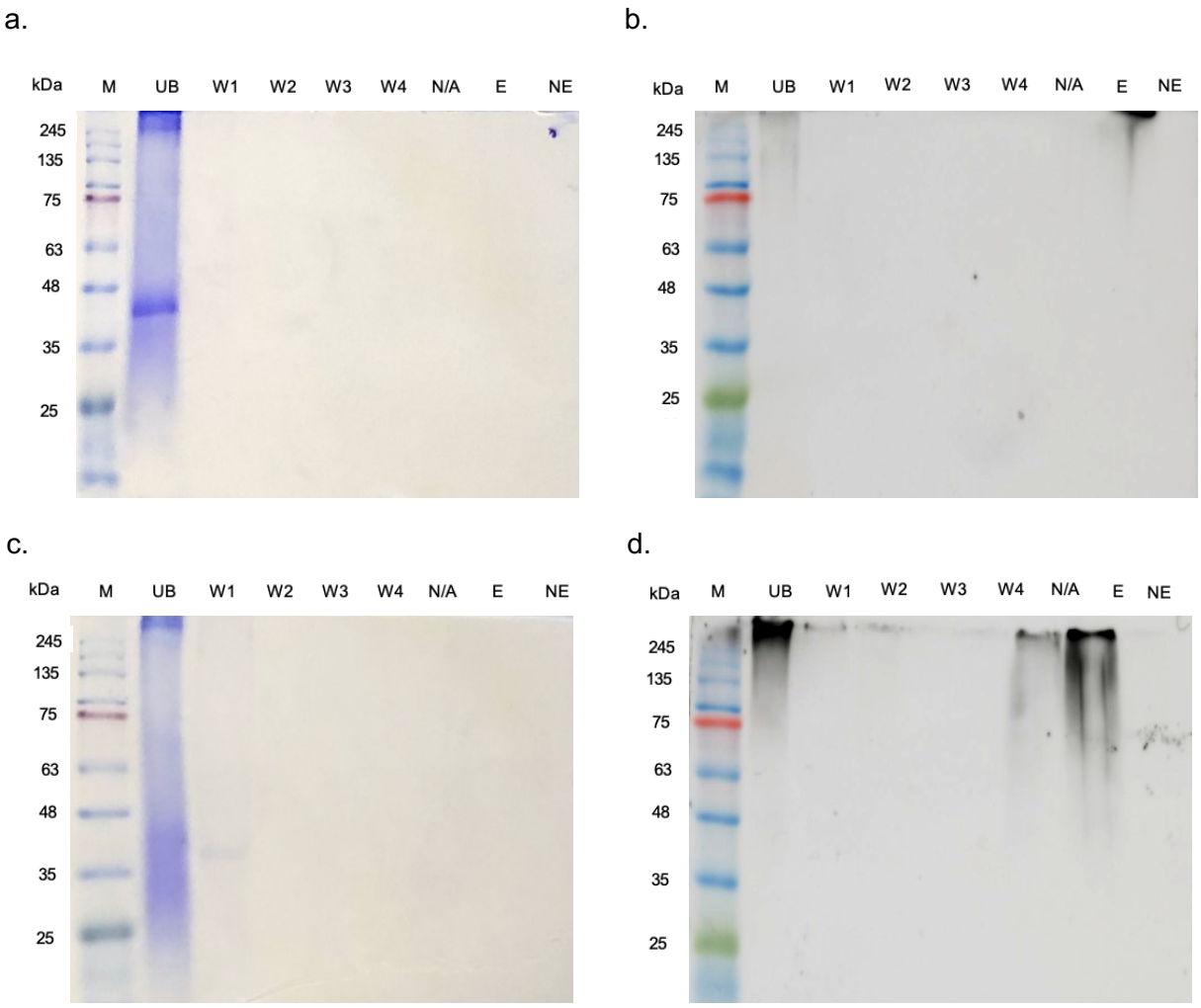

Supplementary Figure 3 - Pulldown assay (second optimization) of glycoproteins from *Paracentrotus lividus* tube feet disc extracts using LEL-bounded agarose beads | One-dimensional gel electrophoresis protein profile (**a,c**) and corresponding lectin blot (**b,d**) using non-precipitated **(a,b)** and precipitated (**c,d)** sample. Abbreviations: E – eluted fraction; M - molecular weight markers; NE – non-eluted fraction; UB- unbound fraction; W1-4 – wash fractions. 15 seconds of exposure time.

a.

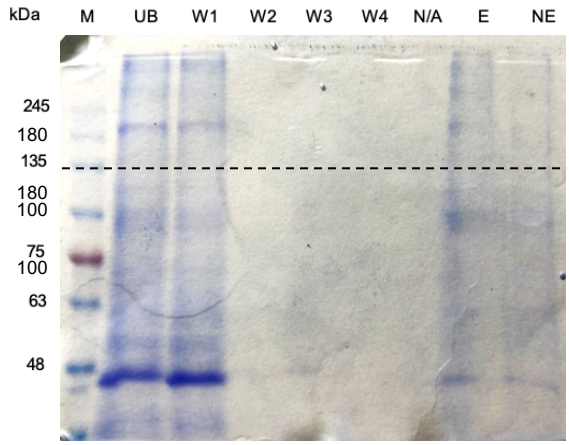

b.

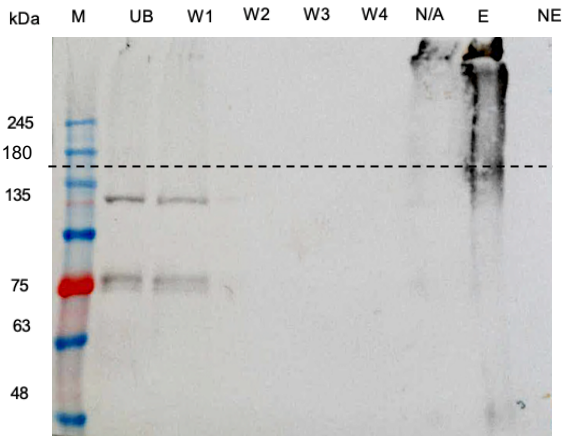

Supplementary Figure 4 - Pulldown assay (third optimization) of glycoproteins from *Paracentrotus lividus* tube feet disc extracts using LEL-bounded agarose beads | One-dimensional gel electrophoresis protein profile (**a**) and corresponding lectin blot (**b**) using lower acrylamide percentage gels (stacking gel 3% and resolving gel 7.5%. Abbreviations: E – eluted fraction; M - molecular weight markers; NE – non-eluted fraction; UB- unbound fraction; W1-4 – wash fractions. 15 seconds of exposure time. Dashed line indicates the separation between stacking and resolving gel. Dashed line indicates the separation between stacking and resolving gel.

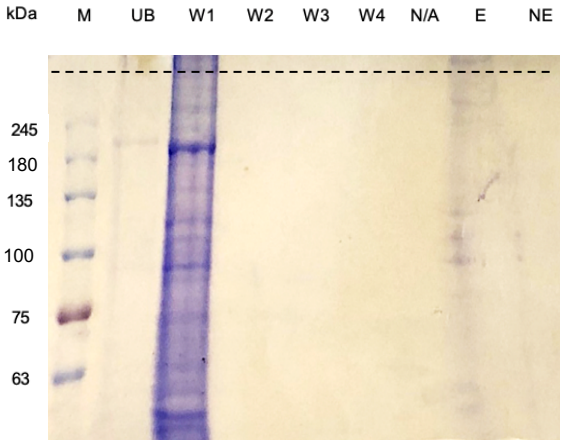

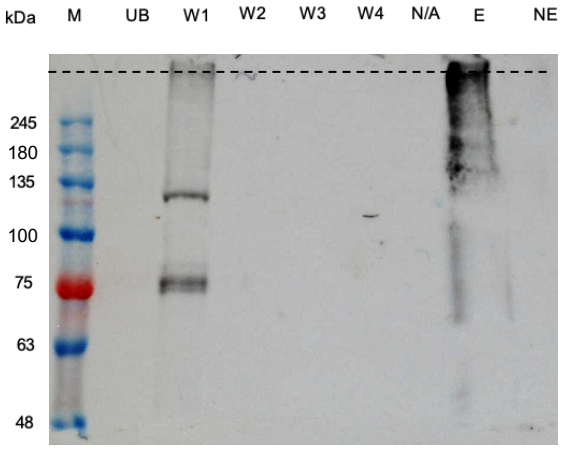

Supplementary Figure 5 - Pulldown assay of glycoproteins from *Paracentrotus lividus* tube feet disc extracts using SBA-bounded agarose beads | One-dimensional gel electrophoresis protein profile (**a**) and corresponding lectin blot (**b**) using lower acrylamide percentage gels (stacking gel 3% and resolving gel 7.5%. Abbreviations: E – eluted fraction; M - molecular weight markers; NE – non-eluted fraction; UB- unbound fraction; W1-4 – wash fractions. 5 seconds of exposure time. Dashed line indicates the separation between stacking and resolving gel. Dashed line indicates the separation between stacking and resolving gel.

Supplementary Table 2 – Unique peptides obtained by MS/MS for *Paracentrotus lividus* Nectin variant 3 | In bolt, the peptides were present in both replicates. When present in the first replicate is identified in black and in the second replicate, in grey. Absent peptides were marked with a black square.

Protein	**Nectin variant 3 (TR60905_c1_g1_i1_5)**				
Numer of peptides	**Peptides**	**GSL II** (38,7 e 35)	**WGA** (40,5 e 33,9)	**LEL** (37,3 e 31,4)	**SBA** (39,1 e 35,2)
1	LGIEDGR	**yes**	**yes**	**yes**	**yes**
2	VFVGNGDR	**yes**	**yes**	yes	
3	LGMEDGR	**yes**	**yes**	yes	**yes**
4	IFTANTDR	**yes**	**yes**	**yes**	**yes**
5	VTGIITQGR	yes		**yes**	
6	IFAVATQGR	**yes**	**yes**	**yes**	**yes**
7	LNLPLSGALK	yes	yes	yes	**yes**
8	SRLDTAAGAGK	**yes**	**yes**	**yes**	**yes**
9	FEVLGSIASK	**yes**	**yes**	**yes**	**yes**
10	QDANQWVTGFR	yes	**yes**	yes	yes
11	NGYSQWVTSFR	**yes**	**yes**	yes	yes
12	QDLNQWVTSYK	**yes**	**yes**	**yes**	**yes**
13	FEPLKLGMEDGR	**yes**	yes	**yes**	yes
14	QAFEVTGIITQGR	**yes**	**yes**	**yes**	yes
15	QLHEVSGVMTQGR	**yes**	**yes**	**yes**	**yes**
16	VLPDEWHGHISMR	yes	**yes**	yes	yes
17	LLPATWNSHISLR		yes	yes	
18	TNDQDQYIQVDLR	**yes**	**yes**	**yes**	**yes**
19	DSLVISMLPLPVTAR	**yes**	**yes**	**yes**	**yes**
20	TNDLDQWIQVDLR	**yes**	**yes**	**yes**	**yes**
21	WELIGMGPTTLAGSSR	**yes**	yes	**yes**	yes
22	NTIVTNSLPVPQVCR	**yes**	**yes**	**yes**	**yes**
23	STQVTNYFAPPFTAR	**yes**	**yes**	**yes**	**yes**
24	FELLGDGPINVVSTPGK	**yes**	**yes**	**yes**	**yes**
25	TNNVNQWIQVDLLSPYR	**yes**	**yes**	yes	**yes**
26	IPDSAITASTQYDANHGPQR	**yes**	**yes**	**yes**	**yes**
27	IAASSLSASSCYDGNHCVDR	**yes**	**yes**	**yes**	**yes**
28	LTDVQITASSCFDGNHCTDR	**yes**	**yes**	**yes**	**yes**
29	IADSQLSSSTCYDVNHCVDR	**yes**	**yes**	**yes**	**yes**
30	IACSSDGATFDTVQGICTNAAADR	**yes**	**yes**	**yes**	**yes**
31	VESSDDGVTFNPILDCSGNQQVFTGNADR	**yes**	yes	**yes**	**yes**
32	VLSSLDGLTFTPIPNAMMAGSDIFNGNSDR	yes	yes	yes	**yes**
33	GCLAETQIFPGNFDADSLVENAISPPVTAR	**yes**	**yes**	**yes**	**yes**
34	VESSDDGVTFNPILDCSGNQQVFTGNADRNTK	**yes**	yes	yes	**yes**
35	IHPETWSGHISMR		yes		yes
36	FEPVTWANHISMR		yes		yes
37	NGEDFTTISSPSTPLQDK	yes	**yes**		**yes**
38	KLGLEDYR	yes	yes		
39	QDANQWVTGFRVESSDDGVTFNPILDCSGNQQVFTGNADR		yes		
40	TGAWSAR	yes			
Total		40 peptides			

Supplementary Table 3 - Unique peptides obtained by MS/MS for *Paracentrotus lividus* alpha-tectorin | In bolt, the peptides were present in both replicates. When present in the first replicate is identified in black and in the second replicate, in grey. Absent peptides were marked with a black square.

Protein	**Alpha tectorin like** (TR46688_c0_g1_i1_6)				
Numer of peptides	**Peptides**	**GSL II** (12,1 e 10,1	**WGA** (7,4 e 5,1)	**LEL** (6,4 e 11,2)	**SBA** (12,5 e 4,5)
1	SYCDSLEAYVSR	**yes**	yes	**yes**	**yes**
2	ELFLDECSYDVCR	**yes**		**yes**	yes
3	IDGLPVQLDFTDSSTPPLFR	**yes**	**yes**	**yes**	**yes**
4	NIPLPDWR	yes		yes	
5	CQGIESCAFQVSTGLFSADPCPLTPK	**yes**		yes	yes
6	TGACIEMQCQNGGYCIR				yes
7	HEAHIGETFDVLAR		yes		
8	LGEDVRIDGLPVQLDFTDSSTPPLFR	yes	**yes**		
9	CVCQPDFILK		yes		
Total	9 peptides				
Protein	**Alpha tectorin like** (TR63383_c2_g1_i1_5)				
Numer of peptides	**Peptides**	**GSL II** (8,7 e 6,4)	**WGA** (9,5 e 0,5)	**LEL** (7,6 e 4,3)	**SBA** (15 e 4,5)
1	ECGCLVEGK	**yes**	**yes**	yes	yes
2	LFGDPCFTK	**yes**	yes	**yes**	yes
3	VYQACSEGVTK			yes	yes
4	CYEVCECPPGK	**yes**	yes	**yes**	yes
5	DSTGCSYMCPLGK	**yes**	yes	**yes**	yes
6	HCGLTDLQVSCSK	yes	yes	**yes**	yes
7	YLEVEYECLETK	**yes**	yes	**yes**	yes
8	CAHYEAYADACQAK			yes	yes
9	CELWANGEYFPDPCPATFK	**yes**	yes	**yes**	yes
10	DICAADNIGDQSCHEPTSLGVVMSK	**yes**	yes	yes	yes
11	EFYLDGER		yes		yes
12	VAMTCQGLTR		yes		yes
13	EESCFSATAEVR				yes
14	IICQDNPVMLNCR	yes	yes		yes
15	DCTICNGCQDIEACTR	yes			yes
16	VQHHCTQQPLASEVPQTPVR				yes
17	GGSVVASAPAFGFSWASNSPDCPTR				yes
18	DNIHEVDDYDVEAPFSVSTGDAMLSV		yes		yes
19	SYCDSLEAYVSR				yes
20	IDGLPVQLDFTDSSTPPLFR				yes
21	CPFCTQDPSCTDQIAQLDASSVCSEMI	yes			
Total	21 peptides				
	For all sequence				
Total	30 peptides				

Supplementary Table 4 - Unique peptides obtained by MS/MS for *Paracentrotus lividus* alpha-2-macroglobulin | In bolt, the peptides were present in both replicates. When present in the first replicate is identified in black and in the second replicate, in grey. Absent peptides were marked with a black square.

Protein	**Alpha macroglobulin** (TR61622_c8_g1_i2_4)				
Numer of peptides	**Peptides**	**GSL II** (10,3 e 9,5)	**WGA** (10,6 e 9,8)	**LEL** (7,6 e 9,5)	**SBA** (13,6 e 11)
1	IDNNDLQR	**yes**	yes	yes	yes
2	TEVVSFLNR			yes	**yes**
3	WLVSQQGPR	**yes**	**yes**	yes	**yes**
4	GYQGQLNFR	**yes**	**yes**	yes	yes
5	EFEELGLVR	yes	**yes**	yes	**yes**
6	IEEGVTHSDGLR	**yes**	yes	yes	**yes**
7	VHTTCDCPGGVK	**yes**	yes	yes	**yes**
8	GSGEFDLVDSSNR	**yes**	**yes**	yes	**yes**
9	AVALEAVAVGGPPAIR	**yes**	yes	yes	yes
10	YTDVTKEFEELGLVR	**yes**	**yes**	yes	**yes**
11	DLDSLIQGDLTLIEYR	**yes**	**yes**	yes	**yes**
12	HTFEVTVPEEYVADSGR			yes	yes
13	TSGAYSAFGNSDPEGSAWLSAYVVR	**yes**	**yes**	yes	**yes**
14	KASDVLQVR			yes	
15	EAEAAVFHR			yes	
16	TGLLAGGGSAEVK			yes	
17	SVETLMDMIK			yes	
18	TCSIAVALDTK			yes	
19	NSGIICTIGPVSR			yes	
20	VVTANTFLDHCSK			yes	
21	FFEDNTPVIVVTGWR			yes	
22	VLDVGGTIFVDDGLIALK			yes	
23	KGVNLPNAEVDLPALSDK			yes	
24	EVDMPTSAGLTVAIAAVEASYK			yes	
25	VAEIGADYLDCQIVNGGMLGSR			yes	
26	AETSDVANAVLDGADCVMLSGETAK			yes	
27	SFAQAGQFIK	yes	yes		**yes**
28	WLLNNLGQQDNGCFMNR		**yes**		**yes**
29	VIIFLSGDILGNSLTNIDSLLR		yes		**yes**
Total		29 peptides			

Supplementary Table 5 - Unique peptides obtained by MS/MS for *Paracentrotus lividus* uncharacterized protein | In bolt, the peptides were present in both replicates. When present in the first replicate is identified in black and in the second replicate, in grey. Absent peptides were marked with a black square.

Protein	**Uncharacterized protein** (TR46467_c1_g1_i2)				
Numer of peptides	**Peptides**	**GSL II** (24,6 **e ---)**	**WGA** (24,6 e ---)	**LEL** (13,9 e 24,6)	**SBA** (18,8 e 27)
1	AGEGWEFFK	yes	yes	**yes**	**yes**
2	HAFPDDIPSLR	yes	yes	**yes**	**yes**
3	MVVLPCDEELGYLCK	yes	yes	**yes**	**yes**
4	DANAACKPWDEEICSASR	yes	yes	**yes**	**yes**
5	NGYLFWSGVK	yes	yes	yes	**yes**
6	ECVAFDMSGDR	yes	yes	yes	yes
7	GWQSYLASYLTDGELEGAFR	yes	yes	yes	yes
8	KAYDAACIK				**yes**
Total		8 peptides			

Supplementary Table 6 - Unique peptides obtained by MS/MS for *Paracentrotus lividus* myeloperoxidase | In bolt, the peptides were present in both replicates. When present in the first replicate is identified in black and in the second replicate, in grey. Absent peptides were marked with a black square.

Protein	**Myeloperoxidase** (TR57217_c2_g1_i1_5)				
Numer of peptides	**Peptides**	**GSL II** (5 e 5)	**WGA** (10,5 e 12,7)	**LEL** (3 e 3,8)	**SBA** (7,6 e 8,2)
1	VLCETLDNPVTFQK	**yes**	**yes**	yes	**yes**
2	YLIDSETGEATPLDPLPITK	**yes**	**yes**	**yes**	**yes**
3	LFVDPDDDEDATGLDLMSLNVLR	**yes**	**yes**	yes	**yes**
4	NPAWVLDSDR		yes		yes
5	FHTSPDAEPSDVDLALSAGR				**yes**
6	FFYLNQDGPQAFTEDQR		yes		yes
7	NAIHDVTMAR		**yes**		
8	FVDDIDPFIGFIAEEPANDDGTLGPTLSCIIGSQFK		**yes**		
9	GSLLPHPEEISGNCFGEDETTGIICGDAGDFR		yes		
Total	9 peptides				

Supplementary Table 26 - Amino acid substitutions between Nectin variants | | Legend: nonpolar amino acids – yellow, polar amino acids – green, basic amino acids – blue, acidic amino acids – orange.

Non conservative substitutions between variants

	161 - 240 D II	**161 - 240 D II**	**401 - 480 D III**	**561 - 640 D IV**	**561 - 640 D IV**	**641 - 720 D V**	**721 - 800 D V**	**721 - 800 D V**	**721 - 800 D V**	**721 - 800 D V**	**801 - 874 D VI**	**801 - 874 D VI**
Nectin variant 1	Glycine (G)	Asparagine (N)	Alanine (A)	Glycine (G)	Histidine (H)	Phenylalanine (F)	Lysine (K)	Glycine (G)	Aspartic acid (D)	Serine (S)	Proline (P)	Arginine (R)
Nectin variant 2	Arginine (R)	Aspartic acid (D)	Threonine (T)	Serine (S)	Asparagine (N)	Tyrosine (Y)	Lysine (K)	Serine (S)	Valine (V)	Glycine (G)	Glutamine (Q)	Glutamine (Q)
Nectin variant 3	Glycine (G)	Aspartic acid (D)	Alanine (A)	Serine (S)	Asparagine (N)	Tyrosine (Y)	Threonine (T)	Serine (S)	Valine (V)	Glycine (G)	Proline (P)	Arginine (R)

Conservative substitutions between variants

	1 - 80 O/D	**80 - 160 D I**	481 - 560 O/D	**641 - 720 D IV**	**721 - 800 D V**	**801 - 874 D VI**
Nectin variant 1	Histidine (H)	Isoleucine (I)	Valine (V)	Arginine (R)	Isoleucine (I)	Alanine (A)
Nectin variant 2	Histidine (H)	Isoleucine (I)	Isoleucine (I)	Histidine (H)	Valine (V)	Alanine (A)
Nectin variant 3	Arginine (R)	Phenylalanine (F)	Isoleucine (I)	Histidine (H)	Valine (V)	Proline (P)